GEOMETRIC TRANSITIONS:
FROM HYPERBOLIC TO AdS GEOMETRY

A DISSERTATION
SUBMITTED TO THE DEPARTMENT OF MATHEMATICS
AND THE COMMITTEE ON GRADUATE STUDIES
OF STANFORD UNIVERSITY
IN PARTIAL FULFILLMENT OF THE REQUIREMENTS
FOR THE DEGREE OF
DOCTOR OF PHILOSOPHY

Jeffrey Danciger

June 2011

This dissertation is online at: http://purl.stanford.edu/ww956ty2392

I certify that I have read this dissertation and that, in my opinion, it is fully adequate in scope and quality as a dissertation for the degree of Doctor of Philosophy.

Steven Kerckhoff, Primary Adviser

I certify that I have read this dissertation and that, in my opinion, it is fully adequate in scope and quality as a dissertation for the degree of Doctor of Philosophy.

Gunnar Carlsson

I certify that I have read this dissertation and that, in my opinion, it is fully adequate in scope and quality as a dissertation for the degree of Doctor of Philosophy.

Maryam Mirzakhani

Approved for the Stanford University Committee on Graduate Studies.

Patricia J. Gumport, Vice Provost Graduate Education

This signature page was generated electronically upon submission of this dissertation in electronic format. An original signed hard copy of the signature page is on file in University Archives.

Abstract

We introduce a geometric transition between two homogeneous three-dimensional geometries: hyperbolic geometry and anti de Sitter (AdS) geometry. Given a path of three-dimensional hyperbolic structures that collapse down onto a hyperbolic plane, we describe a method for constructing a natural continuation of this path into AdS structures. In particular, when hyperbolic cone manifolds collapse, the AdS manifolds generated on the "other side" of the transition have tachyon singularities. The method involves the study of a new transitional geometry called *half-pipe* geometry.

We also discuss combinatorial/algebraic tools for constructing transitions using ideal tetrahedra. Using these tools we prove that transitions can always be constructed when the underlying manifold is a punctured torus bundle.

Preface

This thesis focuses on connections between two particular types of geometry: *hyperbolic* geometry and *anti de Sitter* (AdS) geometry. Though hyperbolic manifolds have been studied for over a century, it was Thurston's ground-breaking work starting in the late 1970s that established hyperbolic geometry as a vital tool for understanding three-manifolds. Today, with Perelman's proof of Thurston's Geometrization Conjecture, the study of hyperbolic manifolds is at the heart of the most important questions in low-dimensional topology. Anti de Sitter geometry is a Lorentzian analogue of hyperbolic geometry. Witten [Wit88] and others have studied such constant curvature Lorentzian spaces as simple models for $2+1$ dimensional gravity. In the last ten years, AdS geometry has drawn much renewed interest due to its role in the most successful realizations of the holographic principle in string theory [Mal99].

Though historically the studies of hyperbolic geometry and anti de Sitter geometry have been somewhat disjoint, many parallels have appeared in recent years. One breakthrough along these lines is Mess's classification of maximal AdS space-times [Mes07, ABB$^+$07] and its remarkable similarity to the Simultaneous Uniformization Theorem of Bers [Ber60] for quasi-Fuchsian hyperbolic manifolds. Stemming from Mess's work, results and questions in hyperbolic and AdS geometry have begun to appear in tandem, suggesting the existence of a deeper link between the two geometries. The search for such a link is one motivating force behind this research.

The work presented here on *geometric transitions* establishes an explicit connection between three-dimensional hyperbolic and AdS geometry, strengthening the analogies described above. Many of the ideas are inspired by Craig Hodgson's study of degeneration and regeneration of hyperbolic structures [Hod86] and by the work of Joan Porti and collaborators on regeneration of hyperbolic structures from various other geometric structures [Por98, HPS01, Por02, Por10].

Acknowledgements

Over the last five years as a Ph.D. student, I was fortunate to benefit from the insight, advice, and encouragement of mentors, colleagues, and many dear friends. Without them, I am sure it would have been impossible to complete this thesis.

First, I thank my advisor Steven Kerckhoff for abundant patience and generosity. I feel very fortunate to have worked with an advisor who was so involved with my research. With luck, I will leave Stanford having absorbed some small fraction of Steve's geometric intuition. I thank Gunnar Carlsson for many interesting conversations and general guidance during my graduate career. It was also a great pleasure discussing geometry with Maryam Mirzakhani; I wish she had arrived at Stanford sooner! I also thank the other members of my thesis committee, Joan Licata and Eva Silverstein.

Some ideas in this thesis were influenced by conversations with Jean-Marc Schlenker, Joan Porti, Craig Hodgson, and many others at the Workshop on Geometry, Topology, and Dynamics of Character Varieties at the National University of Singapore in July 2010.

The exceptional group of graduate students and postdocs at Stanford also deserve acknowledgement. I have greatly enjoyed discussing mathematics with Jason DeBlois and Kenji Kozai. I thank my dear friends Jesse Gell-Redman, for on-demand geometric analysis consultation, and Daniel Murphy, for emergency thesis formatting advice. My experience at Stanford has been greatly enhanced by the comradery of classmates Olena Bormashenko and Jóse Perea as well as past and current office-mates David Ayala, Eric Malm, Dean Baskin, Henry Adams, and Chris Henderson.

To my dearest Marika, your love is a stabilizing force in my life. Thank you for supporting me through the difficult times of the past five years. Also, your editing was clutch.

Finally, I thank my family for endless love and support. Mom, your unfaltering devotion has lifted me beyond what I thought I was capable of. Dad, your passion, perseverance, and dedication inspire me in every endeavor; This thesis is dedicated to you.

Contents

List of Figures

Chapter 1

Introduction

1.1 Geometric transitions: from $\mathbb{H}^3$ to AdS^3

The study of deformation spaces of geometric structures is a rich subject with many interesting questions. Of particular interest is the question of how and why geometric structures degenerate. The overarching philosophy in three dimensions, based loosely on Thurston's geometrization program, is that when a path of geometric manifolds degenerates, the degeneration is calling for a transition to a different type of geometry in order to continue the path. One prominent example of this is the transition from hyperbolic to spherical, studied by Hodgson [Hod86] and Porti [Por98]. A path of hyperbolic structures (say compact with

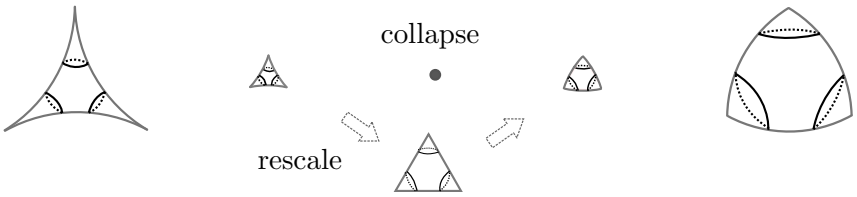

Figure 1.1: Hyperbolic structures on a sphere with three cone points (of equal angle) collapse down to a point as the cone angles increase to $\frac{2\pi}{3}$. After rescaling the metric, the structures limit to a Euclidean sphere with cone points and then transition to spherical cone structures.

singularities) that collapses down to a point can be isotropically *rescaled* and made to converge to a Euclidean structure. This Euclidean structure in turn determines a regeneration from the collapsed structure (a point) to a path of expanding spherical structures (which when rescaled also approximate the Euclidean structure). This phenomenon is an example

of a *geometric transition*. The focus of this thesis is the study of geometric transitions in the context of a different degeneration behavior, that of three-dimensional structures collapsing down onto a hyperbolic plane.

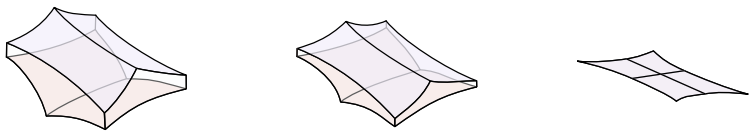

Figure 1.2: Fundamental domains for hyperbolic cone manifolds collapse onto a hyperbolic plane.

To begin the discussion, we focus our attention on hyperbolic structures on a compact three-manifold M with boundary. Let $D_t : \widetilde{M} \to \mathbb{H}^3$ be a family of developing maps defined for $t > 0$ and suppose D_t converges to D_0 a local submersion onto a two dimensional hyperbolic plane $\mathfrak{P}$. Then D_0 defines a co-dimension one *transversely hyperbolic foliation*. The problem of regenerating hyperbolic structures from this data was examined by Hodgson [Hod86], and later in a specific case by Porti [Por10]. However, it had not yet been established how to construct a geometric transition in this context. Our point of view, based on projective geometry, is that such a degeneration naturally suggests a transition to AdS geometry. As motivation, note that the isometry groups $\mathrm{Isom}(\mathbb{H}^3) = \mathrm{SO}(3,1)$ and $\mathrm{Isom}(\mathrm{AdS}^3) = \mathrm{SO}(2,2)$ are naturally subgroups of the projective group $\mathrm{PGL}(4,\mathbb{R})$. The intersection $\mathrm{SO}(3,1) \cap \mathrm{SO}(2,2)$ is, with suitable choice of coordinates, exactly the copy of $\mathrm{O}(2,1)$ that preserves the hyperbolic plane $\mathfrak{P}$.

Roughly, the transition from hyperbolic to AdS geometry is constructed similarly to the transition from hyperbolic to spherical, alluded to above. As the hyperbolic structures degenerate, the collapsing direction is rescaled so that the structures converge to a robust three-dimensional structure called a *half-pipe* (HP) structure. Interpreting the hyperbolic structures as projective structures, this rescaling is really a projective change of coordinates. This construction is given in Chapter 3.

The key for constructing transitions is that HP structures contain precisely the information needed to regenerate to both hyperbolic and AdS structures. In fact, if a regeneration can be constructed on the level of representations, then an HP structure can be "exponentiated" to produce a regeneration to robust geometric structures. We simply note here that HP geometry plays the same central role in the transition between hyperbolic and AdS

geometry as Euclidean geometry plays in the transition between hyperbolic and spherical.

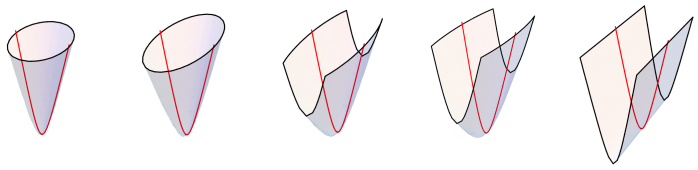

Figure 1.3: Rescaling the hyperboloid model for $\mathbb{H}^2$. The limit is the hyperboloid model for *half-pipe* (HP) geometry.

1.1.1 Cone/tachyon transitions

Chapter 4 focuses on transitions in the context of hyperbolic cone structures (see Section 4.3 or e.g. [CHK00, BLP05, Bro07]). In this case, the AdS structures generated on the "other side" of the transition have *tachyon singularities*, a natural Lorentzian analogue to cone singularities (see [BBS09], or Section 4.4). Recall that a cone singularity is a singularity along a geodesic axis such that the holonomy of a meridian encircling the axis is a rotation around the axis. Similarly, a tachyon is a singularity along a space-like axis such that the holonomy of a meridian encircling the axis is a Lorentz boost perpendicular to the axis. The magnitude of the boost is called the *tachyon mass*. The following is proved in Chapter 4:

Theorem 6. *Let N be a closed three-manifold, with Σ a knot, and let $M = N \setminus \Sigma$. Let h_t be a path of hyperbolic cone structures on (N, Σ) defined for $t > 0$. Suppose that:*

- *As $t \to 0$, the cone angle approaches 2π and h_t limits to a transversely hyperbolic foliation with holonomy $\rho : \pi_1 M \to \mathrm{O}(2,1)$.*
- *There are projective structures $\mathscr{P}_t$, defined for $t > 0$, equivalent to h_t, and which converge to an* HP *structure.*
- $H^1(\pi_1 M, \mathfrak{so}(2,1)_{Ad\rho}) = \mathbb{R}$.

Then a transition to AdS *structures with tachyons exists: We can continue the path $\mathscr{P}_t$ to $t < 0$ so that $\mathscr{P}_t$ is projectively equivalent to an* AdS *structure with a tachyon singularity (of mass $O(t)$). The same result holds when the roles of hyperbolic and* AdS *structures are interchanged.*

The proof of the theorem involves a generalization of cone singularities to projective geometry (Section 4.2). This class of singularities, called *cone-like* singularities, includes cone singularities in hyperbolic geometry, tachyons in AdS geometry, and the corresponding singularity in HP geometry. We prove that deformations of a projective structure with cone-like singularities are locally in correspondence with appropriate deformations of the holonomy representation. Then, we analyze the representation variety to produce representations with the needed properties and prove a regeneration theorem going from singular HP structures to singular hyperbolic and AdS structures (Theorem 4 of 4.7) which implies the result.

The cohomology condition in Theorem 6 is satisfied by a variety of examples, including examples coming from small Seifert fiber spaces and Anosov torus bundles. This condition, reminiscent of a similar condition appearing in Porti's regeneration theorem for Euclidean cone structures [Por98], is simply a way to guarantee smoothness of the representation variety. Our construction of a geometric transition really only requires that a transition exists *on the level of representations* which is implied by (but does not require) smoothness. In Section 4.11, we study examples of collapsing structures for which the singular locus has two components. In this case the $\mathrm{SO}(2,1)$ representation variety is not smooth, but we can still produce transitions. We also observe an interesting flexibility phenomenon in this case: A transitional HP structure can be deformed so that it no longer regenerates to hyperbolic structures.

1.2 Ideal triangulations

In Chapter 5, we introduce tools for studying many of the above questions in the case when an ideal triangulation is available. Ideal triangulations are featured in the volume maximization program of Casson-Rivin [Riv94], the recent variational formulation of the Poincaré conjecture by Luo [Luo10], and many other articles (e.g. [PP00, Lac00]). Perhaps the most widespread use of ideal triangulations is in the study of deformation spaces of singular hyperbolic structures, which are constructed as varieties of solutions to Thurston's equations ([Thu80] or see [NZ85]). We generalize this construction to study deformation spaces of triangulated AdS structures, transversely hyperbolic foliations, and HP structures. Let M^3 have a union of tori as boundary and assume that M^3 has a fixed topological ideal triangulation $\mathcal{T} = \{\mathcal{T}_1, \ldots, \mathcal{T}_n\}$.

1.2.1 Deformation Varieties

Recall that a hyperbolic ideal tetrahedron is described up to isometry by a complex *shape parameter* (See [Thu80] or Section 2.2.4 for a description). Defining a hyperbolic structure on $(M, \mathcal{T})$ amounts to assigning complex numbers z_j to each tetrahedron $\mathcal{T}_j$ such that the z_j satisfy Thurston's *edge consistency equations*. Solutions to these algebraic equations make up the *hyperbolic deformation variety*. A point (z_j) for which all tetrahedra are positively oriented (i.e. $\mathrm{Im}(z_j) > 0$) determines a robust hyperbolic structure. A *degenerate* $\mathbb{H}^2$ *ideal tetrahedron* is a hyperbolic tetrahedron with real shape parameter. Such a tetrahedron is collapsed onto a plane. The *real deformation variety* of real solutions to Thurston's equations describes transversely hyperbolic foliations built out of these degenerate tetrahedra. These foliations have Dehn surgery singularities as defined by Hodgson in [Hod86].

In Section 5.2.3, deformation spaces of AdS structures built of *anti de Sitter ideal tetrahedra* are constructed. All faces of these tetrahedra are space-like hyperbolic ideal triangles. It turns out that the shape of a tetrahedron is determined by a parameter z lying in the algebra $\mathbb{R} + \mathbb{R}\tau$ where τ commutes with $\mathbb{R}$ and satisfies $\tau^2 = +1$. An element $a + b\tau$ has square-norm defined by $|a+b\tau|^2 = a^2 - b^2$. The parameter z determines an ideal tetrahedron if and only if z, $\frac{1}{1-z}$, and $\frac{z-1}{z}$ (are defined and) have positive square-norm (such elements are called *space-like*). The AdS *deformation variety* consists of space-like solutions to the edge consistency equations over $\mathbb{R}+\mathbb{R}\tau$. A point (z_j) for which all tetrahedra are positively oriented ($\mathrm{Im}(z_j) > 0$) determines a robust AdS structure. We emphasize that the absence of a Riemannian metric makes AdS structures very difficult to study. These combinatorial and algebraic methods give an easy way to construct and deform AdS structures.

Remark 1. A half-space model of AdS^3, with isometries given by $\mathrm{PGL}^+(2, \mathbb{R}+\mathbb{R}\tau)$ acting by Mobius transformations, is constructed in Appendix A. The ideal boundary in this model is a projectivization of $(\mathbb{R} + \mathbb{R}\tau)^2$.

1.2.2 Regeneration results

The study of the real deformation variety is crucial for constructing regenerations to hyperbolic and AdS structures on $(M, \mathcal{T})$. In fact, if the real deformation variety is smooth at a point, then any positive tangent vector determines regenerations to robust hyperbolic and anti de Sitter structures (Section 5.3). In the case that M is a punctured torus bundle with anosov monodromy, we identify two canonical connected components of the deformation

variety for which every point has the best possible properties. The following theorem is discussed in Chapter 6:

Theorem 7. *Let M^3 be a punctured torus bundle with Anosov monodromy and let $\mathcal{T}$ be the monodromy ideal triangulation on M. Let $\mathscr{D}_{\mathbb{R}}$ be the deformation variety of of transversely hyperbolic foliations on $(M, \mathcal{T})$. Then, there are two canonical smooth, one dimensional, connected components $\mathscr{V}_+$ of $\mathscr{D}_{\mathbb{R}}$ with positive tangent vectors at every point. Further, each component of $\mathscr{V}_+$ is parameterized by the (signed) length of the puncture curve.*

Corollary. *Any transversely hyperbolic foliation on $(M, \mathcal{T})$ belonging to $\mathscr{V}_+$ regenerates to hyperbolic and* AdS *structures.*

1.2.3 Triangulated transitions and HP tetrahedra

It is possible to frame the *triangulated transition problem* in terms of solving Thurston's edge consistency equations over a varying path of sub-algebras of a larger Clifford algebra. These sub-algebras smoothly transition from $\mathbb{C}$ to $\mathbb{R} + \mathbb{R}\tau$ and pass through a transitional shape parameter algebra $\mathbb{R}+\mathbb{R}\sigma$, where $\sigma^2 = 0$, that describes shape parameters for *half-pipe ideal tetrahedra*. This construction is discussed in Section 5.4.

Chapter 2

Geometric structures

In this chapter we give a description of the (X, G) formalism that is ubiquitous in the study of locally homogeneous geometric structures. We will then describe hyperbolic geometry, AdS geometry, and a few other examples using this formalism. The material in this chapter is standard; references will be given along the way. We give an intuitive account of the important concepts rather than rigorous proofs.

2.1 (X, G) structures

Let X be a smooth manifold with G a Lie group of diffeomorphisms of X acting transitively. We assume further that the elements of G are *analytic* in the sense that an element is determined by its restriction to any open set in X. The following definition is originally due to Ehresmann [Ehr36], though much of the modern study of homogeneous geometric structures is based on the work of Thurston [Thu80] (or see Goldman's expository article [Gol10]).

Definition 1. An (X, G) structure on a manifold M is given by a family of charts $\varphi_\alpha : U_\alpha \to X$ which cover M such that each transition map $\varphi_\alpha \varphi_\beta^{-1}$ is the restriction of an element $g_{\alpha\beta} \in G$.

Note that the transition map $\varphi_\alpha \varphi_\beta^{-1}$ is only defined on the intersection $\varphi_\beta(U_\alpha \cap U_\beta)$. However, if this intersection is non-empty, the element $g_{\alpha\beta}$ is uniquely determined because of the analytic condition.

Choosing a base chart $\varphi_0 : U_0 \to X$, we build a *developing map* $D : \widetilde{M} \to X$ as follows.

Fix a basepoint $p \in U_0$. We identify $\widetilde{M}$ with the space of paths in M originating at p up to homotopy rel endpoints. Begin by defining $D(p) = \varphi_0(p)$ and define D along paths originating from p via analytic continuation as follows. Consider a path $\gamma : [0,1] \to M$, with $\gamma(0) = p$. Find finitely many charts $U_0, U_1, \ldots, U_k$ covering γ, where we assume the first chart to be our base chart. Further assume that consecutive charts overlap. If $\gamma(t)$ lies in U_0, define $D(\gamma(t)) = \varphi_0(\gamma(t))$. If $\gamma(t)$ lies in U_1, then define $D(\gamma(t)) = g_{01}\varphi_1(\gamma(t))$. In general, if $\gamma(t)$ lies in the j^{th} open set U_j, define

$$D(\gamma(t)) = g_{01}g_{12}\cdots g_{j-1,j}\varphi_j(\gamma(t)).$$

Note that D is well-defined, for on the overlap $U_j \cap U_{j+1}$, we have $\varphi_j = g_{j,j+1}\varphi_{j+1}$ which implies that

$$g_{01}g_{12}\cdots g_{j-1,j}\varphi_j = g_{01}g_{12}\cdots g_{j-1,j}g_{j,j+1}\varphi_{j+1}.$$

It is a straightforward exercise to show that D is well defined independent of the covering $U_1, \ldots, U_k$ of γ and independent of γ up to homotopy rel endpoints. Thus D is a well-defined local diffeomorphism.

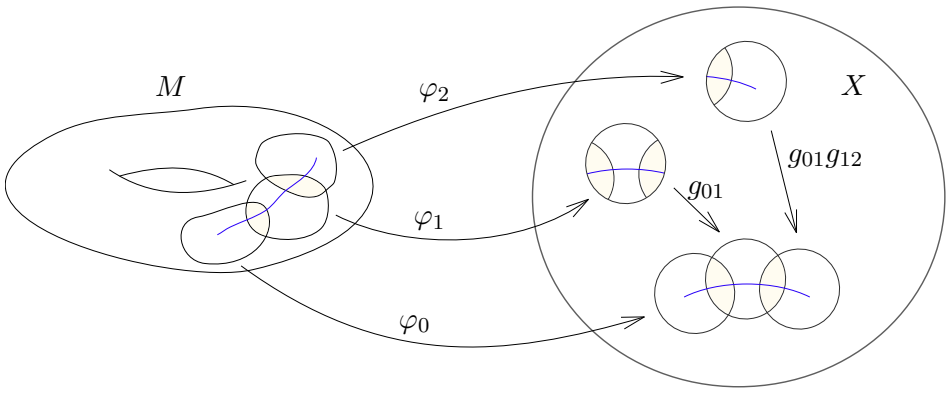

Figure 2.1: A developing map is constructed via analytic continuation of the charts along paths.

Given an (X, G) manifold M with charts $(U_\alpha, \varphi_\alpha)$ and another (X, G) manifold N with charts (V_β, ψ_β), an (X, G) *isometry* or *equivalence* is a diffeomorphism $\Phi : M \to N$ so that $\varphi_\alpha \circ \Phi \circ \psi_\beta^{-1}$ is the restriction of an element $g \in G$ whenever defined. Each lift $\widetilde{\Phi} : \widetilde{M} \to \widetilde{N}$ of Φ is an (X, G) isometry of the universal covers. Let D_M, D_N be developing maps for M and N. In a small neighborhood of $x \in \widetilde{M}$, D_M is a diffeomorphism and $D_N \circ \widetilde{\Phi} \circ D_M^{-1}$ is

the restriction of an element $g(x, \widetilde{\Phi}) \in G$. However, $g(x, \widetilde{\Phi})$ is locally constant in x and so it does not depend on x at all. That is, for any $\widetilde{\Phi}$ there is a unique $g(\widetilde{\Phi}) \in G$ such that

$$D_N \circ \widetilde{\Phi} = g(\widetilde{\Phi}) \circ D_M.$$

In the case that $M = N$, with $\Phi = \mathrm{Id}$, the lifts $\widetilde{\Phi}$ are exactly the deck transformations of $\widetilde{M}$ corresponding to elements $\gamma \in \pi_1 M$. The homomorphism $\rho : \gamma \mapsto g(\gamma)$ is called the *holonomy representation*. We record this information in a proposition:

Proposition 1. *Given an (X, G) structure on M, the choice of a base chart (U_0, φ_0) determines a* developing map $D : \widetilde{M} \to X$ *and* holonomy representation $\rho : \pi_1 M \to G$. *Note that D is a local diffeomorphism and is equivariant with respect to ρ:*

$$D(\gamma \cdot x) = \rho(\gamma) D(x)$$

where on the left hand side $\gamma \cdot x$ refers to deck translation by $\gamma \in \pi_1 M$.

Definition 2. An (X, G) structure is *complete* if the developing map is a covering map.

Assume that X is simply connected and that M is a complete (X, G) manifold. Then the developing map is a diffeomorphism and we identify $\widetilde{M} = X$. Note that the holonomy representation ρ must be discrete and faithful. Further, $\Gamma = \rho(\pi_1 M)$ acts properly discontinuously on X and we may identify M with the quotient $M = X/\Gamma$.

Remark 2. In the case that X has a G-invariant Riemannian metric, this definition of completeness is equivalent to geodesic completeness.

2.1.1 Deforming (X, G) structures

A smooth family of (X, G) structures on a manifold M with boundary is given by a smooth family of developing maps $D_t : \widetilde{M} \to X$ equivariant with respect to a smooth family of holonomy representations $\rho_t : \pi_1 M \to G$.

Definition 3. Two deformations D_t and F_t of a given structure D_0 are considered equivalent if there exists a path $g_t \in G$ and a path Φ_t of diffeomorphisms *defined on all but a small neighborhood of ∂M* so that

$$D_t = g_t \circ F_t \circ \widetilde{\Phi}_t$$

where $\widetilde{\Phi}_t$ is a lift of Φ_t to $\widetilde{M}$ and we assume $g_0 = 1$ and $\widetilde{\Phi}_0 = \mathrm{Id}$.

A *trivial* deformation of D_0 is of the form $D_t = g_t \circ D_0 \circ \widetilde{\Phi}_t$. In this case, the holonomy representations differ by a path of conjugations:

$$\rho_t = g_t \rho_0 g_t^{-1}.$$

Such a deformation of the holonomy representation is also called trivial. Let $\mathscr{R}(\pi_1 M; G)$ be the space of representations up to conjugation (we only consider points at which this quotient is reasonable). Let $\mathscr{D}(M; X, G)$ be the space of all (X, G) structures on M up to the equivalence described above. The following fact is crucial for the study of deformations of (X, G) structures.

Proposition 2 (Thurston)**.** *The map* hol : $\mathscr{D}(M; X, G) \to \mathscr{R}(\pi_1 M; G)$*, which maps an* (X, G) *structure to its holonomy representation, is (well-defined and) a local homeomorphism.*

The injectivity and well-defined-ness is not hard to see. For if we have two paths of (X, G) developing maps D_t, F_t with corresponding holonomy representations ρ_t and σ_t so that $\rho_t = g_t \sigma_t g_t^{-1}$. Then, by replacing F_t with the equivalent deformation $g_t^{-1} F_t$, we may assume that $\rho_t = \sigma_t$. Next, since $F_0 = D_0$, we can find diffeomorphisms Ψ_t such that $F_t = D_t \circ \Psi_t$. Since F_t and D_t are both equivariant with respect to ρ_t, we must have Ψ_t invariant under the action of $\pi_1 M$, so that $\Psi_t = \widetilde{\Phi}_t$ is a lift of a diffeomorphism of M. The local surjectivity is a little bit harder. We give the proof in Lemma 5 of Section 3.6.

Remark 3. We emphasize that the definition of $\mathscr{D}(M; X, G)$ above does not consider behavior at the boundary. In particular, given a structure D_0 with special geometric features at ∂M, Proposition 2 may produce nearby (X, G) structures with very different boundary geometry. Often, it is desirable to deform (X, G) structures with control over the geometry at the boundary. This is the case, for example, in the study of hyperbolic cone structures (see [HK98]). The Proposition is not strong enough in these cases, and a thorough study of the boundary geometry is needed. In Chapter 4 we will pay careful attention to this issue as we deform from hyperbolic cone structures to AdS tachyon structures.

2.1.2 Infinitesimal Deformations

Consider a smooth family of representations $\rho_t : \pi_1 M \to G$. The derivative of the homomorphism condition (evaluated at $t = 0$) gives that

$$\rho'(ab) = \rho'(a)\rho_0(b) + \rho_0(a)\rho'(b).$$

This is a statement in the tangent space at $\rho_0(ab)$ in G. In order to translate all of the tangent vectors back to the identity, we multiply this equation by $\rho_0(ab)^{-1}$:

$$\begin{aligned} \rho'(ab)\rho_0(ab)^{-1} &= \rho'(a)\rho_0(a)^{-1} + \rho_0(a)\rho'(b)\rho_0(b)^{-1}\rho_0(a)^{-1} \\ &= \rho'(a)\rho_0(a)^{-1} + Ad_{\rho_0(a)}(\rho'(b)\rho_0(b)^{-1}). \end{aligned}$$

Letting $\mathfrak{g} = T_{\mathrm{Id}}G$ denote the Lie algebra of G, define $z : \pi_1 M \to \mathfrak{g}$ by $z(\gamma) = \rho'(\gamma)\rho_0(\gamma)^{-1}$. Then z satisfies the *cocycle condition*:

$$z(ab) = z(a) + Ad_{\rho_0(a)} z(b). \tag{2.1}$$

The group cocycles $Z^1(\pi_1 M, \mathfrak{g}_{Ad\rho_0})$ are defined to be all functions z satisfying Equation 2.1 for all $a, b \in \pi_1 M$. We call $z \in Z^1(\pi_1 M, \mathfrak{g}_{Ad\rho_0})$ an *infinitesimal deformation* of the representation ρ_0. Next, suppose $\rho_t = g_t \rho_0 g_t^{-1}$ is a trivial deformation of ρ_0. Differentiating shows that

$$\rho'(\gamma)\rho_0(\gamma)^{-1} = g' - Ad_{\rho_0(\gamma)} g'.$$

The co-boundaries $B^1(\pi_1 M, \mathfrak{g}_{Ad\rho_0})$ are defined to be all group cocycles z such that

$$z(\gamma) = u - Ad_{\rho_0(\gamma)} u$$

for some $u \in \mathfrak{g}$. These are thought of as trivial infinitesimal deformations. Now define the cohomology group

$$H^1(\pi_1 M, \mathfrak{g}_{Ad\rho_0}) = Z^1(\pi_1 M, \mathfrak{g}_{Ad\rho_0}) / B^1(\pi_1 M, \mathfrak{g}_{Ad\rho_0}).$$

Proposition 3. *If $\mathscr{R}(\pi_1 M; G)$ is a smooth manifold at ρ_0, then $H^1(\pi_1 M, \mathfrak{g}_{Ad\rho_0})$ describes the tangent space at ρ_0.*

Remark 4. In all cases of interest in this thesis, G is an algebraic group. In this case the

representation space $\mathscr{R}(\pi_1 M; G)$ can be given the structure of an algebraic variety.

2.1.3 Projective Geometry

We close this section with an important example of an (X, G) geometry which does not come from a homogeneous Riemannian model space. The real projective space $\mathbb{RP}^n$ is the space of lines in $\mathbb{R}^{n+1}$. It is an n-dimensional manifold, orientable if and only if n is odd. The group $\mathrm{GL}(n+1, \mathbb{R})$ acts by diffeomorphisms on $\mathbb{RP}^n$, with kernel given by its center $\{\lambda I : \lambda \in \mathbb{R}^*\}$. Thus $\mathrm{PGL}(n+1, \mathbb{R})$, defined to be the quotient of $\mathrm{GL}(n+1, \mathbb{R})$ by its center, acts faithfully by diffeomorphisms on $\mathbb{RP}^n$. A hyperplane of dimension $k+1$ in $\mathbb{R}^{n+1}$ descends to a copy of $\mathbb{RP}^k$ inside $\mathbb{RP}^n$, which we call a *k-plane*. The *lines* in $\mathbb{RP}^n$ are described by the case $k = 1$. They correspond to two-dimensional planes in $\mathbb{R}^{n+1}$. Note that k-planes in $\mathbb{RP}^n$ are taken to other k-planes by $\mathrm{PGL}(n+1, \mathbb{R})$, so these are well defined geometric objects in projective geometry; they play the role of totally geodesic hyperplanes in a Riemannian model geometry.

Definition 4. A *projective structure* on a manifold M^n is an (X, G) structure for $X = \mathbb{RP}^n$, $G = \mathrm{PGL}(n+1, \mathbb{R})$.

Remark 5. Usually, it most convenient to work with a simply connected model space. If desired, $\widetilde{\mathbb{RP}^n}$ can be used as the model for projective geometry. However, it turns out that $\mathbb{RP}^n$ has nicer global geometry than its universal cover. The best example of this is that any two points in $\mathbb{RP}^n$ are connected by a unique line, while this is not true in $\widetilde{\mathbb{RP}^n}$.

The geometry of projective structures is a vast subject with may interesting problems. We mention in particular the rich theory of convex projective structures developed by Goldman [Gol90], Choi-Goldman [CG97], Labourie [Lab97], Fock-Goncharov [FG07], and others. We do not attempt to give an introduction to these ideas here. Rather, we continue on to the main geometries of interest in this thesis: hyperbolic and anti de Sitter geometry. Both are specializations of projective geometry.

2.2 Hyperbolic geometry

Hyperbolic space $\mathbb{H}^n$ is the unique simply connected Riemannian manifold with constant sectional curvatures equal to negative one. Given a smooth manifold M, the data of a hyperbolic metric on M (i.e. a Riemannian metric with sectional curvatures equal to -1) is

equivalent to an (X, G) structure on M, where $X = \mathbb{H}^n$ and $G = \mathrm{Isom}(\mathbb{H}^n)$ is the group of isometries of $\mathbb{H}^n$. We study hyperbolic structures on M using the formalism described in the previous section. In this section we discuss several useful models for hyperbolic geometry, along the way reviewing a small selection of well-known facts from this vast subject. For a more thorough treatment, see [Thu80, Thu97, Rat94].

2.2.1 The hyperboloid model

Let $\mathbb{R}^{n,1}$ denote $\mathbb{R}^{n+1}$ equipped with the $(n, 1)$ Minkowski form η:

$$\eta = \begin{pmatrix} -1 & 0 \\ 0 & I_n \end{pmatrix}.$$

The hyperboloid defined by $x^T \eta x = -1$ has two sheets, distinguished by the sign of the first coordinate x_1. Commonly, hyperbolic space is taken to be the sheet with $x_1 > 0$. We choose to define $\mathbb{H}^n$ as a quotient of the two-sheeted hyperboloid by the action of $\pm I$, which identifies the two sheets.

$$\mathbb{H}^n = \{x \in \mathbb{R}^{n+1} : x^T \eta x = -1\}/\{\pm I\}.$$

The hyperboloid $x^T \eta x = -1$ inherits a Riemannian metric of constant curvature -1 from the form η. The tangent space to a point x is given by the hyperplane $x^\perp$ in $\mathbb{R}^{n,1}$ and the metric on that tangent space is the restriction of η. We also note that distances are easily calculated in the hyperboloid model by $-\cosh d(x, x') = x^T \eta x'$.

The isometries of $\mathbb{H}^n$ are exactly the isometries of η considered up to $\pm I$:

$$\mathrm{Isom}(\mathbb{H}^n) = \mathrm{PO}(n, 1) := \{A \in \mathrm{GL}(n + 1, \mathbb{R}) : A^T \eta A = \eta\}/\{\pm I\}.$$

The orientation preserving isometries are the isometries lying in the identity component of $\mathrm{PO}(n, 1)$:

$$\mathrm{Isom}^+(\mathbb{H}^n) = \mathrm{PO}_0(n, 1).$$

For n even, $\mathrm{PO}(n, 1) \cong \mathrm{SO}(n, 1)$ and $\mathrm{PO}_0(n, 1) \cong \mathrm{SO}_0(n, 1)$. For n odd, $\mathrm{PO}_0(n, 1) \cong \mathrm{PSO}(n, 1)$.

Remark 6. If we had chosen to think of $\mathbb{H}^n$ as the positive sheet of the hyperboloid $x^T \eta x$,

rather than as a quotient, we would think of $\mathrm{PO}(n,1)$ as the subgroup of $O(n,1)$ that preserves the positive sheet.

The hyperboloid model is very useful for calculating geometric quantities like lengths and angles because the metric η is easy to work with. In dimensions two and three, the upper half-space model (Sections 2.2.3 and 2.2.4) is more visually appealing and so it is usually the model of choice. For the purposes of studying geometric transitions, the projective model, next up, will be most natural.

2.2.2 The projective model

The hyperboloid model for $\mathbb{H}^n$ intersects each line in $\mathbb{R}^{n+1}$ in exactly one point or zero points. Hence, the hyperboloid model defines a domain in $\mathbb{RP}^n$, which is known as the projective model. This domain is given by

$$\mathbb{H}^n = \{x : x^T \eta x < 0\}/\text{scale}.$$

The group $\mathrm{PO}(n,1) \subset \mathrm{PGL}(n+1,\mathbb{R})$ is exactly the subgroup that preserves the domain $\mathbb{H}^n \subset \mathbb{RP}^n$. So, every hyperbolic structure is also a projective structure and we say that hyperbolic geometry is a *specialization* of projective geometry. Geodesic lines and hyperplanes in $\mathbb{H}^n$ are given by lines and hyperplanes in $\mathbb{RP}^n$ that intersect $\mathbb{H}^n$.

The *ideal boundary at infinity* $\partial^\infty \mathbb{H}^n$, given by

$$\partial^\infty \mathbb{H}^n = \{x \neq 0 : x^T \eta x = 0\}/\text{scale}$$

is precisely the boundary of (the closure of) $\mathbb{H}^n$ in $\mathbb{RP}^n$. The action of $\mathrm{PO}(n,1)$ preserves the boundary and it is often useful to describe the action of an isometry by its action on the boundary. Although $\partial^\infty \mathbb{H}^n$ does not have an invariant Riemannian metric, it does have an invariant flat conformal structure.

Proposition 4. *A geodesic in $\mathbb{H}^n$ is determined by two distinct endpoints on $\partial^\infty \mathbb{H}^n$.*

We digress here to mention an important theorem about hyperbolic structures.

Theorem 1 (Mostow Rigidity)**.** *Let M be a closed manifold of dimension $n \geq 3$. Then, if M has a hyperbolic structure, it is unique. More specifically, if M and N are two closed hyperbolic n-manifolds, then a homotopy equivalence $M \to N$ is homotopic to an isometry.*

The theorem implies, in particular, that a hyperbolic structure on a closed manifold M can not be deformed. However, a natural question is whether or not a hyperbolic structure on M can deform as a projective structure. It turns out, rather mysteriously, that sometimes it can and sometimes it can not. See [CLT07].

2.2.3 $n = 2$: the upper half-plane model

The *upper half-plane model* is perhaps the most popular model for working with two-dimensional hyperbolic geometry. It is defined as follows:

$$\mathbb{H}^2 = \{z = x + iy \in \mathbb{C} : \mathrm{Im}(z) = y > 0\}$$

with metric given by

$$h = \frac{dx^2 + dy^2}{y^2}.$$

The ideal boundary is given by $\mathbb{RP}^1 = \mathbb{R} \cup \infty$. The group of orientation preserving isometries is $\mathrm{PSL}(2, \mathbb{R})$ acting by Mobius transformations. The orientation reversing isometries are the 2×2 matrices of determinant equal to -1 acting by anti-holomorphic Mobius transformations. Hence the entire isometry group is described by $\mathrm{PGL}(2, \mathbb{R})$.

One can check fairly easily that the geodesics in this model are half-circles in the complex plane which meet the real axis at right angles. So every geodesic is determined by two endpoints on $\partial^\infty \mathbb{H}^2 = \mathbb{RP}^1$.

Definition 5. An *ideal triangle* is a geodesic triangle in $\mathbb{H}^2$ determined by three distinct vertices on the ideal boundary.

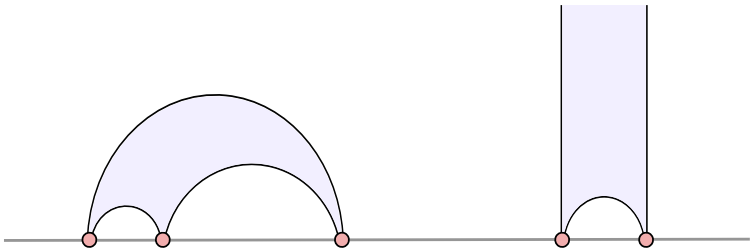

Figure 2.2: Two ideal triangles in the upper half-plane model of $\mathbb{H}^2$.

The following is an immediate corollary of the properties of Mobius transformations:

Proposition 5. *For any two ideal triangles $\triangle_1, \triangle_2$ (with labeled vertices) in $\mathbb{H}^2$, there is a unique isometry taking $\triangle_1$ to $\triangle_2$ (and preserving the labeling).*

The correspondence between the upper half-plane model and the hyperboloid (or projective model) is given, on the level of isometry groups, by the following construction. We identify $\mathbb{R}^3$ with the space of 2×2 symmetric matrices Y using the coordinates

$$Y = \begin{pmatrix} x_1 + x_2 & x_3 \\ x_3 & x_1 - x_2 \end{pmatrix}.$$

We identify $\mathrm{PGL}(2, \mathbb{R})$ with 2×2 matrices of determinant ± 1 up to multiplication by $\pm I$. Then $A \in \mathrm{PGL}(2, \mathbb{R})$ acts on $\mathbb{R}^3$ by

$$Y \mapsto AYA^T.$$

Note that the action preserves the determinant $\det Y = x_1^2 - x_2^2 - x_3^3 = -x^T \eta x$, where $x = (x_1, x_2, x_3)$. So, this gives a map $\mathrm{PGL}(2, \mathbb{R}) \to \mathrm{PO}(2, 1)$. A straightforward (but annoying) computation shows the map is an isomorphism.

2.2.4 $n = 3$: the upper half-space model

Similar to the half-plane model for $\mathbb{H}^2$, the *upper half-space model* for $\mathbb{H}^3$ is very popular for explicit computation. We define it as follows:

$$\mathbb{H}^3 = \{(x, y, z) \in \mathbb{R}^3 : z > 0\}$$

with metric given by

$$h = \frac{dx^2 + dy^2 + dz^2}{z^2}.$$

Geodesics are again half-circles meeting the boundary, $z = 0$, at right angles. Totally geodesic planes, which are isometric copies of $\mathbb{H}^2$, are half-spheres meeting the boundary at right angles. All of the isometries of a given plane extend to unique orientation preserving isometries of $\mathbb{H}^3$.

The ideal boundary $\partial^\infty \mathbb{H}^3$ can be identified with $\mathbb{CP}^1 = \mathbb{C} \cup \infty$. As the action of an isometry is determined by its action on $\partial^\infty \mathbb{H}^3$, we can describe $\mathrm{Isom}(\mathbb{H}^3)$ as a subgroup of diffeomorphisms of $\mathbb{CP}^1$. In fact, the orientation preserving isometries are given by

$\mathrm{Isom}^+(\mathbb{H}^3) = \mathrm{PSL}(2,\mathbb{C})$ acting by Mobius transformations on the ideal boundary. The orientation reversing isometries are given by another copy of $\mathrm{PSL}(2,\mathbb{C})$ acting by anti-holomorphic Mobius tranformations.

The correspondence between the upper half-space model and the hyperboloid (or projective model) is given, on the level of isometry groups, by the following construction. We identify $\mathbb{R}^4$ with the space of 2×2 Hermitian matrices Y over $\mathbb{C}$ using the coordinates

$$Y = \begin{pmatrix} x_1 + x_2 & x_3 + ix_4 \\ x_3 - ix_4 & x_1 - x_2 \end{pmatrix}.$$

Then $A \in \mathrm{PSL}(2,\mathbb{C})$ acts on $\mathbb{R}^4$ by

$$Y \mapsto AYA^*.$$

Note that the action preserves the determinant $\det Y = x_1^2 - x_2^2 - x_3^3 - x_4^2 = -x^T \eta x$, where $x = (x_1, x_2, x_3, x_4)$. So, this gives a map $\mathrm{PSL}(2,\mathbb{C}) \to \mathrm{PO}(3,1)$. A straightforward (but annoying) computation shows the map is an isomorphism onto $\mathrm{PSO}(3,1)$. In order to get all of $\mathrm{PO}(3,1)$, one must include the orientation reversing isometries, which are (as a set) another copy of $\mathrm{PSL}(2,\mathbb{C})$ acting by $Y \mapsto A\overline{Y}A^*$.

The group preserving a geodesic

In order to study *cone* singularities (in Section 4.3), we will need a description of the group that preserves a geodesic γ in $\mathbb{H}^3$. We may translate γ so that its endpoints are at 0 and ∞. Let H_γ be the subgroup of orientation preserving isometries that preserve γ and its orientation. Then H_γ consists of the Mobius transformations that preserve 0 and ∞. So each $A \in H_\gamma$ is a complex dilation by its *exponential complex length* $e^{d+i\theta}$. The quantity d gives the distance that A translates along γ, while θ gives the angle of rotation around γ. The quantities d, θ give a natural parametrization: $H_\gamma = \mathbb{R}_d \times S^1_\theta$.

Ideal tetrahedra and Thurston's Equations

Any three distinct points on $\partial^\infty \mathbb{H}^3$ determine a geodesic ideal triangle and there is a unique orientation preserving isometry of $\mathbb{H}^3$ transforming one ideal triangle to another. On the other hand, an arrangements of four points in $\partial^\infty \mathbb{H}^3$ can be transformed to another such

arrangement if and only if the arrangements share the same *cross-ratio*, defined by:

$$(t, u : v, w) = \frac{(t - v)(u - w)}{(t - w)(u - v)}$$

Definition 6. An *ideal tetrahedron* T is a geodesic tetrahedron in $\mathbb{H}^3$ determined by four distinct vertices t, u, v, w on the ideal boundary.

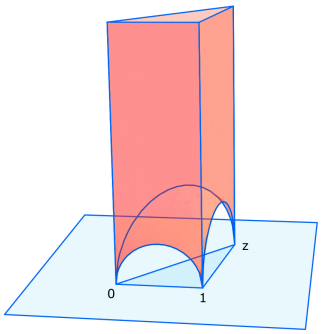

Figure 2.3: An ideal tetrahedron with one vertices $\infty, 0, 1, z$ in the upper half-space model of $\mathbb{H}^3$.

The properties of Mobius transformations immediately imply that

Proposition 6. *The cross ratio $z = (t, u : v, w)$ is a complete invariant of the isometry type (with vertices labeled) of the ideal tetrahedron T. For this reason, z is called the* shape parameter *of the tetrahedron.*

There is a nice geometric interpretation of the cross ratio, which justifies the name "shape parameter". Let e be the edge in T connecting u to t. Then $f_1 = \triangle utw$ and $f_2 = \triangle utv$ are the two faces of T that meet at e. Write the shape parameter z in polar coordinates as $z = e^d e^{i\theta}$. Then θ is the dihedral angle between the faces f_1 and f_2. Next, there are unique circles C_1, C_2 inscribed in each of the faces f_1, f_2 respectively. Then, C_1 and C_2 are tangent to the edge e at points which are distance d apart. Thus, the shape parameter z is the exponential complex length of the unique isometry which transforms f_1 into f_2. Note that, by this interpretation, the shape parameter $z = (t, u; v, w)$ really describes the geometry of the tetrahedron T from the point of view of the edge e. The shape parameters of the other five edges are determined by z according to Figure 2.4.

As the faces of an ideal tetrahedron are ideal triangles, there is a unique isometry glueing

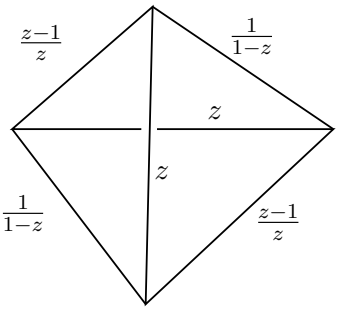

Figure 2.4: The shape parameters corresponding to the six edges of an ideal tetrahedron.

together two ideal tetrahedra along a face. Thus ideal tetrahedra in $\mathbb{H}^3$ are convenient building blocks for constructing hyperbolic structures on a three-manifold (with torus boundary). Consider ideal tetrahedra $T_1, \ldots, T_n$ that are glued together around a common edge e. The resulting identification space S has a hyperbolic structure on the complement of e. The hyperbolic structure extends over e if and only if S embeds isometrically in $\mathbb{H}^3$. That is, isometric copies of the tetrahedra must fit together neatly around an edge in $\mathbb{H}^3$. This is the case if and only if the shape parameters $z_1, \ldots, z_n$ of $T_1, \ldots, T_n$ corresponding to the edge e satisfy

$$\begin{aligned} z_1 \ldots z_n &= 1 \\ \arg z_1 + \ldots + \arg z_n &= 2\pi \end{aligned} \tag{2.2}$$

where $0 < \arg z_i < \pi$ is the dihedral angle at the edge e of tetrahedron T_i. The second condition requires that the *total dihedral angle* around e is 2π. Note that the first condition only implies that the total dihedral angle is an integer multiple of 2π. One way to see Equations 2.2 is by placing all of the tetrahedra in standard position so that the vertices of each T_i are $t_i = \infty, u_i = 0, v_i = 1, w_i = z_i$ (yes, the location of the fourth vertex *is* the shape parameter). We let the edge e correspond to 0∞. Now, the glueing maps which arrange the tetrahedra around 0∞ are given by complex dilations. To glue T_2 to T_1, we must apply dilation by z_1 to T_2. To glue T_3 to $T_1 \cup T_2$, we must apply dilation by $z_1 z_2$ to T_3. Continuing inductively, we find that the glueing map which identifies T_n to T_1 is exactly dilation by $z_1 z_2 \ldots z_n$ (see Figure 5.4).

Given a three-manifold M with a topological ideal triangulation $\mathcal{T} = \{\mathcal{T}_1, \ldots \mathcal{T}_n\}$, one way to produce hyperbolic structures on M is to realize each $\mathcal{T}_i$ as an ideal tetrahedron T_i in

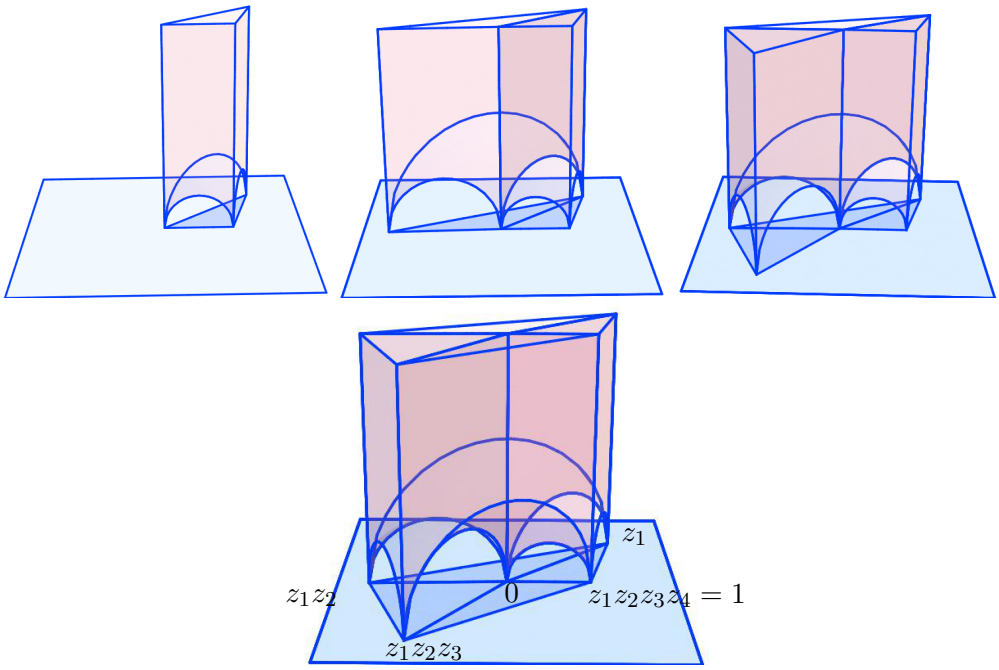

Figure 2.5: Glueing tetrahedra together around an edge.

$\mathbb{H}^3$ so that the T_i fit together correctly around each interior edge. This amounts to solving Equations 2.2 for each edge in $\mathcal{T}$. All of these equations together are called Thurston's *edge consistency equations*. The solutions make up the *deformation variety*; they parameterize the hyperbolic structures on $(M, \mathcal{T})$ with Dehn surgery type singularities (see [Thu80]). In Chapter 5, we generalize this triangulated deformation theory to build many concrete examples of geometric transitions.

Higher dimensional half-space models

As a final remark in our brief discussion of hyperbolic geometry, we mention that Ahlfors [Ahl85] constructed upper half-space models for $\mathbb{H}^n$ in higher dimensions $n \geq 4$. The construction of $\mathbb{H}^n$ uses the Clifford algebra $\mathcal{C}_{n-1}$, generated by $n-1$ square roots of -1 which pairwise anti-commute. The isometries in this model are Mobius transformations with coefficients in $\mathcal{C}_{n-2}$.

2.3 AdS geometry

Anti de Sitter (AdS) geometry is a Lorentzian analogue of hyperbolic geometry in the sense that AdS^n has all sectional curvatures equal to -1. However, the metric on AdS^n is Lorentzian, meaning it has signature $(n-1,1)$. Vectors of negative length-squared are called *time-like*, vectors of positive length-squared are called *space-like*, and non-zero vectors with zero length are called *light-like* or *null*. For basics on Lorentzian geometry, see [BEE96]. The implications of negative curvature in Lorentzian geometry are somewhat different than in Riemannian geometry. For example, AdS^n has an ideal boundary at infinity. But only space-like and light-like geodesics have endpoints on this ideal boundary. Time-like geodesics, on the other hand, are periodic. The geometry in the time-like directions acts more like a positively curved Riemannian space. We review some pertinent facts about AdS geometry, and refer the reader to [BB09] for a more thorough description.

2.3.1 The hyperboloid model

Let $\mathbb{R}^{n-1,2}$ denote $\mathbb{R}^{n+1}$ equipped with the $(n-1,2)$ Minkowski form η, which we choose to write as follows

$$\eta = \begin{pmatrix} -1 & 0 & 0 \\ 0 & I_{n-1} & 0 \\ 0 & 0 & -1 \end{pmatrix}.$$

The hyperboloid defined by $x^T\eta x = -1$ has one sheet. Nonetheless, we mimic our construction in the hyperbolic case, and define

$$\mathrm{AdS}^n = \{x \in \mathbb{R}^{n+1} : x^T\eta x = -1\}/\{\pm I\}.$$

The hyperboloid $x^T\eta x = -1$ inherits a Lorentzian metric of constant curvature -1 from the form η. The tangent space to a point x is given by the hyperplane $x^\perp$ in $\mathbb{R}^{n-1,2}$ and the metric on that tangent space is the restriction of η. We also note that distances are easily calculated in the hyperboloid model by $-\cosh d(x,x') = x^T\eta x'$. These distances can be positive, zero, or imaginary depending on whether the geodesic connecting x to x' is space-like, light-like, or time-like.

Before the quotient by $\pm I$, $\{x \in \mathbb{R}^{n+1} : x^T\eta x = -1\}$ is topologically $S^1 \times \mathbb{R}^{n-1}$. AdS^n is the $\mathbb{R}^{n-1}$ bundle over the circle with monodromy the antipodal map. So, $\pi_1 \mathrm{AdS}^n = \mathbb{Z}$

and if n is even, AdS^n is non-orientable, while if n is odd, AdS^n is orientable. In either case AdS^n is *time-orientable*. The AdS metric defines a *light-cone* in every tangent space which divides the time-like vectors into two components. Time orientable means that one component can be labeled *future* and the other component labeled *past*, and that this can be done consistently over all of AdS^n.

Remark 7. Usually, it most convenient to work with a simply connected model space. If desired, $\widetilde{\mathrm{AdS}^n}$ can be used as the model for AdS geometry. However, it turns out that the definition of AdS^n given above is geometrically most convenient to work with. For example, any two points in AdS^n are connected by a geodesic. However, this not true in $\widetilde{\mathrm{AdS}^n}$, nor is it true in the double cover $\{x \in \mathbb{R}^{n+1} : x^T \eta x = -1\}$ of AdS^n. This is similar to the case of projective geometry, where $\mathbb{RP}^n$ has nicer global geometric properties than its universal cover.

The isometries of AdS^n are the linear transformations preserving η, up to $\pm$:

$$\mathrm{Isom}(\mathrm{AdS}^n) = \mathrm{PO}(n-1,2) := \{A \in \mathrm{GL}(n+1,\mathbb{R}) : A^T \eta A = \eta\}/\{\pm I\}.$$

If n is even, this group has two components, one that preserves time-orientation and one that reverses it. In this case $\mathrm{PO}(n-1,2) \cong \mathrm{SO}(n-1,2)$. If n is odd, $\mathrm{Isom}(\mathrm{AdS}^n)$ has four components corresponding to the binary conditions orientation-preserving (or not), and time-orientation preserving (or not). The orientation preserving, time-orientation preserving subgroup is the component of the identity $\mathrm{PO}_0(n-1,2) = \mathrm{PSO}_0(n-1,2)$. The orientation preserving subgroup is $\mathrm{PSO}(n-1,2)$.

2.3.2 The projective model

The hyperboloid model for AdS^n intersects each line in $\mathbb{R}^{n+1}$ in exactly one point or zero points. Hence, the hyperboloid model projects to a domain in $\mathbb{RP}^n$, which is known as the projective model. This domain is given by

$$\mathrm{AdS}^n = \{x : x^T \eta x < 0\}/\text{scale}.$$

The group $\mathrm{PO}(n-1,2) \subset \mathrm{PGL}(n+1,\mathbb{R})$ is exactly the subgroup that preserves the domain $\mathrm{AdS}^n \subset \mathbb{RP}^n$. So, every AdS structure is also a projective structure. We say that AdS

geometry is a *specialization* of projective geometry. Geodesic lines and hyperplanes in AdS^n are given by lines and hyperplanes in $\mathbb{RP}^n$ that intersect AdS^n.

The *ideal boundary at infinity* $\partial^\infty \mathrm{AdS}^n$, given by

$$\partial^\infty \mathrm{AdS}^n = \{x \neq 0 : x^T \eta x = 0\}/\text{scale}$$

is precisely the boundary of (the closure of) AdS^n in $\mathbb{RP}^n$. The action of $\mathrm{PO}(n-1,2)$ preserves the boundary and it is often useful to describe the action of an isometry by its action on the boundary. Although, $\partial^\infty \mathrm{AdS}^n$ does not have an invariant metric, it does have a flat Lorentzian metric (of signature $(n-2,1)$) which is invariant up to a conformal factor.

Proposition 7. *The asymptotic behavior of geodesics in* AdS^n *is characterized as follows:*

- *A space-like geodesic in* AdS^n *is determined by two distinct endpoints on* $\partial^\infty \mathrm{AdS}^n$*.*
- *A light-like geodesic limits, in both directions, to the same point on* $\partial^\infty \mathrm{AdS}^n$*.*
- *A time-like geodesic is periodic (closed), with length* 2π*.*

Proof. A geodesic is represented by a two-plane in $\mathbb{R}^{n-1,2}$ which contains negative lines. If the two-plane has signature $(1,1)$, then it descends to a space-like geodesic in AdS^n. Every two plane of signature $(1,1)$ contains exactly two null-lines which represent the endpoints of the geodesic on the ideal boundary. Conversely, any two non-orthogonal null lines in $\mathbb{R}^{n-1,2}$ span a plane of signature $(1,1)$. There is no geodesic (space-like or otherwise) connecting two endpoints corresponding to orthogonal null lines within AdS^n. The plane spanned by two orthogonal (distinct) null lines descends to a null geodesic contained in the ideal boundary.

Next, a two plane which contains one null line and (many) negative lines descends to a geodesic with one endpoint on $\partial^\infty \mathrm{AdS}^n$. This geodesic is light-like: its tangent direction is null.

Finally, a two plane of signature $(0,2)$ descends to a time-like geodesic. Since every line in such a plane is negative, the projectivization of the entire plane lies inside AdS^n, and so the geodesic is a copy of $\mathbb{RP}^1$. The length computation can be done easily in the hyperboloid model. □

Another important fact which is easy to check:

Proposition 8. *Every space-like k-dimensional totally geodesic plane is isometric to $\mathbb{H}^k$. Every time-like (meaning it has negative directions) non-degenerate k-dimensional totally geodesic plane is isometric to AdS^k.*

2.3.3 $n = 3$: The $\mathrm{PSL}(2, \mathbb{R})$ model

In dimension 3, a simple change of coordinates transforms the η-norm into the determinant on 2×2 matrices. We may identify the 2×2 matrices $M(2, \mathbb{R})$ with $\mathbb{R}^{2,2}$ by associating the vector $(x_1, x_2, x_3, x_4) \in \mathbb{R}^{2,2}$ with the matrix

$$Y = \begin{pmatrix} x_1 + x_2 & x_3 + x_4 \\ x_3 - x_4 & x_1 - x_2 \end{pmatrix}.$$

Then $x^T \eta x = -\det(Y)$. Hence, we can think of the hyperboloid model of AdS^3 as the matrices of determinant equal to one up to $\pm I$:

$$\mathrm{AdS}^3 = \mathrm{PSL}(2, \mathbb{R}).$$

As we will see, this identification reveals a close connection between AdS^3 geometry and the geometry of the hyperbolic plane. The inner product induced by $-\det$ (which represents η in these coordinates) is given by:

$$\left\langle \begin{pmatrix} a & b \\ c & d \end{pmatrix}, \begin{pmatrix} e & f \\ g & h \end{pmatrix} \right\rangle = -\frac{1}{2}\mathrm{tr}\left(\begin{pmatrix} a & b \\ c & d \end{pmatrix} \begin{pmatrix} h & -f \\ -g & e \end{pmatrix} \right)$$

where $\mathrm{tr}(A)$ denotes the trace of A. The product can be expressed by

$$\langle Y, Z \rangle = -\frac{1}{2} \det(Z) \mathrm{tr}(Y Z^{-1})$$

when Z is invertible. Hence, the action of $\mathrm{PSL}(2, \mathbb{R}) \times \mathrm{PSL}(2, \mathbb{R})$ on AdS^3 defined by

$$(A, B) \cdot Y := A Y B^{-1}$$

preserves the AdS^3 metric. In fact $(A, B) \in \mathrm{GL}(2, \mathbb{R}) \times \mathrm{GL}(2, \mathbb{R})$ acts by isometries as long as $\det A = \det B = \pm 1$. Let $\mathrm{PGL}(2, \mathbb{R})^{2,+}$ be the group of (A, B) such that $\det A = \det B = \pm 1$, where A and B are each defined up to $\pm I$. The map we have described is an

isomorphism

$$\mathrm{PGL}(2,\mathbb{R})^{2,+} \to \mathrm{PSO}(2,2).$$

We note that the orientation reversing isometries in this model are given by another copy of $\mathrm{PGL}(2,\mathbb{R})^{2,+}$ acting by $\left(\begin{smallmatrix} a & b \\ c & d \end{smallmatrix}\right) \mapsto A \left(\begin{smallmatrix} d & -b \\ -c & a \end{smallmatrix}\right) B^{-1}$.

In AdS^n, the stabilizer of a point is $\mathrm{O}(n-1,1)$ which is not compact. For this reason, a discrete group $\Gamma \subset \mathrm{PO}(n-1,2)$ of isometries may or may not act properly discontinuously on AdS^n. We give an example of both possibilities in dimension $n = 3$ using the $\mathrm{PSL}(2,\mathbb{R})$ model. Let Γ_0 be a discrete subgroup of $\mathrm{PSL}(2,\mathbb{R})$ so that $\mathbb{H}^2/\Gamma_0$ is a hyperbolic surface or orbifold. Define $\Gamma = \Gamma_0 \times \{1\} = \{(\gamma, 1) : \gamma \in \Gamma_0\}$. In other words, we act on the left by Γ_0 and on the right by the identity. The action is properly discontinuous, and taking the quotient $M = \mathrm{AdS}^3/\Gamma$ gives the unit tangent bundle of the hyperbolic surface $S = \mathbb{H}^2/\Gamma_0$. In this case, the manifold AdS^3/Γ naturally has a structure modeled on $\widetilde{\mathrm{PSL}}$ geometry. $\widetilde{\mathrm{PSL}}$ is a Riemannian model space with a four-dimensional isometry group (see [Sco83]). However, from the point of view of (X, G) structures $\widetilde{\mathrm{PSL}}$ is a specialization of AdS^3 geometry: Every $\widetilde{\mathrm{PSL}}$ structure can be interpreted as an AdS^3 structure.

Remark 8. The manifold $M = \mathrm{AdS}^3/\Gamma$ is a closed Seifert fibered manifold. The AdS structure can easily be deformed, for example, by deforming the group Γ_0 in $\mathrm{PSL}(2,\mathbb{R})$. Thus the deformation space of AdS^3 structures on M includes the entire Teichmuller space of $S = \mathbb{H}^2/\Gamma_0$. In fact, there are even more deformations (see [Gol85]). Hence, the analogue of Mostow Rigidity for closed AdS^3 manifolds does not hold.

On the other hand, we can also let Γ_0 act diagonally. Let $\Gamma_\Delta = \{(\gamma, \gamma) : \gamma \in \Gamma_0\}$. The action of Γ_Δ on AdS^3 is just the action of Γ_0 on $\mathrm{PSL}(2,\mathbb{R})$ by conjugation. It is easy to see that Γ_Δ does not act discontinuously on AdS^3. For, let $\gamma \in \Gamma_0$ be of infinite order. Then $\langle(\gamma,\gamma)\rangle$ is an infinite subgroup of Γ_Δ which fixes the point $\gamma \in \mathrm{AdS}^3$. Nonetheless, there is an open domain in AdS^3 on which Γ_Δ acts discontinuously. A maximal domain of discontinuity Ω for Γ_Δ is the space of elliptics in $\mathrm{PSL}(2,\mathbb{R})$ (where A is elliptic if $|\mathrm{tr}(A)| < 2$). The quotient Ω/Γ_Δ is a basic example of a *globally hyperbolic maximal compact* AdS *space-time* (see [Mes07, ABB$^+$07]). It is topologically $\mathbb{H}^2/\Gamma_0 \times (0, 2\pi)$ and $\mathbb{H}^2/\Gamma_0 \times \{\pi\}$ is a totally geodesic surface. The other level surfaces $\mathbb{H}^2/\Gamma_0 \times \{\theta\}$ are curved space-like surfaces and have arbitrarily small diameter as $\theta \to 0$ or $\theta \to 2\pi$.

The ideal boundary

In this model, the ideal boundary is given by the rank one 2×2 matrices modulo scale factors.

$$\partial^\infty \mathrm{AdS} = \{A : \mathrm{rank}(A) = 1\}/\mathrm{scale}.$$

Any rank one matrix A can be written as

$$A = vw^T$$

where $v, w \in \mathbb{R}^2$ are vectors, uniquely determined up to scale. This gives a diffeomorphism $\partial^\infty \mathrm{AdS} \cong \mathbb{RP}^1 \times \mathbb{RP}^1$. It is more convenient to use a slightly different identification. Define the operation $w \mapsto w^\dagger$ by

$$\begin{pmatrix} a \\ b \end{pmatrix}^\dagger = \begin{pmatrix} -b & a \end{pmatrix}$$

and note that $(Bw)^\dagger = w^\dagger \det(B) B^{-1}$ (as long as B^{-1} exists). Now, any rank one matrix can be written as

$$A = vw^\dagger$$

and the vectors v, w are uniquely determined up to scale. Under this identification $\partial^\infty \mathrm{AdS} = \mathbb{RP}^1 \times \mathbb{RP}^1$, the action of $\mathrm{Isom}^+(\mathrm{AdS}) = \mathrm{PGL}(2,\mathbb{R})^{2,+}$ on $\partial^\infty \mathrm{AdS}$ is exactly the product action:

$$A(vw^\dagger)B^{-1} = (Av)(Bw)^\dagger.$$

The group preserving a geodesic

In order to study *tachyon* singularities (in Section 4.4), we will need a description of the isometries preserving a space-like geodesic. We give a few proofs in this section to demonstrate the interplay between AdS geometry and the geometry of the hyperbolic plane.

A space-like geodesic γ in AdS is determined by its endpoints (p_L, p_R) and (q_L, q_R) on $\partial^\infty \mathrm{AdS} = \mathbb{RP}^1 \times \mathbb{RP}^1$. Let H_γ be the group of orientation preserving isometries that preserve γ and its orientation. Then

$$H_\gamma = \{(A, B) \in \mathrm{PGL}(2,\mathbb{R})^{2,+} : Ap_L = p_L, Aq_L = q_L, Bp_R = p_R, Bq_R = q_R\}.$$

Let γ_L be the geodesic in $\mathbb{H}^2$ connecting p_L to q_L and let $H_{\gamma_L} \subset \mathrm{PSL}(2,\mathbb{R})$ be the subgroup

translating along γ_L. Define γ_R and H_{γ_R} similarly. Then

$$H_\gamma = H_{\gamma_L} \times H_{\gamma_R} \times \mathbb{Z}/2$$

where the $\mathbb{Z}/2$ factor is generated by the element $(\mathrm{ref}_{\gamma_L}, \mathrm{ref}_{\gamma_R})$ which reflects about γ_L in the first factor and reflects about γ_R in the second factor. The element $(\mathrm{ref}_{\gamma_L}, \mathrm{ref}_{\gamma_R})$ acts on AdS^3 as a time-orientation reversing involution that point-wise fixes γ.

Note H_γ also preserves a different geodesic $\hat{\gamma}$ which has endpoints at (q_L, p_R) and (p_L, q_R). $\hat{\gamma}$ is the *dual* of γ in the following sense:

Proposition 9. *Let P_γ and $P_{\hat{\gamma}}$ be the two-planes in $M(2,\mathbb{R})$ whose intersection with AdS^3 gives γ and $\hat{\gamma}$ respectively. Then P_γ and $P_{\hat{\gamma}}$ are orthogonal with respect to $\langle \cdot, \cdot \rangle$.*

Proof. The proposition can be easily checked because γ and $\hat{\gamma}$ are given explicitly by:

$$\begin{aligned} \gamma &= \{Y \in \mathrm{PSL}(2,\mathbb{R}) : Yp_R = p_L, Yq_R = q_L\} \\ \hat{\gamma} &= \{Z \in \mathrm{PSL}(2,\mathbb{R}) : Zp_R = q_L, Zq_R = p_L\}. \end{aligned}$$

So, if $Y \in \gamma$ and $Z \in \hat{\gamma}$, then YZ^{-1} maps $p_L \mapsto q_L$ and $q_L \mapsto p_L$. So YZ^{-1} is elliptic of order two. Hence $< Y, Z >= -\frac{1}{2}\mathrm{tr}(YZ^{-1}) = 0$. □

Suppose $(A, B) \in H_\gamma$ point-wise fixes γ and preserves time orientation. This will be the case if and only if the signed translation length a of A along γ_L is equal to the signed translation length b of B along γ_R in $\mathbb{H}^2$. The action orthogonal to γ is that of a *Lorentz boost* of *hyperbolic angle* $\varphi = a$. In general, an element of H_γ will translate along γ by a distance d and boost by a hyperbolic angle φ. The parameters d, φ are global parameters for the time-orientation preserving subgroup of H_γ.

Proposition 10. *Suppose $(A, B) \in H_\gamma$ translates by distance d along γ and acts as a Lorentz boost of hyperbolic angle φ orthogonal to γ. Then (A, B) translates by distance φ along $\hat{\gamma}$ and acts as a boost of hyperbolic angle d orthogonal to $\hat{\varphi}$. Further, if a, b are the signed translation lengths of A along γ_L and B along γ_R respectively, then*

$$\begin{aligned} d &= \frac{a-b}{2} \\ \varphi &= \frac{a+b}{2}. \end{aligned}$$

Proof. Let P_γ and $P_{\hat\gamma}$ be the planes representing γ and $\hat\gamma$ respectively in $M(2,\mathbb{R})$. Then, for any point $x \in \hat\gamma$ the plane orthogonal to the direction of $\hat\gamma$ in $T_x\,\mathrm{AdS}^3$ is exactly P_γ independent of x (and this identification is parallel along $\hat\gamma$). The action of (A,B) on P_γ is described, in an orthonormal basis, by $\begin{pmatrix}\cosh(d) & \sinh(d)\\ \sinh(d) & \cosh(d)\end{pmatrix}$, while the action on $P_{\hat\gamma}$ is described, in an orthonormal basis, by $\begin{pmatrix}\cosh(\varphi) & \sinh(\varphi)\\ \sinh(\varphi) & \cosh(\varphi)\end{pmatrix}$. The duality of translation distance and boost angle is clear.

The formulas for d,φ in terms of a,b are most easily checked by assuming $\gamma_L = \gamma_R$. In this case γ consists of all hyperbolic translations in $\mathrm{PSL}(2,\mathbb{R})$ along γ_L, while $\hat\gamma$ consists of all rotations by π about points along γ_L. For any $Y_1, Y_2 \in \mathrm{PSL}(2,\mathbb{R})$,

$$\begin{aligned} -\cosh d(Y_1,Y_2) &= -\langle Y_1, Y_2\rangle \\ &= -\frac{1}{2}\mathrm{tr}(Y_1 Y_2^{-1}) \\ &= -\cosh(\mathrm{tl}(Y_1Y_2^{-1})/2) \end{aligned}$$

where tl denotes the translation length in $\mathbb{H}^2$ (and we assume $Y_1Y_2^{-1}$ is a hyperbolic translation). Hence, for $Y_1, Y_2 \in \gamma$, $d(Y_1,Y_2)$ is half the difference of the translation lengths $(\mathrm{tl}(Y_1)-\mathrm{tl}(Y_2))/2$. For $Z_1, Z_2 \in \hat\gamma$, $d(Z_1,Z_2) = \mathrm{tl}(Z_1Z_2^{-1})/2$ is exactly the distance between the fixed points of Z_1, Z_2 in $\mathbb{H}^2$.

Now, the formulas are easily verified as for $Y \in \gamma$, $Z \in \hat\gamma$,

$$\begin{aligned} AYB^{-1} &= AB^{-1}Y \\ AZB^{-1} &= (AB)^{1/2}Z(AB)^{-1/2} \end{aligned}$$

where the last equality follows because A, B anti-commute with Z ($AZ = ZA^{-1}$). □

A half-space model for AdS

Ahlfors [Ahl85] constructed upper half-space models for hyperbolic geometry $\mathbb{H}^n$ in all dimensions. The construction of $\mathbb{H}^n$ uses the Clifford algebra $\mathcal{C}_{n-1}$, generated by $n-1$ square roots of -1 which pairwise anti-commute. Following Ahlfors, we construct a conformal half-space model for anti de Sitter three-space using generalized Clifford numbers in Appendix A. The model has some advantages over the $\mathrm{PSL}(2,\mathbb{R})$ model, the main one being that it allows

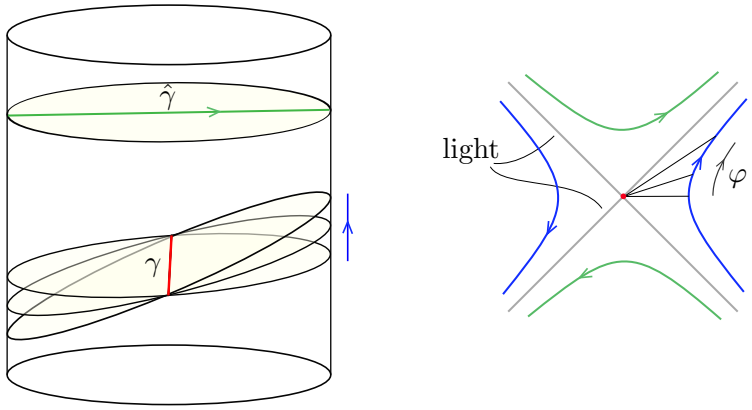

Figure 2.6: An isometry that point-wise fixes γ acts as a Lorentz boost on tangent planes orthogonal to γ (shown right) and as a pure translation along $\hat{\gamma}$.

for better visualization of the geometry.

2.4 Transversely hyperbolic foliations

Let X be a $(n-k)$-dimensional model geometry. A *transversely* (X,G) *foliation* on a manifold M^n is a smooth foliation by k-dimensional leaves so that locally the space of leaves has an (X,G) structure. More concretely, a transversely (X,G) foliation is defined by charts $\varphi_\alpha : U_\alpha \to \mathbb{R}^k \times X$ so that each transition map $\varphi_\alpha \circ \varphi_\beta^{-1} = (f,g)$ respects the product structure and acts on the first factor by a smooth function f (not necessarily defined on all of $\mathbb{R}^k$) and on the second factor by the restriction of an element $g \in G$. As we do not require the smooth functions f to be analytic, a transversely (X,G) foliation is not itself an (X',G') structure.

Consider the case $k = 1$, with $X = \mathbb{H}^{n-1}$, $G = \mathrm{Isom}(\mathbb{H}^{n-1})$. Then a transversely (X,G) structure on M is called a *transversely hyperbolic foliation*. By the same analytic continuation process described in Section 2.1, we can build a pseudo-developing map $D : \widetilde{M} \to X$, which is a local submersion equivariant with respect to a representation $\rho : \pi_1 M \to G$, again called the holonomy representation. This degenerate developing map encapsulates all of the information about the foliation and its transverse structure.

Transversely hyperbolic foliations arise as limits of degenerating hyperbolic structures. Assume for simplicity that M is orientable. Consider a path $D_t : \widetilde{M} \to \mathbb{H}^n$ of developing maps for hyperbolic structures such that $D_0 = \lim_{t\to 0} D_t$ collapses to a local submersion

onto a codimension one hyperbolic space $\mathfrak{P} \cong \mathbb{H}^{n-1}$. The limit D_0 will be equivariant with respect to the limiting holonomy representation ρ_0. The image of ρ_0 must lie in the subgroup H of $\mathrm{Isom}^+(\mathbb{H}^n)$ that preserves the plane $\mathfrak{P}$. This group H is exactly the isometries of $\mathfrak{P}$, so D_0 defines a transversely $(\mathfrak{P}, H) \cong (\mathbb{H}^{n-1}, \mathrm{Isom}(\mathbb{H}^{n-1}))$ structure on M. In the case of dimension $n = 3$, Hodgson [Hod86] studied the following *regeneration problem*:

Question. Given a transversely hyperbolic foliation $\mathcal{F}$ on a manifold M, what data is needed to produce a family of hyperbolic structures that collapse to $\mathcal{F}$.

This question and its generalization to other geometric contexts was then studied by Porti and collaborators [Por98, HPS01, Por02, Por10]. The works of Hodgson and Porti lead to natural questions about geometric transitions and are the basic motivation for the questions addressed in this thesis.

There is a notion of completeness for transversely (X, G) foliations.

Definition 7. A transversely (X, G) foliation is *complete* if its pseudo-developing map is a fibration.

Any n-manifold M with a complete dimension one transversely hyperbolic foliation has universal cover $\mathbb{R} \times \mathbb{H}^{n-1}$ with deck transformations acting by isometries in the second factor. This puts a restriction on the topology of M. The following theorem of Thurston [Thu80] classifies the topology of closed three-manifolds M that admit a transversely hyperbolic foliation:

Theorem 2 (Thurston)**.** *Suppose M^3 is a closed manifold endowed with a transversely hyperbolic foliation. Let D be a pseudo-developing map with holonomy ρ. Then one of the following holds.*

(a) The holonomy group $\rho(\pi_1 M)$ is discrete and D descends to a Seifert fibration

$$D_{/\pi_1 M} : M \to \mathbb{H}^2/\rho(\pi_1 M).$$

(b) The holonomy group $\rho(\pi_1 M)$ is not discrete, and M fibers over the circle with fiber a torus.

The case (b) of the Theorem is of particular interest. A torus bundle M with Anosov monodromy has *Sol geometry* (see, for example [Sco83]). In Sol geometry, there are two

natural projection maps to $\mathbb{H}^2$ which can be used to define two transversely hyperbolic foliations on M. In Section 6.2.3, we show how to build these hyperbolic foliations directly using *degenerate* $\mathbb{H}^2$ *ideal tetrahedra*. We study deformation varieties of singular hyperbolic foliations on torus bundles in Chapter 6.

Chapter 3

Transition theory: half-pipe structures

Our description of the transition between hyperbolic and AdS geometry hinges on the understanding of an interesting new transitional geometry, which we call *half-pipe* or HP geometry, that bridges the gap between hyperbolic and AdS geometry. Recall that we wish to construct transitions in the context of hyperbolic and anti de Sitter structures that collapse onto a co-dimension one hyperbolic space. Therefore our model for HP^n should be the "midpoint" in a family of models $\mathbb{X}_s$ which share a common embedded co-dimension one hyperbolic space. We give a natural construction of such a family of models inside of real projective geometry. Though the main focus will be the case $n = 3$, we develop this part of the theory in all dimensions $n \geq 2$.

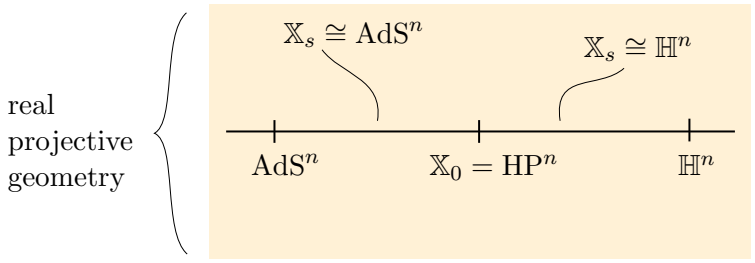

3.1 $\mathbb{H}^n$ and AdS^n as domains in $\mathbb{RP}^n$

Consider the family η_s of diagonal forms on $\mathbb{R}^{n+1}$ given by

$$\eta_s = \begin{pmatrix} -1 & 0 & 0 \\ 0 & I_{n-1} & 0 \\ 0 & 0 & \mathrm{sign}(s)s^2 \end{pmatrix}$$

where s is a real parameter and I_{n-1} represents the identity matrix. Each form η_s defines a convex region $\mathbb{X}_s$ in $\mathbb{RP}^n$ by the inequality

$$x^T \eta_s x = -x_1^2 + x_2^2 + \ldots + x_n^2 + \mathrm{sign}(s)s^2 x_{n+1}^2 < 0.$$

For each s, $\mathbb{X}_s$ is a homogeneous sub-space of $\mathbb{RP}^n$ which is preserved by the group G_s of linear transformations that preserve η_s. The usual projective model for hyperbolic geometry is given by $\mathbb{H}^n = \mathbb{X}_{+1}$, with $G_{+1} = \mathrm{PO}(n,1)$. In fact, for all $s > 0$ an isomorphism $\mathbb{X}_{+1} \to \mathbb{X}_s$ is given by the *rescaling map*

$$\mathfrak{r}_s = \begin{pmatrix} I_n & 0 \\ 0 & |s|^{-1} \end{pmatrix} \in \mathrm{PGL}(n+1, \mathbb{R}).$$

Note that $\mathfrak{r}_s$ conjugates $\mathrm{PO}(n,1)$ into G_s. Similarly, $\mathbb{X}_{-1}$ is the usual projective model for anti de Sitter geometry, AdS^n, with $G_{-1} = \mathrm{PO}(n-1,2)$. For all $s < 0$, the map $\mathfrak{r}_s$ gives an isomorphism $\mathbb{X}_{-1} \to \mathbb{X}_s$, conjugating $\mathrm{PO}(n-1,2)$ into G_s. The rescaling map $\mathfrak{r}_s$ should be thought of as a projective change of coordinates which does not change intrinsic geometric properties.

Remark 9. For $s \neq 0$, a constant curvature -1 metric on $\mathbb{X}_s$ is obtained by considering the hyperboloid model, defined by $x^T \eta_s x = -1$. In this sense, the maps $\mathfrak{r}_s$ are isometries.

There is a distinguished codimension one hyperbolic space $\mathfrak{P}^{n-1}$ defined by

$$x_{n+1} = 0 \quad \text{and} \quad -x_1^2 + x_2^2 + \ldots + x_n^2 < 0.$$

Note that $\mathfrak{P}^{n-1}$ is contained in $\mathbb{X}_s$ for all s. For $s \neq 0$, the rescaling map $\mathfrak{r}_s$ point-wise fixes $\mathfrak{P}^{n-1}$.

3.2 Rescaling the degeneration - definition of HP^n

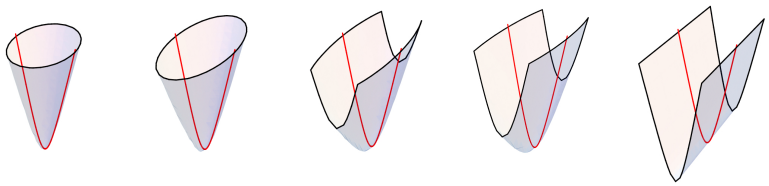

Figure 3.1: For each $s > 0$, the hyperboloid $x^T \eta_s x = -1$ gives a model for $\mathbb{H}^2$ (left four figures). As $s \to 0^+$, the limit is the hyperboloid model for HP^2 (shown right). The distinguished codimension one hyperbolic space $\mathfrak{P} \cong \mathbb{H}^1$ is shown in red.

The space $\mathbb{X}_0$ is a natural intermediary space between $\mathbb{H}^n$ and AdS^n. However, as the metric η_0 is degenerate, the full group of isometries of $\mathbb{X}_0$ makes the structure too flimsy to be of much use in our transition context. In order to determine a useful structure group for $\mathbb{X}_0$ we examine the degeneration context in which we hope to construct a transition. In this section, we will not pay close attention to technical details about collapsing.

Consider a family of developing maps

$$D_t : \widetilde{M} \to \mathbb{X}_1 \text{ with holonomy } \rho_t : \pi_1 M \to G_1 = \mathrm{SO}(n,1),$$

defined for $t > 0$. Suppose that at time $t = 0$, our developing maps collapse to D_0, a local submersion onto the co-dimension one hyperbolic space $\mathfrak{P}^{n-1}$. In particular the last coordinate x_{n+1} converges to the zero function. The holonomy representations ρ_t then converge to a representation ρ_0 with image in the subgroup $H_0 \cong \mathrm{PO}(n-1,1)$ that preserves $\mathfrak{P}^{n-1}$. The one dimensional foliation defined by the local submersion D_0 has a natural transverse $\mathbb{H}^{n-1}$ structure. The foliation together with its transverse structure is called a *transversely hyperbolic foliation* (see Section 2.4). We assume for simplicity that the the fibers of the foliation can be consistently oriented so that in particular the holonomy representation ρ_0 of the transverse structure has image in the subgroup

$$H_0^+ = \left\{ \begin{pmatrix} A & 0 \\ 0 & 1 \end{pmatrix} : A \in \mathrm{SO}(n-1,1) \right\} / \{\pm I\} \quad \cong \quad \mathrm{PSO}(n-1,1).$$

Next, apply the rescaling map $\mathfrak{r}_t$ to get the family $\mathfrak{r}_t D_t : \widetilde{M} \to \mathbb{X}_t$. This does not change the intrinsic hyperbolic geometry, but extrinsically in $\mathbb{RP}^n$ this stretches out the collapsing

direction: $\mathfrak{r}_t$ rescales the x_{n+1} coordinate by $1/t$. Let us assume that $\mathfrak{r}_t D_t$ converges as $t \to 0$ to a local diffeomorphism $\mathcal{D} : \widetilde{M} \to \mathbb{X}_0$ (see Section 3.5). The map $\mathcal{D}$ will be equivariant with respect to a representation $\rho_{\mathcal{D}} : \pi_1 M \to \mathrm{PGL}(n+1, \mathbb{R})$. This representation is the limit of the holonomy representations for the $\mathbb{X}_t$ structures determined by $\mathfrak{r}_t D_t$, which are given by the representations $\mathfrak{r}_t \rho_t \mathfrak{r}_t^{-1}$. For a particular $\gamma \in \pi_1 M$, we write

$$\rho_t(\gamma) = \begin{pmatrix} A(t) & w(t) \\ v(t) & a(t) \end{pmatrix}$$

where A is $n \times n$, $w, v^T \in \mathbb{R}^n$, and $a \in \mathbb{R}$. Then

$$\mathfrak{r}_t \rho_t(\gamma) \mathfrak{r}_t^{-1} = \begin{pmatrix} A(t) & tw(t) \\ \frac{v(t)}{t} & a(t) \end{pmatrix} \xrightarrow[t \to 0]{} \begin{pmatrix} A(0) & 0 \\ v'(0) & 1 \end{pmatrix} = \rho_{\mathcal{D}}(\gamma). \tag{3.1}$$

The special form of $\rho_{\mathcal{D}}$ motivates the following definition.

Definition 8. Define $\mathrm{HP}^n = \mathbb{X}_0$ and G_{HP} to be the subgroup of $\mathrm{PGL}(n+1, \mathbb{R})$ of matrices (defined up to $\pm I$) with the form $\begin{pmatrix} A & 0 \\ v & \pm 1 \end{pmatrix}$ where $A \in \mathrm{O}(n-1, 1)$ and $v^T \in \mathbb{R}^n$. We refer to G_{HP} as the group of *half-pipe isometries*. A structure modeled on $(\mathrm{HP}^n, G_{\mathrm{HP}})$ is called a *half-pipe structure*.

Definition 9. We say that any path of $\mathrm{O}(n, 1)$ representations ρ_t satisfying the limit (3.1) is *compatible to first order* at $t = 0$ with $\rho_{\mathcal{D}}$.

Remark 10. Both Lie algebras $\mathfrak{so}(n, 1)$ and $\mathfrak{so}(n-1, 2)$ split with respect to the adjoint action of $\mathrm{O}(n-1, 1)$ as the direct sum $\mathfrak{so}(n-1, 1) \oplus \mathbb{R}^{n-1,1}$. In both cases, the $\mathbb{R}^{n-1,1}$ factor describes the tangent directions normal to $\mathrm{O}(n-1, 1)$. The group G_{HP} is really a semi-direct product

$$G_{\mathrm{HP}} \cong \mathbb{R}^{n-1,1} \rtimes \mathrm{O}(n-1, 1)$$

where an element $\begin{pmatrix} A & 0 \\ v' & \pm 1 \end{pmatrix}$ is thought of as an infinitesimal deformation v' of the element A normal to $\mathrm{O}(n-1, 1)$ (into either $\mathrm{O}(n, 1)$ or $\mathrm{O}(n-1, 2)$).

Remark 11. We also note that the isotropy group of a point in HP^n is

$$\mathbb{R}^{n-1} \rtimes (\mathrm{O}(n-1) \times \mathbb{Z}^2).$$

The the subgroup that fixes a point and also preserves orientation and the orientation of the degenerate direction is $\mathbb{R}^{n-1} \rtimes \mathrm{SO}(n-1)$.

3.3 Example: singular torus

We give an illustrative example in dimension $n = 2$ of transitioning singular structures on a torus. Let $F_2 = \langle a, b \rangle$ be the free group on two generators. For $t > 0$ define the following representations into $G_{+1} = \mathrm{PSO}(2, 1)$:

$$\rho_t(a) = \begin{pmatrix} 3 & 2\sqrt{2} & 0 \\ 2\sqrt{2} & 3 & 0 \\ 0 & 0 & 1 \end{pmatrix}, \qquad \rho_t(b) = \begin{pmatrix} \sqrt{1+t^2} & 0 & t \\ 0 & 1 & 0 \\ t & 0 & \sqrt{1+t^2} \end{pmatrix}.$$

For small t, the commutator $\rho_t[a, b]$ is elliptic, rotating by an amount $\theta(t) = 2\pi - 2t + O(t^2)$. These representations describe a family of hyperbolic cone tori with cone angle $\theta(t)$. As $t \to 0$ these tori collapse onto a circle (the geodesic representing a). Next, we rescale this family to produce a limiting half-pipe representation:

$$\begin{aligned} \mathfrak{r}_t \rho_t(a) \mathfrak{r}_t^{-1} &= \rho_t(a) \qquad\qquad \text{(independent of } t\text{)} \\ \mathfrak{r}_t \rho_t(b) \mathfrak{r}^{-1} &= \begin{pmatrix} \sqrt{1+t^2} & 0 & t^2 \\ 0 & 1 & 0 \\ 1 & 0 & \sqrt{1+t^2} \end{pmatrix} \xrightarrow[t \to 0]{} \begin{pmatrix} 1 & 0 & 0 \\ 0 & 1 & 0 \\ 1 & 0 & 1 \end{pmatrix}. \end{aligned}$$

After applying $\mathfrak{r}_t$, the fundamental domains for the hyperbolic cone tori limit to a fundamental domain for a singular HP structure on the torus (see figure 3.2). The commutator

$$\mathfrak{r}_t \rho_t([a, b]) \mathfrak{r}_t^{-1} \xrightarrow[t \to 0]{} \begin{pmatrix} 1 & 0 & 0 \\ 0 & 1 & 0 \\ 2 & -2\sqrt{2} & 1 \end{pmatrix}$$

fixes the singular point and shears in the degenerate direction. This half-pipe isometry can be thought of as an infinitesimal rotation in $\mathbb{H}^2$.

Next consider the family of singular AdS^2 structures on the torus given by the following

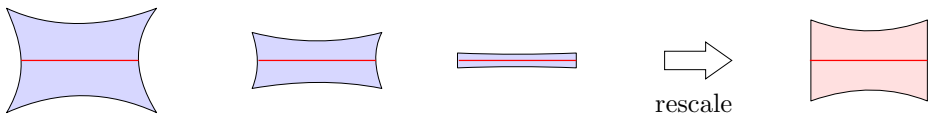

Figure 3.2: Fundamental domains for hyperbolic cone tori collapsing to a circle (shown in red). The collapsing structures are rescaled to converge to an HP structure (right).

$G_{-1} = \mathrm{PSO}(1,2)$ representations defined for $t < 0$:

$$\sigma_t(a) = \begin{pmatrix} 3 & 2\sqrt{2} & 0 \\ 2\sqrt{2} & 3 & 0 \\ 0 & 0 & 1 \end{pmatrix}, \qquad \sigma_t(b) = \begin{pmatrix} \sqrt{1-t^2} & 0 & -t \\ 0 & 1 & 0 \\ t & 0 & \sqrt{1-t^2} \end{pmatrix}.$$

Here the commutator $\sigma_t[a,b]$ acts as a Lorentz boost by hyperbolic angle $\varphi(t) = -2t + O(t^2)$ about a fixed point in AdS^2. These representations describe a family of AdS tori with a singular point of *hyperbolic angle* $\varphi(t)$. The singular point is the Lorentzian analogue of a cone point in Riemannian gometry. We describe the three-dimensional version of this singularity in more detail in Section 4.4. Again, as $t \to 0$ these tori collapse onto a circle (the geodesic representing a). Similar to the above, we have that

$$\mathfrak{r}_t \sigma_t(b) \mathfrak{r}_t^{-1} \xrightarrow[t\to 0]{} \begin{pmatrix} 1 & 0 & 0 \\ 0 & 1 & 0 \\ 1 & 0 & 1 \end{pmatrix}$$

showing that the limiting HP representation for these collapsing AdS structures is the same as for the above hyperbolic structures. So we have described a transition on the level of representations. Indeed, applying $\mathfrak{r}_t$ to fundamental domains for the collapsing AdS structures gives the same limiting HP structure as in the hyperbolic case above.

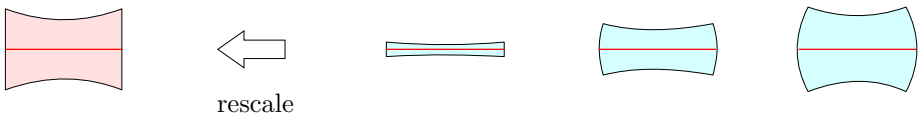

Figure 3.3: The HP structure (left) from Figure 3.2 is also the rescaled limit of AdS tori with "boost" singularities. Fundamental domains for the AdS structures are shown right.

3.4 The geometry of HP^n

Though no Riemannian metric on HP^n exists, there are some useful geometric tools for studying HP structures. To begin with, the form η_0 induces a degenerate metric on HP^n. The degenerate direction defines a foliation of HP^n by degenerate lines. These are exactly the lines of constant $x_1, \ldots, x_n$ coordinates, with x_{n+1} allowed to vary. There is a projection map $p : \mathrm{HP}^n \to \mathfrak{P}^{n-1} \cong \mathbb{H}^{n-1}$, given in coordinates by

$$p(x_1, \ldots, x_n, x_{n+1}) = (x_1, \ldots, x_n, 0)$$

which makes the foliation by degenerate lines into a (trivial) $\mathbb{R}$-bundle over $\mathbb{H}^{n-1}$. The projection commutes with the action of G_{HP} in the sense that if $g \in G_{\mathrm{HP}}$, then

$$p \circ g = \pi(g) \circ p.$$

where $\pi : G_{\mathrm{HP}} \to \mathrm{O}(n-1, 1)$ is given by $\pi \begin{pmatrix} A & 0 \\ v & \pm 1 \end{pmatrix} = A$. Thus p defines a transverse hyperbolic structure on the degenerate lines of HP^n. This transverse structure descends to any HP^n structure on a manifold M. So an HP structure on M induces a *transversely hyperbolic foliation* on M (see Section 2.4). This can be described directly with developing maps: If $D : \widetilde{M} \to \mathrm{HP}^n$ is a local diffeomorphism, equivariant with respect to $\rho : \pi_1 M \to G_{\mathrm{HP}}$, then $D_0 = p \circ D$ is a local submersion onto $\mathbb{H}^{n-1}$ which is equivariant with respect to $\pi \circ \rho : \pi_1 M \to \mathrm{O}(n-1, 1)$. Thinking of the induced transversely hyperbolic foliation, we will sometimes refer to the degenerate direction as the *fiber direction*.

Topologically, HP^n is just $\mathbb{H}^{n-1} \times \mathbb{R}$. A particularly useful diffeomorphism is given by $(p, L) : \mathrm{HP}^n \to \mathbb{H}^{n-1} \times \mathbb{R}$, where p is the projection defined above and L is defined in coordinates by

$$L(x_1, \ldots, x_n, x_{n+1}) = \frac{x_{n+1}}{x_1 \sqrt{1 - (\frac{x_2}{x_1})^2 - \cdots - (\frac{x_n}{x_1})^2}}.$$

Our choice of structure group G_{HP} makes the geometry more stiff than the geometry of the degenerate metric alone. In particular, the non-zero vector field

$$X_{fiber} = x_1 \sqrt{1 - \left(\frac{x_2}{x_1}\right)^2 - \cdots - \left(\frac{x_n}{x_1}\right)^2} \frac{\partial}{\partial x_{n+1}}$$

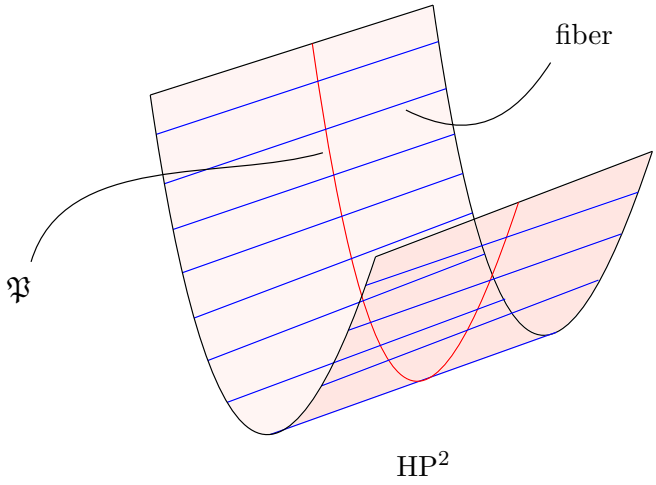

Figure 3.4: The hyperboloid model of half-pipe geometry in dimension two. The degenerate fibers (blue) foliate HP^2.

descends to $\mathrm{HP}^n \subset \mathbb{RP}^n$ and is invariant under G_{HP} up to $\pm$. It is tangent to the degenerate direction. The group G_{HP} has four components, corresponding to the conditions orientation preserving (or not) and preserving X_{fiber} (or flipping it). We denote the two components that preserve X_{fiber} by G^f_{HP}. Declaring X_{fiber} to have length one, we can measure lengths along degenerate fibers, as follows. Let $\gamma(t)$ be a path parallel to the degenerate direction, defined for $t \in [a, b]$. Then

$$\gamma'(t) \quad = \quad f(t)X_{fiber}$$

and we define

$$L_{fiber}(\gamma) \quad = \quad \int_a^b f(t)dt.$$

We note that $L_{fiber}(\gamma) = L(\gamma(b)) - L(\gamma(a))$.

Proposition 11. *$|L_{fiber}(\gamma)|$ is invariant under G_{HP}. The sign of $L_{fiber}(\gamma)$ is preserved by the subgroup G^f_{HP} that preserves the fiber direction.*

Note that we can not measure such a fiber length for a path transverse to the fiber direction because there is no invariant projection onto the fiber direction. This is the

reason that no Riemannian metric exists on HP^n.

We have already seen an example of an HP structure on the torus with a singular point. Though we have not yet given a detailed discussion of singularities in HP geometry (see Section 4.5), we show here that, at least in dimensions $n = 2$ and $n = 3$, all HP structures on closed manifolds must have singularities. This should not be surprising as HP geometry was designed for the purpose of transitioning from singular hyperbolic structures to singular AdS structures.

Proposition 12. *Let S be any closed surface. Then any* HP *structure on S must be singular.*

Proof. Suppose S has a non-singular HP structure. All elements of G_{HP} preserve the foliation of HP^2 by degenerate lines (these are lines of constant x_1, x_2 coordinate). Thus the HP structure on S defines a line field on S which is nowhere zero. So S has Euler characteristic $\chi = 0$. Hence S is either a torus or a Klein bottle. We show that no HP structure on the torus exists. It then follows that no (non-singular) HP structure could exist on the Klein bottle (as the torus double covers the Klein bottle).

Suppose $S = T^2$, with $\pi_1 S = \mathbb{Z} \times \mathbb{Z}$. We may assume that the holonomy $\rho : \pi_1 S \to G_{\mathrm{HP}}$ preserves orientation as well as the fiber direction X_{fiber} (if not, lift to a cover). Thus the holonomy lifts to a representation into $\mathrm{SL}(3, \mathbb{R})$ of the form

$$\rho(\cdot) \quad = \quad \begin{pmatrix} A(\cdot) & 0 \\ v(\cdot) & 1 \end{pmatrix}$$

where $A \in \mathrm{SO}(1,1)$ and $v \in \mathbb{R}^2$. The condition that $\pi_1 T^2$ is abelian implies (after a quick computation) that the entire representation $\rho(\pi_1 T^2)$ lies in a one parameter subgroup of the form

$$\begin{pmatrix} A(t) & 0 \\ u(A(t) - I) & 1 \end{pmatrix}.$$

Thus either the representation has non-trivial kernel or it is not discrete. This is a contradiction in light of the following lemma.

Lemma 1. *An HP^n structure on a closed manifold is complete, meaning the developing map is a diffeomorphism.*

Proof. Let $D : \widetilde{M} \to \mathrm{HP}^n$ be the developing map of an HP structure on a closed n-manifold. To show that D is a diffeomorphism, we must show D is a covering map. First, we construct product neighborhoods around points in M. Let B be an $(n-1)$-dimensional disk embedded in M, transverse to the fiber direction, such that $p \circ D$ maps (any lift of) B diffeomorphically to a disk of radius r in $\mathbb{H}^{n-1}$. Let $x \in M$ be the center of B. For some $\epsilon > 0$, the neighborhood $U_{B,\epsilon}$ of all points in M with L_{fiber} distance from B less than ϵ is an embedded ball:

$$\begin{aligned} U_{B,\epsilon} &= \{y \in M : \exists \gamma(s) \text{ tangent to the fiber, with } \gamma(0) \in B, \gamma(1) = y, L_F(\gamma) < \epsilon\}. \\ &\cong B \times (-\epsilon, \epsilon). \end{aligned}$$

By compactness, the radius r of B and the thickness ϵ can be chosen uniformly, so that every point $x \in M$ is the center of some $U_{B,\epsilon}$.

We use the neighborhoods $U_{B,\epsilon}$ to show that D has the path-lifting property. First, we show that paths along the fiber direction can be lifted. Consider a point $q = D(x)$ in the image of D and consider the fiber f in HP^n that contains q. Let J be an open interval around q in f so that J lifts to an interval I around x in $\widetilde{M}$. Let q' be an endpoint of $\overline{J}$ in HP^n. Then, let q'' be a point in J with L_{fiber} distance less than ϵ from q'. Let $y \in I$ with $D(y) = q''$. Then, there is a lifted neighborhood $\widetilde{U}_{B,\epsilon}$ around y in $\widetilde{M}$. We must have that $D(\widetilde{U}_{B,\epsilon})$ contains q'. Hence we can extend J to include q'. It follows that the entire fiber f lifts to $\widetilde{M}$. Next, consider the neighborhood $T_r(f)$ of all points in HP^n whose η_0 distance to f is less than r. Let $\widetilde{U}_{B',\epsilon}$ be a lifted product neighborhood around x. Then $D(\widetilde{U}_{B',\epsilon})$ is contained in $T_r(f)$ and intersects every fiber of $T_r(f)$ in an open interval. Hence we can lift every fiber of $T_r(f)$ to $\widetilde{M}$ and so we can lift $T_r(f)$ to $\widetilde{M}$.

Finally, let $x \in \widetilde{M}$ and let $\gamma : [0,1] \to \mathrm{HP}^n$ be any path beginning at $\gamma(0) = D(x)$. Let J be the maximal connected sub-interval of $[0,1]$ such that $\gamma(J)$ lifts to $\widetilde{M}$. Then J is open because D is a local diffeomorphism. To show J is closed, consider a sub-interval $[0,a) \subset J$. Let $a' < a$ such that $\gamma([a',a])$ is contained in the neighborhood $T_r(f)$ where f is the fiber containing $\gamma(a')$. Since $T_r(f)$ lifts to $\widetilde{M}$, it follows that we can lift $\gamma([0,a])$ to $\widetilde{M}$. So, J is closed and we must have that $J = [0,1]$. This shows that $D : \widetilde{M} \to \mathrm{HP}^n$ has the path lifting property. So D is a covering map.

□

This completes the proof of the proposition. □

In fact, the same result holds in dimension $n = 3$:

Proposition 13. *Let M be a closed three-manifold. Then any* HP *structure on M must have singularities.*

Proof. Suppose M has a (non-singular) HP structure. Without loss in generality we may assume M is orientable and that the fibers can be consistently oriented (if not lift to a finite cover). Let $D : \widetilde{M} \to \mathrm{HP}^3$ be the developing map and ρ its holonomy representation. As in the previous Proposition, we choose a lift of $\rho(\cdot)$ to $\mathrm{SL}(4, \mathbb{R})$ so that:

$$\rho(\gamma) = \begin{pmatrix} \rho_0(\gamma) & 0 \\ v(\gamma) & 1 \end{pmatrix}.$$

The projection $p \circ D : \widetilde{M} \to \mathbb{H}^2$ is a local submersion defining a transversely hyperbolic foliation with holonomy ρ_0. Now by Theorem 2 (originally from [Thu80]), there are two possibilities for M:

(a) The holonomy group $\rho_0(\pi_1 M)$ is discrete and D descends to a Seifert fibration

$$D_{/\pi_1 M} : M \to \mathbb{H}^2/\rho_0(\pi_1 M).$$

In this case, let $S = \mathbb{H}^2/\rho_0(\pi_1 M)$ denote the base surface (or orbifold) of the fibration. The generic fiber $f \in \pi_1 M$ generates the center of $\pi_1 M$. Hence, $\rho_0(f) = 1$. Next, we may interpret $v(\cdot)$ as an infinitesimal deformation of the representation ρ_0 in $\mathrm{SO}(2, 1)$. However, the deformations of ρ_0 correspond precisely to the deformations of the hyperbolic geometry of the base surface. Thus the ρ_0 component of the representation space $\mathscr{R}(\pi_1 M, \mathrm{SO}(2, 1))$ is a copy of the Teichmuller space of S. In particular, it is smooth and $f \mapsto 1$ for all representations. Hence $v(f) = 0$, and so $\rho(f) = 1$. This contradicts Lemma 1 above.

The other possibility is

(b) The holonomy group $\rho_0(\pi_1 M)$ is not discrete, and M fibers over the circle with fiber a torus.

In fact, from the proof of Theorem 2 (see [Thu80]), we can say precisely what ρ_0 looks like. $\pi_1 M$ is generated by three elements a, b, c with $\langle a, b\rangle = \mathbb{Z} \times \mathbb{Z}$ generating the torus fiber and c corresponding to the circle direction. The conjugation action of c on $\langle a, b\rangle$ is described by

an Anosov element φ of $\mathrm{SL}(2,\mathbb{Z})$:

$$\begin{aligned} \varphi &= \begin{pmatrix} m & n \\ r & s \end{pmatrix} \\ cac^{-1} &= a^m b^r \\ cbc^{-1} &= a^n b^s. \end{aligned}$$

The representation ρ_0 is reducible, mapping a, b to parabolics with fixed point Q and mapping c to a hyperbolic translation with fixed points Q, Q'. The translation length of $\rho_0(c)$ is equal to one of the eigenvalues of φ. In fact, the data of φ entirely determines the representation ρ_0 up to conjugacy. The only infinitesimal deformations of ρ_0 are infinitesimal conjugations. Thus it follows that ρ can be conjugated in G_{HP} so that $v(\cdot) = 0$. Hence, ρ is not discrete (because ρ_0 is not), and we have a contradiction by Lemma 1. □

Remark 12. We study torus bundles with Anosov monodromy in a related context in Chapter 6. We will see that the representation ρ_0 can be deformed if one allows the hyperbolic foliation to have a singularity. The deformation space of these singular hyperbolic foliations is naturally at the boundary of deformation spaces of both hyperbolic and AdS structures.

3.5 Collapsing and Rescaling

In general, a family of diffeomorphisms which collapses in the limit can exhibit complicated behavior. In the case of interest, we have developing maps $D_t : \widetilde{M} \to X$ which collapse as $t \to 0$ to a local submersion D_0 onto a co-dimension one hyperbolic plane. We wish to rescale these maps and obtain convergence to a developing map for an HP structure. Precise conditions for when such convergence can be obtained (possibly after applying a smooth path of re-parameterizations) are beyond the scope of this thesis. We explore the delicate issue of collapsing and rescaling in a future paper. In this section, we produce an HP structure from collapsing $\mathbb{H}^n$ structures under some strong assumptions about the collapse. A similar construction may be possible in the AdS setting, but we omit this case.

We consider incomplete $X = \mathbb{H}^n$ structures on a compact manifold M with boundary. The main example to keep in mind is a hyperbolic cone three-manifold with a tubular neighborhood of the singular locus removed.

In order for the rescaling process to have a chance of working correctly, we need to know that one part of the manifold is not collapsing faster than the rest. To make this more concrete, we make the following definition which generalizes the usual notion of maximal and minimal injectivity radius for a complete Riemannian manifold.

Definition 10. Let (M, g) be a compact Riemannian manifold (with or without boundary). Consider an embedded open ball $B(p, r)$ in M. We say that $B(p, r)$ is maximal if one of the following holds

1. The closure $\bar{B}(p, r)$ is no longer embedded.
2. The closure $\bar{B}(p, r)$ of B intersects the boundary ∂M.

The *maximal injectivity radius* R_{max} of (M, g) is the supremal radius r over all maximal balls $B(p, r)$. The *minimal injectivity radius* R_{min} of (M, g) is the infimal radius r over all maximal balls $B(p, r)$.

We will assume that the rate at which the minimal injectivity radius collapses is on the order of t. We construct examples of collapsing $\mathbb{H}^3$ structures using ideal tetrahedra in Chapter 5. In all of these examples, the hypotheses of the following proposition are satisfied.

Proposition 14 (Rescaling)**.** *Let M be a compact oriented n-manifold with boundary. Consider collapsing $\mathbb{H}^n$ structures defined by developing maps $D_t : \widetilde{M} \to \mathbb{H}^n$ that converge to a local submersion D_0 onto a co-dimension one hyperbolic space $\mathfrak{P}^{n-1}$. Assume the family D_t is smooth in t at $t = 0$, that the convergence is uniform in $\mathscr{C}^2$ on compacts, and that*

$$R_{min}(M, h_t) \geq ct$$

where $h_t = D_t^* h$ is the hyperbolic metric at time t. Then the limit $F : \widetilde{M} \to \mathrm{HP}^n$ of the rescaled developing maps is equivariantly homotopic to a map D, which restricts to a developing map for an HP *structure on a slightly thinner manifold $M_0 \subset M$.*

Remark 13. We note that the assumption that D_t is differentiable in t at time $t = 0$ implies an injectivity radius bound from above

$$R_{max}(M, h_t) \leq Ct$$

where C can be taken to be any number larger than the maximum norm of the derivative of D_t at $t = 0$. So our assumptions require that the injectivity radius is collapsing uniformly.

Proof. For the sake of avoiding fractions of c all over the place, we assume $c = 7$ throughout the proof. Naively, we attempt to rescale the developing maps and take the limit. Let $F : \widetilde{M} \to \mathrm{HP}^n$ be defined by

$$F(\cdot) = \lim_{t\to 0} \mathfrak{r}_t D_t(\cdot)$$

The x_{n+1} coordinate of F is just the t-derivative of the x_{n+1} coordinate of D_t, so F is well defined and $\mathscr{C}^1$. Further, F is equivariant with respect to the rescaled limit $\rho = \lim_{t\to 0} \mathfrak{r}_t \rho_t \mathfrak{r}_t^{-1}$ of the holonomy representations. However, F might not be a local diffeomorphism. Let us assume it is not.

Although F is not a local diffeomorphism everywhere, we can still use it to measure lengths along fibers in HP^n. We have $p \circ F = D_0$, where $p : \mathrm{HP}^n \to \mathfrak{P}$ is the projection defined in Section 3.4. As D_0 is a local submersion, it defines a smooth one-dimensional foliation on M (and in fact the foliation has a tranverse hyperbolic structure). Let $\gamma : [0, 1] \to M$ be a path tangent to this foliation. Define the F-length of γ by

$$L_F(\gamma) = L_{fiber}(F(\tilde{\gamma}))$$

where $\tilde{\gamma}$ is any lift of γ. Using the diffeomorphism $(p, L) : \mathrm{HP}^n \to \mathbb{H}^{n-1} \times \mathbb{R}$ defined in Section 3.4, we note that $L_F(\gamma) = L(\tilde{\gamma}(1)) - L(\tilde{\gamma}(0))$. The following is easy to check in coordinates.

Lemma 2. *$L_F(\gamma)$ can be calculated as follows. Choose any lift $\tilde{\gamma}$ to $\widetilde{M}$. Let $\hat{n}$ be the unit length vector field normal to $\mathfrak{P}^{n-1}$ pointing up out of $\mathfrak{P}$, extended via parallel translation along normal geodesics to all of $\mathbb{H}^n$. Then*

$$L_F(\gamma) = \frac{d}{dt} \int (D_t\tilde{\gamma})'(s) \cdot \hat{n}\ ds.$$

Let $\mathcal{S}$ be the set of all smooth embedded $(n-1)$-dimensional disks B in M such that D_0 maps (a lift of) B diffeomorphically onto a geodesic $(n-1)$-ball in $\mathfrak{P}$. Every point in M is contained in infinitely many of these disks, and all such disks are transverse to the fiber direction. Now for each $B \in \mathcal{S}$ define a corresponding neighborhood U_B by

$$U_B = \{p \in M : \exists \gamma(s) \text{ tangent to the fiber, with } \gamma(0) \in B, \gamma(1) = p, L_F(\gamma) < 1\}.$$

In other words U_B is the set of points with L_F distance (along fibers) to B less than one.

Lemma 3. *For each $B \in \mathcal{S}$, and for sufficiently small t, U_B lies inside a $3t$ neighborhood of B (with respect to h_t).*

Proof of Lemma. Given $B \in \mathcal{S}$, the function that measures L_F distance to B along fibers, defined on $D_0^{-1}(D_0(B))$, is continuous. So, U_B is open. Let $\widetilde{U}_B$ be a lift of U_B to the universal cover. Then $\widetilde{U}_B$ is a product of the corresponding lift $\widetilde{B}$ of B with an interval in the fiber direction, $\widetilde{U}_B = \widetilde{B} \times (-1, 1)$. $D_t(\widetilde{B})$ converges in $\mathscr{C}^2$ to a geodesic $(n-1)$ disk in $\mathfrak{P}$. Thus the normal direction to $D_t(\widetilde{B})$ is very close to $\hat{n}$ and we can use Lemma 2 to bound the distance $d_t(\cdot, \widetilde{B})$ to $\widetilde{B}$. Let $b \in \widetilde{B}$, and let $\gamma(s) = (b, s) \in \widetilde{U}_B$ be a fiber. Then, for t sufficiently small there is an $\epsilon > 0$ so that,

$$\begin{aligned} d_t(\gamma(s), \widetilde{B}) &\leq (1+\epsilon) \left| \int_{-1}^{1} (D_t \tilde{\gamma})'(u) \cdot \hat{n} \, du \right| \\ &\leq (1+\epsilon)^2 t L_F(\gamma) \\ &= 2(1+\epsilon)^2 t. \end{aligned}$$

Hence, $\widetilde{U}_B$ lies inside a $3t$ neighborhood of $\widetilde{B}$ with respect to the metric at time t. □

Lemma 4. *Every point $x \in M$ is the center of some U_B which is an embedded product neighborhood $U_B = B \times (-1, 1)$.*

Proof. Let $B \in \mathcal{S}$ with x as its center. Let $t > 0$ be such that U_B is contained in a $3t$ neighborhood of B with respect to the metric at time t. U_B may not have the desired properties. So, let B' be a sub-disk of B with diameter t. Then $U_{B'} \subset U_B$ has diameter less than or equal to $7t$. By the injectivity radius assumption, $U_{B'}$ must be embedded. In this case, the fibration is trivial. □

Now, let $B \in \mathcal{S}$ have the properties of Lemma 4 and let $\widetilde{U}_B \subset \widetilde{M}$ be a lift of U_B. Let Y be a vector field tangent to the fiber, supported in $\widetilde{U}_B$. Note that $dL_F(Y)$ may be zero at some points. These are precisely the points where F fails to be a local diffeomorphism. Next, $\widetilde{U}_B = \widetilde{B} \times (-1, 1)$, with the second factor giving coordinates along the fiber. The submersion D_0 only depends on the factor $\widetilde{B}$. By definition of U_B, $L_F(\{b\} \times (-1, 1)) = 2$. Replace L_F by a different smooth function $\mathcal{L}$ (which also measures lengths in the fiber direction) so that $d\mathcal{L}(Y)$ is non-zero, while preserving the condition $\mathcal{L}(\{b\} \times (-1, 1)) = 2$. We use the

smoothed out version to modify F on $\widetilde{U}_B$. Recall the coordinates $(p, L) : \mathrm{HP}^n \cong \mathbb{H}^{n-1} \times \mathbb{R}$ from Section 3.4. Then,

$$F(b, s) = (D_0(b), L(b) + L_F(b, s)).$$

So replace F with the local diffeomorphism $\mathcal{F}$ on $\widetilde{U}_B$

$$\mathcal{F}(b, s) = (D_0(b), L(b) + \mathcal{L}(b, s)).$$

As $\widetilde{U}_B$ maps diffeomorphically to $U_B \subset M$, we can perform this adjustment equivariantly to all lifts of U_B.

We use this process on a finite cover to produce D. Specifically, cover a thinner submanifold M_0 by finitely many $U_{B1}, \ldots, U_{Bk}$ having the properties of Lemma 4. Perform the process of smoothing out the length function along the fiber sequentially on each neighborhood U_{Bi}, one at a time. The resulting map D is a local diffeomorphism when restricted to M_0 and is still equivariant with respect to ρ. It is clear from the construction that D is homotopic to F equivariantly with respect to ρ. □

3.6 Regeneration

In this section, we show how to regenerate $\mathbb{H}^n$ and AdS^n structures from HP^n structures. We begin with a useful Lemma, familiar from Thurston's notes, about deformations of (X, G) structures.

Lemma 5. *Let M_0 be a compact n-manifold with boundary and let M be a thickening of M_0, so that $M \setminus M_0$ is a collar neighborhood of ∂M_0. Consider an (X, G) structure on M_0 which extends to M. Then any small deformation of the holonomy representation produces a nearby geometric structure on M_0.*

Proof. Let $D : \widetilde{M} \to X$ be a developing map for the given (X, G) structure on M, and let $\sigma : \pi_1 M \to G$ be the corresponding holonomy representation. Let σ_t be a path of nearby G representations such that $\sigma_t \to \sigma$. We will produce, for short time, nearby developing maps D_t with σ_t as holonomy.

Cover M_0 by finitely many open balls $U_1, \ldots, U_n \subset M$, and then choose lifts $\tilde{U}_1, \ldots, \tilde{U}_n$ to the universal cover $\widetilde{M}$. These lifts, together with all of their translates cover $\widetilde{M_0} \subset \widetilde{M}$. We may assume that D maps each $\tilde{U}_j$ diffeomorphically onto a ball in X. We define D_t as

follows: For each $\tilde{U}_j$, simply let $D_t = D$ on $\tilde{U}_j$. Now, we would like to extend to all of $\widetilde{M}_0$ equivariantly using σ_t. Of course, there is a problem: For any $\gamma \in \pi_1 M$, with $\gamma\tilde{U}_i \cap \tilde{U}_j \neq \emptyset$, it will most likely happen that $\sigma_t(\gamma)D_t\big|_{\tilde{U}_i}$ and $D_t\big|_{\tilde{U}_j}$ do not agree on the overlap. As such overlaps are finite in number, we can use standard bump function techniques to resolve this problem and produce maps $D_t : \widetilde{M}_0 \to X$ which are equivariant with respect to σ_t. Further, we can arrange that D_t depends smoothly on t and converges to D on every compact set in $\widetilde{M}_0$ in the $\mathscr{C}^1$ topology. Thus, by the inverse function theorem, D_t is a local diffeomorphism for small enough t.

□

Proposition 15 (Regeneration)**.** *Let M_0 be a compact n-manifold with boundary and let M be a thickening of M_0, so that $M \setminus M_0$ is a collar neighborhood of ∂M_0. Suppose M has an* HP *structure defined by developing map D_{HP}, and holonomy representation σ_{HP}. Let X be either $\mathbb{H}^n$ or AdS^n and let $\rho_t : \pi_1 M_0 \to \mathrm{Isom}(X)$ be a family of representations compatible to first order at time $t = 0$ with σ_{HP} (in the sense of Equation 3.1). Then we can construct a family of X structures on M_0 with holonomy ρ_t for short time.*

Proof. If $X = \mathbb{H}^3$, we take ρ_t to be defined for $t \geq 0$, while if $X = \mathrm{AdS}^3$ then we take ρ_t to be defined for $t \leq 0$. This allows us to use the notation from Section 3.1 and treat both cases at once.

The representations

$$\sigma_t := \mathfrak{r}_t \rho_t \mathfrak{r}_t^{-1} : \pi_1 M_0 \to G_t \subset \mathrm{PGL}(n+1, \mathbb{R})$$

converge, by assumption, to σ_{HP} in $\mathrm{PGL}(n+1, \mathbb{R})$. Thus, thinking of the HP structure as a projective structure, Lemma 5 above gives that for small time, we have a family of nearby projective structures with holonomies σ_t. These projective structures are given by developing maps $F_t : \widetilde{M}_0 \to \mathbb{RP}^n$ which converge (in the compact open topology) to D as $t \to 0$. We show now that F_t is the developing map for an $(\mathbb{X}_t, G_t)$ structure. We will use the following easy lemma.

Lemma 6. *Let K be a compact set and let $F_t : K \to \mathbb{RP}^3$ be any continuous family of functions. Suppose $F_0(K)$ is contained in $\mathbb{X}_s$. Then there is an $\epsilon > 0$ such that $|t| < \epsilon$ and $|r - s| < \epsilon$ implies that $F_t(K)$ is contained in $\mathbb{X}_r$.*

Consider a compact fundamental domain $K \subset \widetilde{M}_0$. $D(K)$ is a compact set contained

in $\mathrm{HP}^n = \mathbb{X}_0 \subset \mathbb{R}P^n$. By the lemma, $F_t(K)$ is also contained in $\mathbb{X}_t$ for all t sufficiently small. Now, since F_t is equivariant with respect to $\sigma_t : \pi_1 M \to G_t$, we have that the entire image of F_t is contained in $\mathbb{X}_t$. Thus (for small t), F_t determines an $\mathbb{X}_t$ structure with holonomy σ_t. Now, applying the inverse of the rescaling map gives developing maps $D_t = \mathfrak{r}_t^{-1} F_t$ into X which are equivariant with respect to $\rho_t = \mathfrak{r}_t^{-1} \sigma_t \mathfrak{r}_t$. These define the desired X structures. □

3.7 Transitions

Definition 11. Let M be an n-dimensional manifold. A *geometric transition* from $\mathbb{H}^n$ structures to AdS^n structures is a $\mathscr{C}^1$ path of projective structures $\mathscr{P}_t$ on M so that

- for $t > 0$, $\mathscr{P}_t$ is projectively equivalent to a hyperbolic structure
- for $t < 0$, $\mathscr{P}_t$ is projectively equivalent to an AdS structure.

There is no mention of half-pipe geometry in the above definition. However, the main tool for building a geometric transition is an HP structure. The following is a corollary of Proposition 15:

Theorem 3. *Let M be a compact manifold with boundary and let h_t be a path of hyperbolic (resp anti de Sitter) structures on M that degenerate to a transverse hyperbolic foliation. Suppose the h_t limit projectively (after rescaling by $\mathfrak{r}_t$) to an* HP *structure. Then a transition to anti de Sitter (resp. hyperbolic) structures can be constructed if and only if the transition can be constructed on the level of representations.*

Note that while this theorem applies in broader generality than Theorem 6 from the Introduction, it does not guarantee any control of the geometry at the boundary. We study behavior near the boundary in Chapter 4.

Chapter 4

Singular three dimensional structures

In this section, our goal is to build transitions from hyperbolic cone structures to their AdS analogues, tachyon structures. To do this, we generalize the notion of cone singularity to projective structures. Before studying the three-dimensional case, we start with a brief description of the two-dimensional case.

4.1 Cone-like singularities on projective surfaces

Consider a cone point on a Riemannian surface. The Riemannian metric is un-defined at this point, but much of the local geometry extends to the cone point. For example, there are geodesic segments connecting the cone point to all nearby points. Motivated by this, we make the following definition.

Definition 12. Let S be a surface, with $\mathfrak{o} \in S$. A *projective structure with a cone-like singularity* on $(S, \mathfrak{o})$ is a smooth (incomplete) projective structure on $S \setminus \mathfrak{o}$ determined by charts $(\varphi_\alpha, U_\alpha)$ with the following properties:

- Every chart $\varphi_\alpha : U_\alpha \to \mathbb{RP}^2$ extends continuously to the closure $\overline{U_\alpha}$.
- There are finitely many charts $(\varphi_1, U_1), \ldots, (\varphi_k, U_k)$ such that the union

$$U_1 \cup \cdots \cup U_k \cup \{\mathfrak{o}\}$$

is an open neighborhood of $\mathfrak{o}$.

$S \setminus \mathfrak{o}$ is called the *smooth part* and $\mathfrak{o}$ is called the *cone point*. Note that in the case $\overline{U_\alpha \cap U_\beta}$ contains $\mathfrak{o}$, the transition function $g_{\alpha\beta} \in \mathrm{PGL}(3,\mathbb{R})$ maps $\varphi_\beta(\mathfrak{o})$ to $\varphi_\alpha(\mathfrak{o})$.

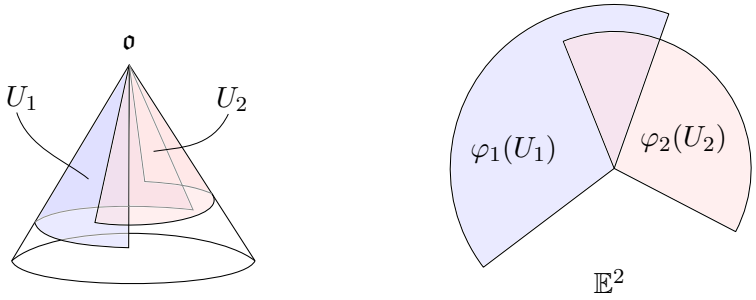

Figure 4.1: A Euclidean cone is the model example of a projective surface with a cone-like point. In this example, a neighborhood of the cone point is covered by two wedge shaped chart neighborhoods U_1, U_2. The respective charts φ_1, φ_2 map U_1, U_2 to wedges in the Euclidean plane. Each φ_i extends to $\overline{U_i}$, mapping $\mathfrak{o}$ to the corner of the wedge.

Definition 13. Let $(S, \mathfrak{o})$ and $(S', \mathfrak{o}')$ be two projective surfaces with cone-like singularities. An *isomorphism* $(S, \mathfrak{o}) \cong (S', \mathfrak{o}')$ is an isomorphism of projective structures

$$\Phi : S \setminus \mathfrak{o} \to S' \setminus \mathfrak{o}'$$

that extends continuously over $\mathfrak{o}$.

The developing map for a projective structure with a cone-like singularity extends to the cone point in the following sense.

Proposition 16. *Let $(S, \mathfrak{o})$ be a projective surface with a cone-like singularity. Let B be a small neighborhood of the cone point $\mathfrak{o}$. Then:*

- *The developing map D on $\widetilde{B \setminus \mathfrak{o}}$ extends to the universal branched cover $\widetilde{B} = \widetilde{B \setminus \mathfrak{o}} \cup \{\mathfrak{o}\}$ of B branched over $\mathfrak{o}$.*
- *The holonomy $\rho(\pi_1(B \setminus \mathfrak{o}))$ fixes $p := D(\mathfrak{o})$.*

In particular, there are "polar coordinates" $(r, x) \in (0,1) \times \mathbb{R}/\mathbb{Z}$ on B which lift to coordinates on $\widetilde{B}$ so that for a fixed x, $D(r, x)$ is a radial line segment with $\lim_{r \to 0} D(x, r) = p$.

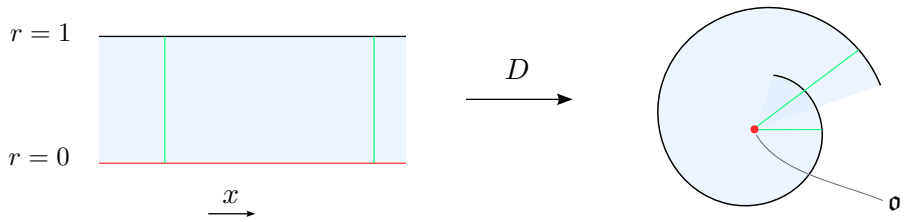

Figure 4.2: The developing map of a cone-like projective surface.

Proof. From the definition, there exist finitely many chart neighborhoods $U_1, \ldots, U_k$ whose union with $\mathfrak{o}$ forms a neighborhood of $\mathfrak{o}$ in S. Let $V_1, \ldots, V_k$ be the intersections with B. By restricting to a smaller neighborhood, we may assume that the following holds:

- $V_i \cap V_j$ is either empty or $\overline{V_i \cap V_j}$ contains $\mathfrak{o}$.

We construct the developing map using $V_1, \ldots, V_k$ by first lifting V_1 to $\widetilde{N \setminus \mathfrak{o}}$ and mapping into $\mathbb{RP}^2$ with the corresponding chart map φ_1. Then, the usual analytic continuation process defines D on the rest of $\widetilde{N \setminus \mathfrak{o}}$. Note that if $\overline{V_i \cap V_j}$ contains $\mathfrak{o}$, then the transition function g_{ij} maps $\varphi_j(\mathfrak{o})$ to $\varphi_i(\mathfrak{o})$. Hence D extends continuously to the universal branched cover $\widetilde{B}$, with $D(\mathfrak{o}) = \varphi_1(\mathfrak{o})$. The coordinates (r, x) are easily obtained by pulling back any choice of polar coordinates around p in $\mathbb{RP}^2$. □

Let G_p denote the elements of $\mathrm{PGL}(3, \mathbb{R})$ which fix p and preserve the local orientation near p. We define the *rotation angle* map $\mathcal{R} : G_p \to S^1$ as follows. Given $[A] \in G_p$, there is a representative A so that the eigenvalue corresponding to p is one. Let λ_2, λ_3 be the other eigenvalues. If $\lambda_2, \lambda_3 = \lambda, \bar{\lambda}$ are complex, then A is similar in $\mathrm{SL}(3, \mathbb{R})$ to the block diagonal form

$$A = \begin{pmatrix} 1 & 0 \\ 0 & |\lambda| R(\theta) \end{pmatrix},$$

where $R(\theta)$ rotates by angle θ in the positive direction. In this case define $\mathcal{R}(A) = e^{i\theta}$. If λ_2, λ_3 are real, then they both have the same sign and we define $\mathcal{R}(A) = \mathrm{sign}(\lambda_2)$.

Proposition 17. *The rotation angle function $\mathcal{R} : G_p \to S^1$ is a homotopy equivalence.*

Proof. A homotopy inverse for $\mathcal{R}$ is given by $e^{i\theta} \longmapsto \begin{pmatrix} 1 & 0 \\ 0 & R(\theta) \end{pmatrix}$. □

Now, consider D and ρ as in Proposition 16 and let $\gamma(t) \in \pi_1(B \setminus \mathfrak{o})$. We can find a path $g(t) \in G_p$ such that $D(\gamma(t)) = g(t) \cdot D(\gamma(0))$ with $g(0) = 1$ and $g(1) = \rho(\gamma)$. The path $g(t)$ is unique up to homotopy and defines the *lifted holonomy* $\widetilde{\rho}(\gamma) \in \widetilde{G}_p$. The lifted rotation angle map $\widetilde{\mathcal{R}} : \widetilde{G}_p \to \mathbb{R}$ defines the *total rotational part* of γ:

$$\widetilde{\mathcal{R}}(\gamma) = \widetilde{\mathcal{R}}([g(t)]).$$

The map $\widetilde{\mathcal{R}} : \pi_1(B \setminus \mathfrak{o}) \to \mathbb{R}$ is a homomorphism. Note that it does not in general extend to a representation of $\pi_1(S \setminus \mathfrak{o})$. Now take γ to be the generator of $\pi_1(B \setminus \mathfrak{o})$ that encircles $\mathfrak{o}$ in the direction consistent with the local orientation of S.

Definition 14. The quantity $\alpha := \widetilde{\mathcal{R}}(\gamma)$ is the *rotational part* of the holonomy at $\mathfrak{o}$. Note that the rotational part of the holonomy must satisfy $e^{i\alpha} = \mathcal{R}(\rho(\gamma))$. In the case that the eigenvalues of $\rho(\gamma)$ are real, α is an integer multiple of π and we call α the *discrete rotational part* of the holonomy at $\mathfrak{o}$.

In the case of a Riemannian cone point, the rotational part of the holonomy is exactly the cone angle. However, in the case that the local geometry is Lorentzian, the rotational part must be an integer multiple of π. In this case the holonomy around the cone point will be a discrete rotation plus a Lorentz tranformation.

4.2 Cone-like singularities for $\mathbb{RP}^3$ structures

We define cone-like singularities in three dimensions in a similar manner. Let N be an orientable three-manifold with $\Sigma \subset N$ an embedded circle. Let $M = N \setminus \Sigma$.

Definition 15. A *projective structure with a cone-like singularity* on (N, Σ) is a smooth projective structure on M defined by charts $(U_\alpha, \varphi_\alpha)$ such that

- Every chart $\varphi_\alpha : U_\alpha \to \mathbb{RP}^3$ extends continuously to the closure $\overline{U_\alpha}$. In the case $\overline{U_\alpha}$ contains points of Σ, we require that φ_α maps $\overline{U_\alpha} \cap \Sigma$ diffeomorphically to a segment of a line $\mathfrak{L}_\alpha$ in $\mathbb{RP}^3$.

- For every point $p \in \Sigma$, there is a neighborhood B of p and finitely many charts $(\varphi_1, U_1), \ldots, (\varphi_k, U_k)$ such that B is covered by $\overline{U_1}, \ldots, \overline{U_k}$ and for each j,

$$B \cap \Sigma \subset \overline{U_j} \cap \Sigma.$$

M is called the *smooth part* and Σ is called the *singular locus*. Note that in the case $\overline{U_\alpha \cap U_\beta}$ contains points of Σ, the transition function $g_{\alpha\beta} \in \mathrm{PGL}(3,\mathbb{R})$ maps $\mathfrak{L}_\beta$ to $\mathfrak{L}_\alpha$.

We note that a projective structure with cone-like singularities on (N,Σ) induces an $\mathbb{RP}^1$ structure on Σ, which is compatible with the projective structure on $M = N \setminus \Sigma$.

Definition 16. Let (N,Σ) and (N',Σ') be two projective three-manifolds with cone-like singularities. An *isomorphism* $(N,\Sigma) \cong (N',\Sigma')$ is an isomorphism of projective structures

$$\Phi : N \setminus \Sigma \to N' \setminus \Sigma'$$

which extends to a diffeomorphism $N \to N'$. We note that $\Phi\big|_\Sigma$ is an isomorphism of the induced $\mathbb{RP}^1$ structures on Σ and Σ'.

Proposition 18. *Let (N,Σ) be a projective manifold with a cone-like singularity. Let B be a small neighborhood of a point $p \in \Sigma$, with $\Sigma_B = \Sigma \cap B$. Then:*

- *The developing map D on $\widetilde{B \setminus \Sigma_B}$ extends to the universal branched cover $\widetilde{B} = \widetilde{B \setminus \Sigma_B} \cup \Sigma_B$ of B branched over Σ_B.*
- *D maps Σ_B diffeomorphically onto an interval of a line $\mathfrak{L}$ in $\mathbb{RP}^3$.*
- *The holonomy $\rho(\pi_1(B \setminus \Sigma_B))$ point-wise fixes $\mathfrak{L}$.*

In particular, there are "cylindrical" coordinates $(r,x,y) \in (0,1) \times \mathbb{R}/\mathbb{Z} \times (0,1)$ around Σ_B which lift to coordinates on $\widetilde{B}$ so that $\lim_{r\to 0} D(r,x,y) =: f(y)$ is a local submersion to $\mathfrak{L}$ independent of x.

Proof. From the definition of cone-like singularity we may choose B and charts $(\varphi_1, U_1), \ldots,$ (φ_k, U_k) so that

$$B = U_1 \cup \cdots \cup U_k \cup \Sigma_B$$

and $\cap_{i=1}^k \overline{U_i} = \overline{\Sigma_B}$. By restricting to a smaller neighborhood, we may assume that the following holds:

- $U_i \cap U_j$ is either empty or $\overline{U_i \cap U_j} \cap \Sigma = \overline{\Sigma_B}$.
- The U_i are arranged in order around Σ.

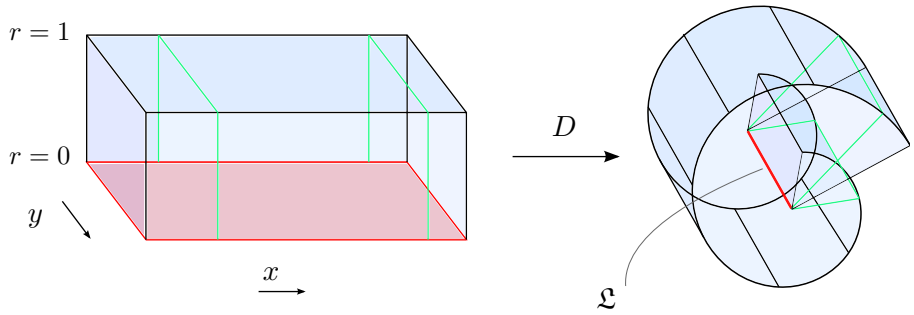

Figure 4.3: The developing map near a cone-like singularity.

We construct the developing map using $U_1, \ldots, U_k$ by first lifting U_1 to $\widetilde{B \setminus \Sigma}$ and mapping into $\mathbb{RP}^3$ with φ_1. Then, the usual analytic continuation process defines D on the rest of $\widetilde{B \setminus \Sigma}$. Note that, by our assumptions $\overline{U_i \cap U_{i+1}} \cap \Sigma$ must be non-empty, and so the transition function $g_{i,i+1}$ maps $\mathfrak{L}_{i+1}$ to $\mathfrak{L}_i$. Since $\Sigma_B \in \overline{U_i}$ for all i, D extends continuously mapping Σ_B to $\mathfrak{L}_1$ by a diffeomorphism. Hence D extends to the universal branched cover $\widetilde{B} = \widetilde{B \setminus \Sigma_B} \cup \Sigma_B$. The coordinates (r, x, y) are easily obtained by pulling back any choice of cylindrical coordinates around $\mathfrak{L}_1$ in $\mathbb{RP}^3$. □

Remark 14. The converse of the proposition is also true: Suppose there is a projective structure on M and assume that Σ is covered by neighborhoods B so that the developing map D on $\widetilde{B \setminus \Sigma}$ extends to the universal branched cover $\widetilde{B}$, mapping $B \cap \Sigma$ diffeomorphically to a line. Then it is easy to construct charts satisfying the requirements of Definition 15. So (N, Σ) is a projective structure with a cone-like singularity.

Let $G_{\mathfrak{L}}$ denote the elements of $\mathrm{PGL}(4, \mathbb{R})$ which point-wise fix $\mathfrak{L}$ and preserve orientation. We fix an orientation of $\mathfrak{L}$ and an orientation $\mathbb{RP}^3$ which determines a positive direction of rotation around $\mathfrak{L}$. Similar to the two-dimensional case. we define the *rotation angle* map $\mathcal{R} : G_{\mathfrak{L}} \to S^1$ as follows. Given $[A] \in G_{\mathfrak{L}}$, there is a representative A so that the eigenvalues corresponding to $\mathfrak{L}$ are both one. Let λ_3, λ_4 be the other eigenvalues. If $\lambda_3, \lambda_4 = \lambda, \bar{\lambda}$ are complex, then A is similar in $\mathrm{SL}(4, \mathbb{R})$ to the block diagonal form

$$A = \begin{pmatrix} I_2 & 0 \\ 0 & |\lambda| R(\theta) \end{pmatrix},$$

where $R(\theta)$ rotates by angle θ in the positive direction. In this case define $\mathcal{R}(A) = e^{i\theta}$. If

λ_3, λ_4 are real, then they both have the same sign and we define $\mathcal{R}(A) = \text{sign}(\lambda_2)$. We again have that the rotation angle function $\mathcal{R} : G_{\mathfrak{L}} \to S^1$ is a homotopy equivalence.

Now, consider D and ρ as in Proposition 18 and let $\gamma(t) \in \pi_1(B \setminus \mathfrak{L})$. We can find a path $g(t) \in G_{\mathfrak{L}}$ such that $D(\gamma(t)) = g(t) \cdot D(\gamma(0))$ with $g(0) = 1$ and $g(1) = \rho(\gamma)$. The path $g(t)$ is unique up to homotopy and defines the *lifted holonomy* $\widetilde{\rho}(\gamma) \in \widetilde{G}_{\mathfrak{L}}$. Let m be a meridian encircling Σ in the direction consistent with the local orientation of Σ. The geometry in a neighborhood of a point of Σ is determined by the lifted holonomy $\widetilde{\rho}(m)$. There is extra information contained in the lifted holonomy $\widetilde{\rho}(m)$ that is missing from $\rho(m)$: $\rho(m)$ does not detect how many times $D(m)$ winds around $\mathfrak{L}$. This information is contained in the *total rotational part* of γ defined by the lifted rotation angle map $\widetilde{\mathcal{R}} : \widetilde{G}_{\mathfrak{L}} \to \mathbb{R}$:

$$\widetilde{\mathcal{R}}(\gamma) := \widetilde{\mathcal{R}}([g(t)]).$$

The map $\widetilde{\mathcal{R}} : \pi_1 B \setminus \Sigma \to \mathbb{R}$ is a homomorphism. Note that it does not in general extend to a representation of $\pi_1 M$.

Definition 17. The quantity $\alpha := \widetilde{\mathcal{R}}(m)$ is the *rotational part* of the holonomy at $\mathfrak{L}$. Note that the rotational part of the holonomy must satisfy $e^{i\alpha} = \mathcal{R}(\rho(\gamma))$. In the case that the eigenvalues of $\rho(\gamma)$ are real, α is an integer multiple of π and we call α the *discrete rotational part* of the holonomy at $\mathfrak{L}$.

Remark 15. One motivating example behind the definition of cone-like singularities is that of cone singularities in a uniform Riemannian geometry. In that case, the rotational part of the holonomy at Σ is exactly the cone angle and determines the local geometry entirely. However, in this more general setting, there can be many geometrically different cones with the same rotational holonomy.

Remark 16. A projective structure with cone-singularities along a multiple component link Σ can be defined analogously. Over the next few sections we will assume Σ has one component; this will be the case in the main theorem we are heading towards, and it also keeps the discussion tidy. However, all of the basic theory we develop can easily be extended to the multiple component case.

4.3 Cone singularities in $\mathbb{H}^3$

Let N be a closed oriented three-manifold, with Σ a knot in N. Let $M = N \setminus \Sigma$. Recall the definition of a hyperbolic cone-manifold:

Definition 18. A *hyperbolic cone structure* on (N, Σ) is given by a smooth hyperbolic structure on M such that the geodesic completion is topologically N. The singular locus Σ is totally geodesic and the holonomy of a meridian m around Σ is a rotation.

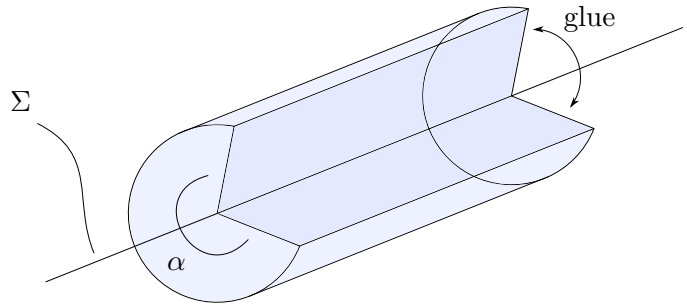

Figure 4.4: Schematic of a cone singularity in $\mathbb{H}^3$ (or any Riemannian model geometry). Perpendicular to the singular locus, the geometry is that of a cone-point on a surface.

Consider a tubular neighborhood T of Σ. The developing map D on $\widetilde{T \setminus \Sigma}$ extends to the geodesic completion $\widetilde{T \setminus \Sigma} \cup \widetilde{\Sigma}$, which is the universal branched cover of T branched over Σ. The image $D(\widetilde{\Sigma})$ is a one-dimensional set in $\mathbb{H}^3$ which must be fixed point-wise by the holonomy $\rho(m)$ of a meridian m around Σ. We will assume $\rho(m)$ is non-trivial. Then $\rho(m)$ is a rotation about a geodesic $\mathfrak{L}$ in $\mathbb{H}^3$ and D maps $\widetilde{\Sigma}$ isometrically onto $\mathfrak{L}$ (this is one sense in which Σ is totally geodesic). Hence from Remark 14:

Proposition 19 (cone singularities are cone-like)**.** *The underlying projective structure of a hyperbolic cone structure on* (N, Σ) *has a cone-like singularity at* Σ*.*

We denote the group of rotations around $\mathfrak{L}$ by $G_{\mathfrak{L}}$. The fundamental group $\pi_1 T \setminus \Sigma$ is generated by the meridian m and a longitude ℓ (which runs once around Σ). $\rho(\pi_1 T \setminus \Sigma)$ must lie in the group $H_{\mathfrak{L}}$ of isometries that preserve $\mathfrak{L}$, the orientation of $\mathfrak{L}$, and the orientation of $\mathbb{H}^3$. Note that $H_{\mathfrak{L}}$ is a product

$$H_{\mathfrak{L}} = G_{\mathfrak{L}} \times \mathcal{T}_{\mathfrak{L}}$$

where $\mathcal{T}_{\mathfrak{L}}$ is the subgroup of pure translations along $\mathfrak{L}$ (See Section 2.2.4). The longitude $\rho(\ell)$ must have non-trivial translational part, for the translational part of $\rho(\ell)$ determines

the length of Σ. It follows that $\pi_1(T \setminus \Sigma) \hookrightarrow \pi_1 M$. In general $\rho(\ell)$ may also have some rotational part.

The local geometry at points of Σ is determined by the *cone angle* α at Σ. Consider a ray orthogonal to Σ, and based at a point $p \in \Sigma$. Then α is the total angle that the ray must rotate through in order to rotate exactly once around Σ. It can be defined to be the rotational part of the holonomy around Σ as in Defintion 17.

Although the hyperbolic metric is not defined on the tangent spaces of points on Σ, much of the local geometry extends up to Σ. For example, for any point q nearby Σ, there is a unique length minimizing geodesic segment connecting q to Σ. This segment meets Σ at a right angle. Let C_p denote the union of all sufficiently short rays that are perpendicular to Σ at a given point p. Then $C \setminus p$ is a totally geodesic embedded hyperbolic surface. The geometry of C_p is exactly that of a two-dimensional hyperbolic cone with cone angle α. For varying p in a small interval $\mathcal{I}$ of Σ, the disks C_p are naturally identified with one another via parallel translation along Σ.

Let $\mathcal{W}$ be a geodesic wedge in C_p with angle $\beta < \alpha, 2\pi$. Define the *product wedge* U as the union of all translates of $\mathcal{W}$ along $\mathcal{I}$. U maps isometrically into the region in $\mathbb{H}^3$ defined in cylindrical coordinates (z, r, θ) around $\mathfrak{L}$ by $0 < \theta < \beta$, $0 < z < L$, where L is the length of $\mathcal{I}$. By covering C_p by wedges $\mathcal{W}_1, \ldots, \mathcal{W}_k$, we construct product wedge charts $\varphi_i : (U_i, \mathcal{I}) \to (\mathbb{H}^3, \mathfrak{L})$ with the desired properties at $\mathcal{I}$ (as in Definition 15). We can do this for every interval $\mathcal{I}$ in Σ. Note that all transition maps will lie in $H_{\mathfrak{L}}$.

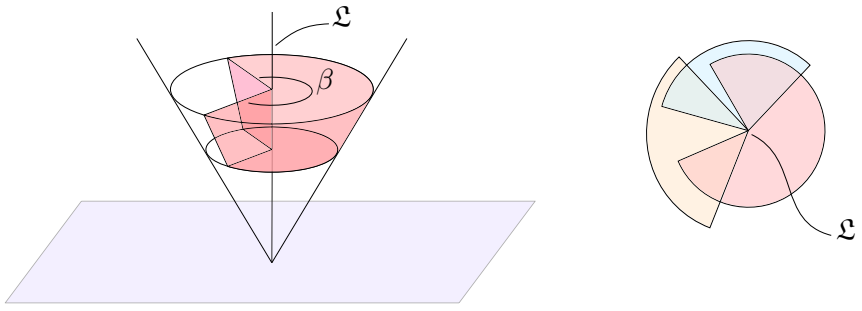

Figure 4.5: Left: A product wedge in $\mathbb{H}^3$, drawn in the upper half-space model. A local neighborhood around a point on the singular locus is covered by product wedge charts. Right: A perpendicular cross section is covered by two-dimensional wedges.

Alternatively, we can construct the geometry around an interval $\mathcal{I}$ by dividing a neighborhood of $\mathcal{I}$ into product wedges which meet only along their faces. Thus the local geometry of a hyperbolic cone singularity is modeled on the union of finitely many product wedges in $\mathbb{H}^3$ glued together along their faces. In the case that the cone angle $\alpha < 2\pi$, this construction can be performed with just one wedge.

4.4 Tachyons in AdS^3

Let N be a closed three-manifold, with Σ a knot in N. Let $M = N \backslash \Sigma$. We give the following definition of an AdS^3 manifold with tachyon singularities. Barbot-Bonsante-Schlenker give an equivalent definition in [BBS09] as well as a detailed discussion of tachyons and other singularities in AdS.

Definition 19. An AdS^3 *structure on N with a tachyon at Σ* is given by a smooth AdS^3 structure on M such that the geodesic completion is topologically N. The singular locus Σ is required to be space-like, and the local future and local past at points of Σ must each be connected and non-empty.

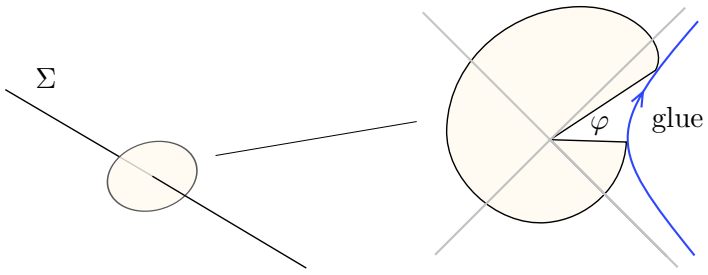

Figure 4.6: Schematic of a tachyon singularity in AdS^3. The geometry orthogonal to the space-like singular locus can be constructed by glueing a wedge in AdS^2 together with a Lorentz boost. The glueing depicted produces a tachyon of mass $-|\varphi|$.

Consider a tubular neighborhood T of Σ. The developing map D on $\widetilde{T \setminus \Sigma}$ extends to the geodesic completion $\widetilde{T \setminus \Sigma} \cup \widetilde{\Sigma}$, which is the universal branched cover of T branched over Σ. The image $D(\widetilde{\Sigma})$ is (locally) a one-dimensional set in AdS^3 which must be fixed by the holonomy $\rho(m)$ of a meridian m around Σ. Assuming $\rho(m)$ is non-trivial, it point-wise

fixes a geodesic $\mathfrak{L}$ in AdS^3 and D maps $\widetilde{\Sigma}$ isometrically onto $\mathfrak{L}$ (this is one sense in which Σ is totally geodesic). Hence, by Remark 14:

Proposition 20 (tachyons are cone-like)**.** *The underlying projective structure of an* AdS *structure with a tachyon on* (N, Σ) *has a cone-like singularity at* Σ*.*

By definition, $\mathfrak{L}$ is required to be *space-like*. The group $G_{\mathfrak{L}}$ of isometries fixing a space-like geodesic is isomorphic to $\mathbb{R}$. It is non-compact, in contrast to the Riemannian case. An element A of $G_{\mathfrak{L}}$ acts as a *Lorentz boost* on each (time-like) tangent plane $\mathfrak{L}^{\perp}$ perpendicular to $\mathfrak{L}$. We choose an orientation of $\mathfrak{L}$ which then determines an orientation on the tangent planes $\mathfrak{L}^{\perp}$. The *hyperbolic angle* φ is determined by

$$\cosh \varphi =< v, Av >$$

where $v \in \mathfrak{L}^{\perp}$ is any space-like unit vector. The sign of φ is determined from the orientation of $\mathfrak{L}^{\perp}$ by the convention: $\varphi > 0$ if $\{v, Av\}$ matches the orientation of $\mathfrak{L}^{\perp}$. The *tachyon mass* is the hyperbolic angle of $\rho(m)$, provided that m is chosen to wind around Σ in the direction consistent with the chosen orientation of $\mathfrak{L}$. Note that if the opposite orientation of $\mathfrak{L}$ is chosen, the sign of the tachyon mass remains unchanged.

The holonomy representation ρ must map $\pi_1 T \setminus \Sigma = \langle m, \ell \rangle$ into the group $H_{\mathfrak{L}}$ of isometries of AdS^3 that preserve $\mathfrak{L}$, the orientation of $\mathfrak{L}$, and the orientation of AdS^3 (See Section 2.3.3). Note that $H_{\mathfrak{L}}$ is a product

$$H_{\mathfrak{L}} = G_{\mathfrak{L}} \times \mathcal{T}_{\mathfrak{L}} \times \mathbb{Z}/2$$

where $\mathcal{T}_{\mathfrak{L}}$ is the subgroup of pure translations along $\mathfrak{L}$ and the $\mathbb{Z}/2$ factor is a rotation by π around $\mathfrak{L}$ that reverses time orientation. The longitude $\rho(\ell)$ must have non-trivial translational part, for the translational part of $\rho(\ell)$ determines the length of Σ. It follows that $\pi_1 T \setminus \Sigma$ injects into $\pi_1 M$. Note that in general $\rho(\ell)$ may also have a component in $G_{\mathfrak{L}}$ and may rotate by π.

The local geometry at points of Σ is determined by the lifted holonomy $\widetilde{\rho}(m)$. We know that $\rho(m)$ is a Lorentz boost by the tachyon mass φ. Hence, to determine the geometry we just need to determine the discrete rotational part of the holonomy around Σ.

Proposition 21. *The discrete rotational part of the holonomy around* Σ *is* 2π *(in the sense of Definition 17).*

Proof. This follows from the condition that the local future and local past at points of Σ must be connected and non-empty. Choose a representative $m(t)$ for the meridian so that for every t, $m(t)$ lies on a ray orthogonal to Σ emanating from p. Then $D(m(t))$ lies entirely in the plane $\mathfrak{L}^\perp$ orthogonal to $\mathfrak{L}$ at the point $q = D(p)$. As the future of p and the past of p each have one component, $D(m(t))$ crosses the four light-like rays emanating from q in $\mathfrak{L}^\perp$ exactly once (counted with sign). □

As in the hyperbolic case, many local geometric quantities are defined at Σ. In a neighborhood of Σ, the union of rays orthogonal to Σ at a point $p \in \Sigma$ forms a totally geodesic disk C_p. The geometry of C_p is that of a disk in AdS^2 with a cone-like point (see Figure 4.6 and 4.8). For varying p in a small interval $\mathcal{I}$ of Σ, the disks C_p are naturally identified with one another via parallel translation along Σ. This defines a product tubular neighborhood of $\mathcal{I}$, foliated by the singular disks C_p. There are four light like rays emanating from p which divide C_p into four regions. Two of the regions are unions of time-like rays, while the other two are unions of space-like rays. Locally, one of the time-like regions can be labeled as the future of p, and the other as the past of p. Let $\mathcal{W}$ be a geodesic wedge in C_p bounded by two geodesic rays. The *product wedge* U is again defined as the

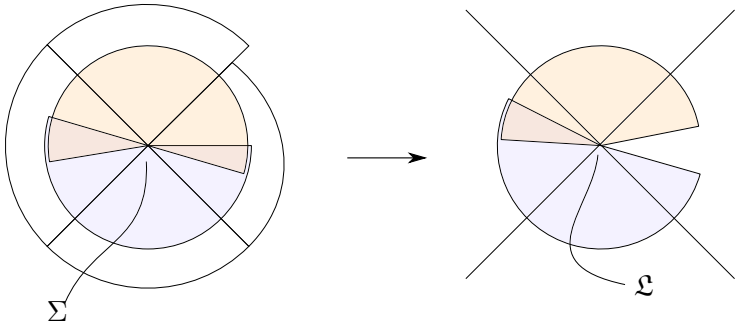

Figure 4.7: A neighborhood of a point on the singular locus is covered by two space-like product wedges. These are mapped to product wedges along $\mathfrak{L}$ in AdS^3 by the developing map. The tachyon mass is negative in this picture.

union of all translates of $\mathcal{W}$ along $\mathcal{I}$. As long as $\mathcal{W}$ is small enough, U maps isometrically to a model product wedge along $\mathfrak{L}$ in AdS^3. By covering C_p by wedges $\mathcal{W}_1, \ldots, \mathcal{W}_k$, we construct product wedge charts $\varphi_i : (U_i, \mathcal{I}) \to (\mathrm{AdS}, \mathfrak{L})$ with the desired properties at $\mathcal{I}$ (as in Definition 15). In fact two wedges are enough in this case. We can do this for every

interval $\mathcal{I}$ in Σ. Note that all transition maps will lie in $H_{\mathfrak{L}}$.

Alternatively, we can construct the geometry around an interval $\mathcal{I}$ by dividing a neighborhood of $\mathcal{I}$ into product wedges which meet only along their faces. Thus the local geometry of a tachyon is modeled on the union of finitely many product wedges in AdS^3 glued together along their faces. Note that two wedges may only be glued together if the signature of the metric is the same along the faces to be glued. In the case that the mass $\varphi < 0$, this construction can be performed with one wedge that has space-like faces. If the mass $\varphi > 0$, this construction can be performed with one wedge that has time-like phases. In either case, there is a useful alternative model. Construct a "wedge" $\mathcal{W}$ by cutting a slit in the

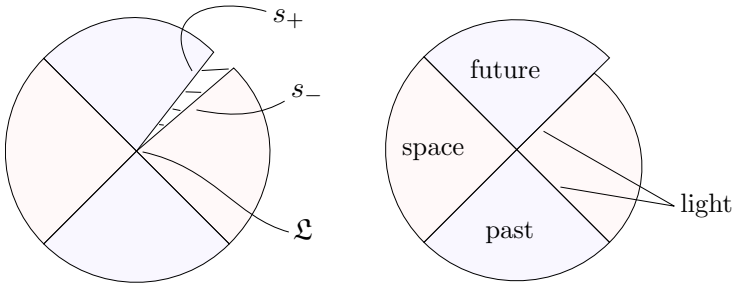

Figure 4.8: A two-dimensional cross-section of a tachyon can be constructed by cutting along a light-like ray and then glueing back together with a Lorentz boost, which act as a dilation along the ray. The figure depicts a tachyon of *negative mass*. This construction should be compared with the construction of Figure 4.6, which produces the same geometry.

disk C_p along a light-like ray r emanating from p. We let r_+ and r_- denote the two sides of the slit which are identified in C_p. Then $\mathcal{W}$ embeds via the developing map in the plane perpendicular to $\mathfrak{L}$ at the point $q = D(p)$. $D(\mathcal{W})$ is slit along the light-like ray s emanating from $q = D(p)$. We denote the two sides of the slit by s_+ and s_-. The identification of r_- with r_+ in C_p corresponds to glueing s_- to s_+ using a Lorentz boost of hyperbolic angle φ as depicted in Figure 4.8. Note that the action of the boost on the ray s_- is dilation by e^{φ}. A model for a tachyon is given by the product of this construction with the space-like geodesic $\mathfrak{L}$.

Remark 17 (Generalized tachyons)**.** A more general class of singularities is produced if we allow for the points of Σ to have disconnected local future and/or local past. These *generalized tachyons* are determined by a hyperbolic angle φ and a discrete rotational part of the holonomy equal to $k\pi$, where $k \neq 0$ could be any non-zero integer. In the case that k is odd, the resulting AdS structure will not be locally time-orientable.

4.5 Infinitesimal cone singularities in HP^3

In order to develop a theory of geometric transitions with singularities, we consider HP structures with a singularity that is cone-like with respect to the underlying projective structure. These singularities arise naturally as rescaled limits of collapsing neighborhoods of cone singularities (resp. tachyons) in $\mathbb{H}^3$ (resp. AdS^3).

Definition 20. Let N be an oriented three-manifold with $\Sigma \subset N$ a knot. Let $M = N \setminus \Sigma$. An HP structure with *infinitesimal cone singularity* on (N, Σ) is a smooth HP structure on M whose underlying projective structure has a cone-like singularity at Σ. Further, we require that there are exactly two degenerate rays emanating from each point of Σ. Hence Σ is a non-degenerate line and the discrete rotational part of the holonomy around Σ is 2π.

In this section, we describe model neighborhoods around an infinitesimal cone singularity using the HP geometry. We will show that the local geometry of any infinitesimal cone singularity is realized as the rescaled limit of a model collapsing neighborhood of a cone (resp. tachyon) singularity in hyperbolic (resp. AdS) geometry. We begin by demonstrating this on the level of holonomy representations.

Let T be a solid torus with core curve Σ and assume that T has an HP structure with infinitesimal cone singularity at Σ. Let m be a meridian encircling Σ in the positive direction with respect to the orientation of Σ. If the holonomy $\rho(m)$ is trivial, then the HP structure extends smoothly over Σ, i.e. there is no singularity. This follows from the requirement that the rotational part of the holonomy around Σ be 2π. So, we assume that $\rho(m)$ is non-trivial. Then $\rho(m)$ lies in the group $G_{\mathfrak{L}}$ of HP isometries that fix a non-degenerate line $\mathfrak{L}$ and preserve both orientation and the direction along degenerate fibers. The holonomy $\rho(\ell)$ of a longitude ℓ will lie in the group $H_{\mathfrak{L}}$ of HP isometries that preserve $\mathfrak{L}$, the orientation of $\mathfrak{L}$, and the orientation of HP^3.

By conjugating in G_{HP}, we may assume $\rho(m)$ and $\rho(\ell)$ have the following forms:

$$\rho(m) = \begin{pmatrix} 1 & 0 & 0 & 0 \\ 0 & 1 & 0 & 0 \\ 0 & 0 & 1 & 0 \\ 0 & 0 & \omega & 1 \end{pmatrix} \quad , \quad \rho(\ell) = \begin{pmatrix} \cosh d & \sinh d & 0 & 0 \\ \sinh d & \cosh d & 0 & 0 \\ 0 & 0 & \pm 1 & 0 \\ 0 & 0 & \mu & \pm 1 \end{pmatrix}.$$

The general form of $\rho(m)$ describes $G_{\mathfrak{L}} \cong \mathbb{R}_\omega$, while the general form of $\rho(\ell)$ describes

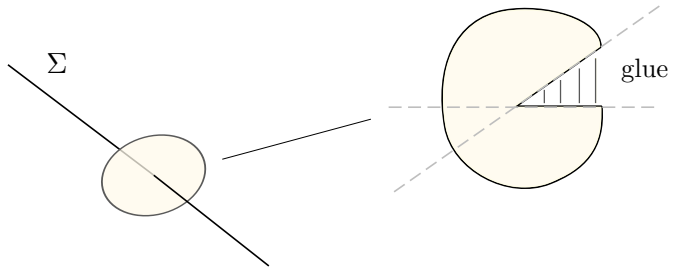

Figure 4.9: Orthogonal to the singular locus, the geometry can be constructed by glueing together the two non-degenerate boundary rays of a wedge with an infinitesimal rotation.

$H_{\mathfrak{L}} \cong \mathbb{R}_d \times \mathbb{R}_\omega \times \mathbb{Z}/2$. The $\mathbb{R}_d$ factor consists of pure translations along $\mathfrak{L}$ and the $\mathbb{Z}/2$ factor is a rotation by π around $\mathfrak{L}$ which reverses direction along degenerate fibers. We will see how to interpret the $\mathbb{R}_\omega$ factor shortly. Recall that there is a hyperbolic plane $\mathfrak{P}^2 \subset \mathrm{HP}^3$, which we think of as simultaneously lying in each of our family of models $\mathbb{X}_s$ (refer to Section 3.1 for notation). Note that if $\rho(m), \rho(\ell)$ are in the form given above, then the preserved line $\mathfrak{L}$ lies in $\mathfrak{P}$. If ρ is the limit of rescaled $\mathrm{PO}(3,1)$ representations ρ_t, then assuming that $\mathfrak{L}$ lies in $\mathfrak{P}$ corresponds to assuming that the axis of $\rho_t(m), \rho_t(\ell)$ in $\mathbb{H}^3$ lies in $\mathfrak{P}$ (at least to first order). Without loss in generality we will assume this throughout the section.

It is easy to construct a path $\rho_t : \langle m, \ell \rangle \to \mathrm{PO}(3,1)$ whose rescaled limit agrees with ρ. Define the path as follows:

$$\rho_t(m) = \begin{pmatrix} 1 & 0 & 0 & 0 \\ 0 & 1 & 0 & 0 \\ 0 & 0 & \cos\omega t & -\sin\omega t \\ 0 & 0 & \sin\omega t & \cos\omega t \end{pmatrix}, \quad \rho_t(\ell) = \begin{pmatrix} \cosh d & \sinh d & 0 & 0 \\ \sinh d & \cosh d & 0 & 0 \\ 0 & 0 & \pm\cos\mu t & -\sin\mu t \\ 0 & 0 & \sin\mu t & \pm\cos\mu t \end{pmatrix}.$$

These representations describe hyperbolic cone structures on a tubular neighborhood of Σ with cone angles approaching 2π. One easily checks that conjugating ρ_t by the rescaling

map $\mathfrak{r}_t$ produces the desired limit as $t \to 0$. For example:

$$\mathfrak{r}_t \rho_t(m) \mathfrak{r}_t^{-1} = \begin{pmatrix} 1 & 0 & 0 & 0 \\ 0 & 1 & 0 & 0 \\ 0 & 0 & \cos \omega t & -t \sin \omega t \\ 0 & 0 & \sin \omega t / t & \cos \omega t \end{pmatrix} \xrightarrow[t \to 0]{} \begin{pmatrix} 1 & 0 & 0 & 0 \\ 0 & 1 & 0 & 0 \\ 0 & 0 & 1 & 0 \\ 0 & 0 & \omega & 1 \end{pmatrix}.$$

The quantity ω describes the first order change in rotation angle of $\rho_t(m)$ at $t = 0$. Hence we call $\rho(m)$ an *infinitesimal rotation*. We note that if $\omega > 0$, the cone angle of nearby hyperbolic cone structures must be increasing, while if $\omega < 0$, the cone angle of nearby hyperbolic structures will be decreasing.

Definition 21. The *infinitesimal cone angle* around Σ is defined to be the quantity ω. Note that the sign is well-defined and that the lifted holonomy $\widetilde{\rho}(m)$ is a rotation by 2π plus an infinitesimal rotation by ω.

It is just as easy to construct a path of representations $\rho_t : \langle m, \ell \rangle \to \mathrm{PO}(2,2)$ whose rescaled limit agrees with ρ. Define the path as follows:

$$\rho_t(m) = \begin{pmatrix} 1 & 0 & 0 & 0 \\ 0 & 1 & 0 & 0 \\ 0 & 0 & \cosh \omega t & \sinh \omega t \\ 0 & 0 & \sinh \omega t & \cosh \omega t \end{pmatrix}, \ \rho_t(\ell) = \begin{pmatrix} \cosh d & \sinh d & 0 & 0 \\ \sinh d & \cosh d & 0 & 0 \\ 0 & 0 & \pm \cosh \mu t & \sinh \mu t \\ 0 & 0 & \sinh \mu t & \pm \cosh \mu t \end{pmatrix}.$$

These representations describe AdS structures on a tubular neighborhood of Σ with a tachyon at Σ of mass ωt. One easily checks that conjugating ρ_t by the rescaling map $\mathfrak{r}_t$ produces the desired limit as $t \to 0$. Hence, the infinitesimal angle ω can also be thought of as an infinitesimal tachyon mass.

Next, we work directly with the HP geometry at Σ. Let $p \in \Sigma$ and consider a neighborhood B of p. The developing map D on $B \setminus \Sigma$ extends to the universal branched cover $\widetilde{B}$, branched over $B \cap \Sigma$. The image of $B \cap \Sigma$ is a segment of a non-degenerate line $\mathfrak{L}$, which we may assume lies in $\mathfrak{P}$. Consider the plane P orthogonal to $\mathfrak{L}$ and passing through $D(p)$. As P is spanned by the fiber direction and a non-degenerate direction orthogonal to $\mathfrak{L}$, the restricted metric is degenerate on P. The inverse image $C_p := D^{-1}(P)$ is a disk in B. Away from p, C_p is locally modeled on HP^2. The singularity at p is a cone-like HP^2 singularity. We may, as in the $\mathbb{H}^3$ and AdS^3 cases, parallel translate C_p (or at least

a smaller neighborhood of p in C_p) along the interval $\mathcal{I} = B \cap \Sigma$, giving the identification $B = C_p \times \mathcal{I}$ near $\mathcal{I}$. Let $\mathcal{W}$ be a wedge in C_p (modeled on a wedge in HP^2), and define the product wedge $U = \mathcal{W} \times \mathcal{I}$. Product wedges are, as in the hyperbolic and AdS case, the most natural geometric charts at the singular locus.

We now construct some particularly useful wedges. For simplicity, this part of the discussion will take place in dimension two. The corresponding three-dimensional behavior is easily described by taking the product with a non-degenerate geodesic. Consider the HP^2 cone C_p defined above. By assumption, there are two degenerate rays emanating from p. Pick one of these rays, r, and let $\mathcal{W}$ be C_p, but with a slit along the ray r, so that the boundary of $\mathcal{W}$ contains two copies r_+, r_- of r with opposite orientation. Though it is a bit of an abuse, we count $\mathcal{W}$ as a wedge. It is isomorphic to a disk V in HP^2 with a slit along a degenerate ray s emanating from the center q of V. The boundary of V contains two copies s_+, s_- of s. We take s_+ to be the positive ray, meaning that it is adjacent to the portion of V containing a small positive rotation of s. The glueing map g identifies s_+ to s_- by an infinitesimal rotation fixing q. Note that g fixes s point-wise. Nonetheless, the geometry at q is singular, for the glueing map does not preserve the lines transverse to s (see Figure 4.10). The holonomy around p is a rotation by 2π composed with g.

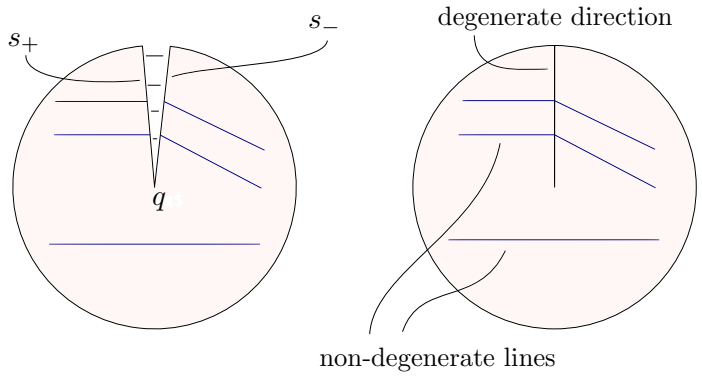

Figure 4.10: A disk V is slit along a ray in the degenerate direction. It is then glued back together using a non-trivial infinitesimal rotation to produce an *infinitesimal cone singularity*. This construction should be compared with the construction of Figure 4.9, which produces the same geometry.

Next, we construct a model degeneration of hyperbolic cones which when rescaled converge to a given HP cone. Again, we give the construction in two dimensions; the three-dimensional case is described by taking the product with a geodesic. We will assume that the infinitesimal cone angle $\omega < 0$, so that we can easily draw a picture. Let $\theta(t) = 2\pi - |\omega| t$.

Construct a polygonal wedge $V(t)$ in $\mathbb{H}^2$ with seven sides, six right angles and a seventh (concave) angle θ at the center point of the wedge as in Figure 4.11. Glueing $V(t)$ together along the sides adjacent to the center point produces a rectangle with a cone point at the center. We arrange for $V(t)$ to be long and skinny, with width roughly equal to one, and thickness $|\omega|t + O(t^2)$. Further, we arrange one ray s_+ of the concave part of the wedge to be aligned with the collapsing direction. The glueing map $g(t)$ is a rotation by ωt. Now, the rescaled limit of these collapsing wedges $V(t)$ produces an HP wedge V of the type described in the previous paragraph. The glueing map g is the rescaled limit of a rotation by ωt, which is an infinitesimal rotation by ω (as demonstrated explicitly above).

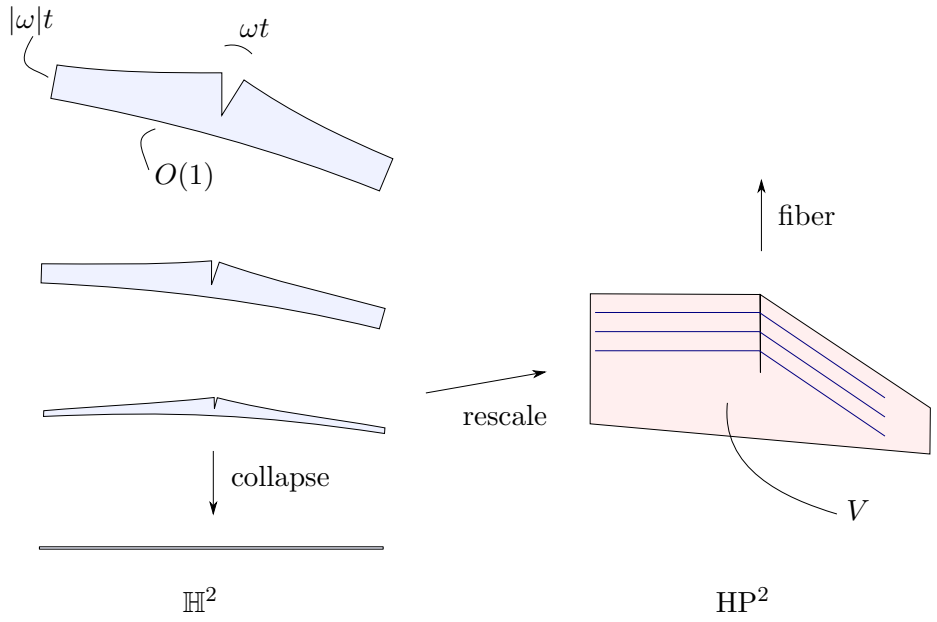

Figure 4.11: Polygonal hyperbolic wedges collapse onto a line as the (interior) wedge angle $2\pi - |\omega|t$ approaches 2π. Each wedge is glued together to form a rectangle with a cone point at the center. The rescaled limit of the wedges V is an HP polygon with a slit along the fiber direction. Glueing the slit together with the rescaled limit of the glueing maps produces an HP infinitesimal cone singularity with infinitesimal angle ω.

Next, we construct a model degeneration of AdS tachyons that when rescaled converge to the given HP cone. Let $\varphi(t) = \omega t$. Let $V(t)$ be a wedge in AdS^2 bounded by seven edges as in Figure 4.12. The five edges along the convex part of the perimeter should alternate space-like, time-like, space-like, time-like, space-like meeting at four right angles. We arrange for the space-like edges to be of roughly constant length, while the time-like

edges have (time-like) length $|\omega|t + O(t^2)$. The two remaining edges s_+, s_- border a slit along a light-like ray emanating from the center q of the wedge. The glueing map $g(t)$, which a is Lorentz boost of hyperbolic angle φ, identifies s_- with s_+; the action of $g(t)$ on s_- is a dilation by e^{φ}. Now, the rescaled limit of these collapsing wedges $V(t)$ produces an HP wedge V of the type described in the previous paragraph. The glueing map g is the rescaled limit of a boost by hyperbolic angle ωt, which is an infinitesimal rotation by ω, alternatively thought of as an infinitesimal boost.

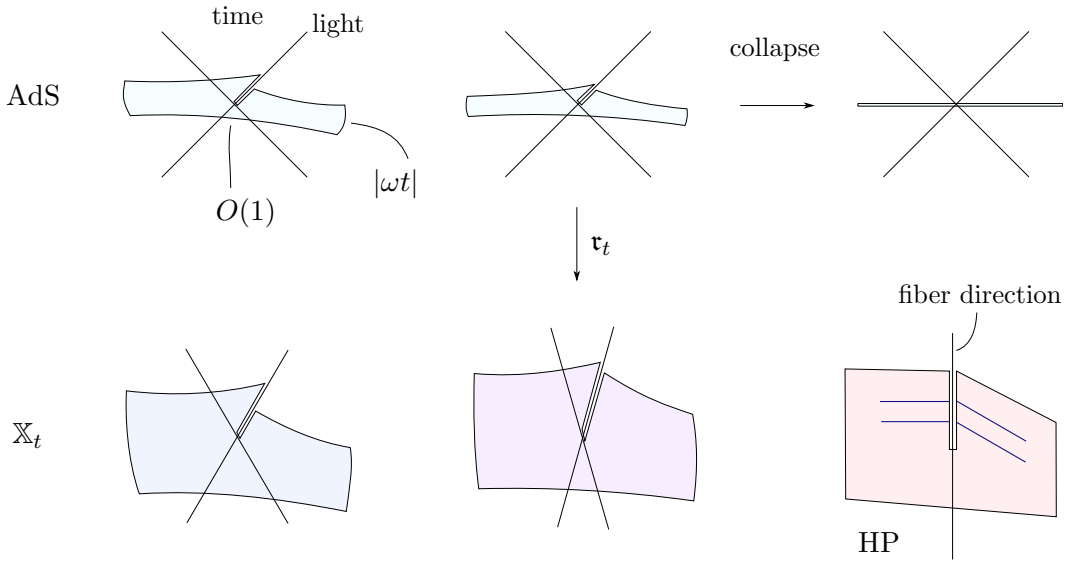

Figure 4.12: Polygons with a slit along a light-like ray in AdS^2 are glued together with a Lorentz boost of hyperbolic angle $\varphi(t) = \omega t$ to form rectangles with a singular point at the center. After rescaling the collapsing time-like direction, these polygons converge to an HP polygon with a slit along a degenerate ray. This "wedge" is glued together with the rescaled limit of the Lorentz boosts: an infinitesimal rotation (thought of as an infinitesimal boost) by angle ω.

Remark 18 (Generalized infinitesimal cone singularities)**.** A more general class of singularities is produced if we allow for an arbitrary number of degenerate rays to meet each point $p \in \Sigma$. These *generalized infinitesimal cone singularities* are determined by the infinitesimal angle ω and a discrete rotational part of the holonomy equal to $k\pi$, where $k \neq 0$ could be any non-negative integer. In the case that k is odd, the fibers of the resulting HP structure can be not be consistently oriented. These generalized singularities naturally appear in the context of geometric transitions: The rescaled limit of collapsing hyperbolic cone manifolds

with cone angle approaching $k\pi$ should be an HP structure with a generalized infinitesimal cone singularity (under appropriate conditions). Similarly collapsing generalized tachyons (see Remark 17) should have rescaled limit a generalized infinitesimal cone singularity.

4.6 Deforming cone-like projective structures

In order to prove a regeneration theorem for hyperbolic cone (resp. AdS tachyon) structures, we need to extend Lemma 5 of Section 3.6 to the case of projective structures with cone-like singularities. That is we must show that an appropriate deformation of the holonomy representation of a cone-like projective structure produces nearby cone-like projective structures.

Let N be a three-manifold, with $\Sigma \subset N$ a knot, and let $M = N \setminus \Sigma$. Let $T \subset M$ be a neighborhood of ∂M (so T is the result of removing Σ from a tubular neighborhood of Σ in N). Let $\widetilde{T}$ be the universal cover of T. We assume that $\pi_1 T \hookrightarrow \pi_1 M$, so that $\widetilde{T}$ embeds in $\widetilde{M}$. The fundamental group $\pi_1 T \cong \mathbb{Z} \times \mathbb{Z}$ is generated by the meridian m around Σ and a longitude ℓ.

Remark 19. The assumption $\pi_1 T \hookrightarrow \pi_1 M$ holds in every application that we are interested in. However, the assumption is not necessary. Everything done below can be easily modified if a longitude $\ell \mapsto 1$ in $\pi_1 M$.

Suppose (N, Σ) has a projective structure with cone-like singularity. Let $D : \widetilde{T} \to \mathbb{RP}^3$ be the developing map on a chosen lift $\widetilde{T}$ of T, and let $\rho : \pi_1 T \to \mathrm{PGL}(4, \mathbb{R})$ be the holonomy. Using Proposition 18 we can construct convenient coordinates $(r, x, y) \in (0, 1) \times \mathbb{R} \times \mathbb{R}$ for $\widetilde{T}$ with the following properties:

- The action of $\pi_1 T$ by deck translations is given by

$$m : (r, x, y) \mapsto (r, x + 1, y) \qquad \ell : (r, x, y) \mapsto (r, x, y + 1).$$

- The limit $\lim_{r \to 0} D(r, x, y) =: f(y)$, is a local submersion, independent of x, to a line $\mathfrak{L}$ in $\mathbb{RP}^3$. The line $\mathfrak{L}$ represents the lift of Σ corresponding to the chosen lift of T.

- $\rho(m)$ point-wise fixes $\mathfrak{L}$ and $\rho(\ell)$ preserves (but does not fix) $\mathfrak{L}$.

These coordinates will be useful for proving the following proposition.

Proposition 22. *Suppose $\rho_t : \pi_1 M \to \mathrm{PGL}(4,\mathbb{R})$ is a path of representations such that*

1. *ρ_0 is the holonomy representation of a projective structure with cone-like singularities on (N,Σ). Let $\mathfrak{L}$ be the line in $\mathbb{RP}^3$ fixed by $\rho(\pi_1 \partial M)$.*

2. *$\rho_t(m)$ point-wise fixes a line $\mathfrak{L}_t$, with $\mathfrak{L}_t \to \mathfrak{L}$.*

Then, for all t sufficiently small, ρ_t is the holonomy representation for a projective structure with cone-like singularities on (N,Σ).

Proof. First, we let $D_0 : \widetilde{M} \to \mathbb{RP}^3$ denote the developing map of our projective structure at time $t = 0$. Let $M_0 \subset M$ be the result of removing a smaller tubular neighborhood $T' \subset T$ of Σ from M, so that M_0 and T overlap in a neighborhood of ∂M_0. By Lemma 5, we can deform the projective structure on M_0 to get developing maps $D_t : \widetilde{M_0} \to \mathbb{RP}^3$ that are equivariant with respect to ρ_t. Further, by the proof of the lemma, we may assume that D_t converges uniformly in the $\mathscr{C}^1$ topology on compacts in $\widetilde{M_0}$. Now we must extend D_t to the rest of $\widetilde{M}$.

We may assume, by conjugating ρ_t in $\mathrm{PGL}(4,\mathbb{R})$, that $\rho_t(m)$ also fixes $\mathfrak{L}$, for all t. That is, we assume $\mathfrak{L}_t = \mathfrak{L}$. In order to define D_t on $\widetilde{T}$ we will need a quick lemma.

Lemma 7. *For each $\gamma \in \pi_1 T$, we can take arbitrary powers $\rho_t(\gamma)^z$ in a way that depends smoothly on z, t.*

Proof of Lemma. First $\rho_t(\pi_1 T) \subset \mathrm{PSL}(4,\mathbb{R})$. So for each $\gamma \in \pi_1 T$, we can find a path $g(t)$ in $\mathrm{PSL}(4,\mathbb{R})$ with $g(0) = \mathrm{Id}$ and $g(1) = \rho_0(\gamma)$. The log function is well-defined sufficiently near to the identity and can be defined by analytic continuation along the path $g(s)$ (this amounts to choosing a branch of log for the eigenvalues; note that we can not have an odd number of negative real eigenvalues). Next, analytically continue log along the path $\rho_t(\gamma)$. Thus $\rho_t(\gamma)^z := \exp(z \log \rho_t(\gamma))$ depends smoothly on z, t. □

Next, using the coordinates defined above, define D_t on $\widetilde{T}$ as follows:

$$D_t(r,x,y) = \rho_t(m)^x \rho_t(\ell)^y \rho_0(m)^{-x} \rho_0(\ell)^{-y} D_0(r,x,y)$$

We check that

$$\begin{aligned} D_t(r, x+k, y+j) &= \rho_t(m)^{x+k}\rho_t(\ell)^{y+j}\rho_0(m)^{-x-k}\rho_0(\ell)^{-y-j}D_0(r, x+k, y+j) \\ &= \rho_t(m)^{x+k}\rho_t(\ell)^{y+j}\rho_0(m)^{-x-k}\rho_0(\ell)^{-y-j}\rho_0(m)^k\rho_0(\ell)^j D_0(r, x, y) \\ &= \rho_t(m)^{x+k}\rho_t(\ell)^{y+j}\rho_0(m)^{-x}\rho_0(\ell)^{-y}D_0(r, x, y) \\ &= \rho_t(m)^k\rho_t(\ell)^j\rho_t(m)^x\rho_t(\ell)^y\rho_0(m)^{-x}\rho_0(\ell)^{-y}D_0(r, x, y) \\ &= \rho_t(m)^k\rho_t(\ell)^j D_t(r, x, y), \end{aligned}$$

so D_t satisfies the right equivariance properties. Next, since $\rho_t(m)$ fixes $\mathfrak{L}$ pointwise, we still have that $\lim_{r\to 0} D_t(r, x, y)$ is independent of x. Further, for small t, $\lim_{r\to 0} D_t(r, x, y)$ will still be a local submersion to $\mathfrak{L}$. So, D_t is the developing map for a structure with cone-like singularities on a neighborhood of the singular locus Σ. Further, D_t converges to D_0 in the $\mathscr{C}^1$ topology (in fact, in $\mathscr{C}^\infty$) on compacts of $\widetilde{T}$. Now, the definition of D_t on $\widetilde{T}$ and the definition of D_t on $\widetilde{M_0}$ may not agree on the overlap. So, we glue these two maps together using a bump function which is supported away from the singular locus. Finally, extend D_t to the other lifts of T in $\widetilde{M}$ by ρ_t equivariance. This gives globally defined maps $D_t : \widetilde{M} \to \mathbb{RP}^3$ which converge in $\mathscr{C}^1$, on compacts, to D_0. Thus for sufficiently small t, the D_t are local diffeomorphisms. □

4.7 Regeneration of $\mathbb{H}^3$ and AdS^3 structures from HP^3

As the class of cone-like singularities specializes to cone singularities in the $\mathbb{H}^3$ case, tachyons in the AdS^3 case, and infinitesimal cone singularities in the HP^3 case, we get the following regeneration statement immediately from Proposition 22.

Proposition 23 (Regeneration with cone-like singularities)**.** *Let N be a closed three-manifold, with Σ a knot, and let $M = N \setminus \Sigma$ with $m \in \pi_1 M$ the meridian around Σ. Let X be either $\mathbb{X}_1 = \mathbb{H}^n$ or $\mathbb{X}_{-1} = \mathrm{AdS}^n$. Let $\rho_t : \pi_1 M \to \mathrm{Isom}(X)$ be a family of representations defined for $t \geq 0$ such that*

- *The path of rescaled representations $\mathfrak{r}_t\rho_t\mathfrak{r}_t^{-1}$ converges as $t \to 0$ in $\mathscr{C}^1$ to a representation ρ_{HP},*
- *ρ_{HP} is the holonomy of an* HP *structure with infinitesimal cone singularities on (N, Σ).*

- *$\rho_t(m)$ is a rotation if $X = \mathbb{H}^3$, or a boost if $X = \mathrm{AdS}^3$.*

Then, for sufficiently small $t > 0$, we can construct a family of X structures on N with singularities at Σ. For each t, the holonomy representation of the smooth part is ρ_t, and the structures have cone singularities if $X = \mathbb{H}^3$ or tachyon singularities if $X = \mathrm{AdS}^3$.

Proof. The proof is the same as the proof of Proposition 15. At time $t = 0$ we have an HP structure with infinitesimal cone singularity. We regard this as a projective structure with cone-like singularities. If $X = \mathbb{H}^3$, then $\sigma_t = \mathfrak{r}_t \rho_t \mathfrak{r}_t^{-1}$ is a representation landing in $G_t = \mathrm{Isom}(\mathbb{X}_t)$. The σ_t limit to ρ_{HP}. By Proposition 22 there is a family of cone-like projective structures very close to the HP structure that realize the σ_t as holonomy (for short time). The developing maps of these structures map a compact fundamental domain K (which includes the singularity) to a compact region inside of $\mathbb{RP}^3$ that for small t is very close to the image of K by the developing map of the HP structure. Thus, for all sufficiently small t, the image will lie inside of $\mathbb{X}_t$ ensuring the developing maps define a family of $(\mathbb{X}_t, G_t)$ structures. Applying the inverse of the rescaling map $\mathfrak{r}_t^{-1}$ gives a family of $\mathbb{X}_1 = \mathbb{H}^3$ structures with cone singularities. If $X = \mathrm{AdS}^3$ everything works the same, except that σ_t lands in G_{-t} and we get $(\mathbb{X}_{-t}, G_{-t})$ structures that, by applying $\mathfrak{r}_t^{-1}$, are equivalent to AdS structures with tachyons. □

This proposition says that we can recover collapsing hyperbolic cone and AdS tachyon structures from an HP structure and a suitable path of representations. We use this proposition to prove the following regeneration theorem.

Theorem 4. *Let (N, Σ) be a closed HP^3 three-manifold with infinitesimal cone singularity of infinitesimal angle $-\omega$ along the knot Σ. Let $M = N \setminus \Sigma$ be the smooth part and let $\rho_{\mathrm{HP}} : \pi_1 M \to G_{\mathrm{HP}}$ be the holonomy representation with ρ_0 its $\mathrm{O}(2,1)$ part. Suppose that $H^1(\pi_1 M, \mathfrak{so}(2,1)_{Ad\rho_0}) = \mathbb{R}$. Then there exists singular geometric structures on (N, Σ) parametrized by $t \in (-\delta, \delta)$ which are*

- *hyperbolic cone structures with cone angle $2\pi - \omega t$ for $t > 0$*
- *AdS structures with a tachyon of mass ωt for $t < 0$.*

To prove this theorem, we use the condition $H^1(\pi_1 M, \mathfrak{so}(2,1)_{Ad\rho_0}) = \mathbb{R}$ to get representations into $\mathrm{PSO}(3,1)$ and $\mathrm{PSO}(2,2)$ satisfying the conditions of Proposition 23. In

the hyperbolic case, the proof of this makes use of the complex structure of the variety of $\mathrm{PSO}(3,1)$ representations coming from the isomorphism $\mathrm{PSO}(3,1) \cong \mathrm{PSL}(2,\mathbb{C})$. This isomorphism can be generalized to give $\mathrm{PGL}(2,\cdot)$ descriptions of all of the isometry groups G_s. Working with the $\mathrm{PGL}(2,\cdot)$ description of isometry groups allows for the most natural proof of Theorem 23. So, we take a detour in the next section and give the proof of the Theorem in Section 4.9.

4.8 The $\mathrm{PGL}(2)$ description of isometry groups

In dimension three, there is a useful alternative description of the isometry groups G_t of our models $\mathbb{X}_t$ which generalizes the isomorphism $\mathrm{PSO}(3,1) \cong \mathrm{PSL}(2,\mathbb{C})$.

Let $\mathcal{B}_s = \mathbb{R} + \mathbb{R}\kappa_s$ be the real two-dimensional (commutative) algebra generated by a non-real element κ_s with $\kappa_s^2 = -\mathrm{sign}(s)s^2$. As a vector space $\mathcal{B}_s$ is spanned by 1 and κ_s. There is a conjugation action:

$$(a + b\kappa_s) \mapsto \overline{(a + b\kappa_s)} := a - b\kappa_s$$

which defines a square-norm

$$|a + b\kappa_s|^2 := (a + b\kappa_s)\overline{(a + b\kappa_s)} = a^2 - b^2\kappa_s^2 \ \in \ \mathbb{R}.$$

Note that $|\cdot|^2$ may not be positive definite. We refer to a as the *real part* and b as the *imaginary part* of $a + b\kappa_s$. It easy to check that $\mathcal{B}_s$ is isomorphic to $\mathbb{C}$ when $s > 0$.

Remark 20. In the case $s = -1$, we will denote κ_s by the letter τ. The algebra $\mathbb{R} + \mathbb{R}\tau$ plays a central role in the study of ideal triangulations of AdS manifolds in Chapter 5. It is also easy to check that when $s < 0$, $\mathcal{B}_s$ is isomorphic to $\mathbb{R} + \mathbb{R}\tau$.

Remark 21. In the case $s = 0$, we will denote κ_s by the letter σ. The algebra $\mathbb{R} + \mathbb{R}\sigma$ plays a central role in the study of ideal triangulations of HP manifolds in Chapter 5.

Now consider the 2×2 matrices $M_2(\mathcal{B}_s)$. There is an adjoint operation $A \mapsto A^*$ which simply takes the conjugate transpose of A. Let $\mathrm{Herm}(2,\mathcal{B}_s)$ denote the 2×2 Hermitian matrices,

$$\mathrm{Herm}(2,\mathcal{B}_s) = \{A \in M_2(\mathcal{B}_s) : A^* = A\}.$$

As a real vector space, $\mathrm{Herm}(2,\mathcal{B}_s) \cong \mathbb{R}^4$. We define the following (real) inner product on $\mathrm{Herm}(2,\mathcal{B}_s)$:

$$\left\langle \begin{bmatrix} a & z \\ \bar{z} & d \end{bmatrix}, \begin{bmatrix} e & w \\ \bar{w} & h \end{bmatrix} \right\rangle = -\frac{1}{2} tr\left(\begin{bmatrix} a & z \\ \bar{z} & d \end{bmatrix} \begin{bmatrix} h & -w \\ -\bar{w} & e \end{bmatrix} \right).$$

The signature of this metric depends on s.

Proposition 24. *The convex region $\mathbb{X}_s$ in $\mathbb{RP}^3$ defined in Section 3.1 can be alternately defined by*

$$\mathbb{X}_s = \{X \in \mathrm{Herm}(2,\mathcal{B}_s) : \langle X, X\rangle < 0\} / X \sim \lambda X \text{ for } \lambda \in \mathbb{R}^*$$

where we use the coordinates $X = \begin{pmatrix} x_1 + x_2 & x_3 + x_4\kappa_s \\ x_3 - x_4\kappa_s & x_1 - x_2 \end{pmatrix}$ *on* $\mathrm{Herm}(2,\mathcal{B}_s)$. *Note that* $\langle X, X\rangle = -det(X) = -x_1^2 + x_2^2 + x_3^2 - \kappa_s^2 x_4^2$.

The ideal boundary $\partial^\infty \mathbb{X}_s$, given by the projectivized light cone with respect to this metric, is exactly the projectivized rank one Hermitian matrices, where for a Hermitian matrix X, rank one means $\det(X) = 0$, $X \neq 0$. Any rank one Hermitian matrix X can be decomposed (uniquely up to $\pm$) as

$$X = vv^*$$

where $v \in \mathcal{B}_s^2$ is a two-dimensional column vector with entries in $\mathcal{B}_s$ (and v^* denotes the transpose conjugate). Further v must satisfy that $\lambda v = 0$ for $\lambda \in \mathcal{B}_s$ if and only if $\lambda = 0$. This gives the identification

$$\partial^\infty \mathbb{X} = \mathbb{P}^1\mathcal{B}_s = \left\{ \begin{bmatrix} x \\ y \end{bmatrix} : x \cdot \alpha = 0 \text{ and } y \cdot \alpha = 0 \text{ for } \alpha \in \mathcal{B}_s \iff \alpha = 0 \right\} / \sim$$

$$\text{where } \begin{bmatrix} x \\ y \end{bmatrix} \sim \begin{bmatrix} x\lambda \\ y\lambda \end{bmatrix} \text{ for } \lambda \in \mathcal{B}_s^\times.$$

Definition 22. We denote by $\mathrm{PGL}^+(2,\mathcal{B}_s)$ the 2×2 matrices A with entries in $\mathcal{B}_s$ such that $|\det(A)|^2 > 0$, up to the equivalence $A \sim \lambda A$ for any $\lambda \in \mathcal{B}_s^\times$.

Remark 22. The condition $|\det(A)|^2 > 0$ is only needed in the case $s < 0$. For $s \geq 0$, PGL^+ and PGL are the same. For $s > 0$, PGL^+ is the same as PSL.

We will think of $\mathrm{PGL}^+(2,\mathcal{B}_s)$ as determinant ± 1 matrices with entries in $\mathcal{B}_s$ up to multiplication by a square root of 1 (if $s < 0$, there will be four such square roots). We note

that $\mathrm{PGL}^+(2,\mathcal{B}_s)$ acts by Mobius transformations on $\partial^\infty \mathbb{X}_s = \mathbb{P}^1\mathcal{B}_s$. This action extends to all of $\mathbb{X}_s$, giving a map $\mathrm{PGL}^+(2,\mathcal{B}_s) \to G_s = \mathrm{Isom}(\mathbb{X}_s)$, as follows:

$$A \cdot X := AXA^* \quad \text{where } X \in \mathbb{X}_s \text{ and } \det(A) = \pm 1.$$

Proposition 25. *For $s \neq 0$ The map $\mathrm{PGL}^+(2,\mathcal{B}_s) \to G_s = \mathrm{Isom}^+(\mathbb{X}_s)$ is an isomorphism. Note that in the case $s = 1$, this is the usual isomorphism $\mathrm{PSL}(2,\mathbb{C}) \cong \mathrm{PSO}(3,1)$.*

Proof. The proof is not hard. Use the coordinates $X = \begin{pmatrix} x_1 + x_2 & x_3 + x_4\kappa_s \\ x_3 - x_4\kappa_s & x_1 - x_2 \end{pmatrix}$ on $\mathrm{Herm}(2,\mathcal{B}_s)$. □

Remark 23. In fact, the orientation reversing isometries are also described by $\mathrm{PGL}^+(2,\mathcal{B})$ acting by $X \mapsto A\overline{X}A^*$.

Note that with the coordinates $X = \begin{pmatrix} x_1 + x_2 & x_3 + x_4\kappa_s \\ x_3 - x_4\kappa_s & x_1 - x_2 \end{pmatrix}$ on $\mathrm{Herm}(2,\mathcal{B}_s)$, the rescaling map $\mathfrak{r}_s : \mathbb{X}_1 \to \mathbb{X}_s$ defined in Section 3.1 corresponds to the algebraic rescaling map $\mathfrak{a}_s : \mathbb{C} = \mathcal{B}_1 \to \mathcal{B}_s$ defined by $i \mapsto \kappa_s/|s|$. This observation gives the following proposition:

Proposition 26. *For $s > 0$, $\mathfrak{a}_s$ defines an isomorphism $\mathrm{PSL}(2,\mathcal{B}_1) \to \mathrm{PSL}(2,\mathcal{B}_s)$ which corresponds to the isomorphism $G_1 \to G_s$ given by conjugation by $\mathfrak{r}_s$.*

$$\begin{array}{ccc} \mathrm{PSL}(2,\mathbb{C}) & \xrightarrow{\mathfrak{a}_s} & \mathrm{PSL}(2,\mathcal{B}_s) \\ \downarrow \cong & & \downarrow \cong \\ \mathrm{PSO}(3,1) & \xrightarrow{\mathfrak{r}_s} & G_s \end{array} \tag{4.1}$$

Similarly, for $s < 0$, the rescaling map $\mathfrak{r}_s : \mathbb{X}_{-1} \to \mathbb{X}_s$ defined in Section 3.1 corresponds to the algebraic rescaling map $\mathfrak{a}_s : \mathcal{B}_{-1} \to \mathcal{B}_s$ defined by $\tau \mapsto \kappa_s/|s|$. Again, we get

Proposition 27. *For $s < 0$, $\mathfrak{a}_s$ defines an isomorphism $\mathrm{PGL}^+(2,\mathcal{B}_{-1}) \to \mathrm{PGL}^+(2,\mathcal{B}_s)$, which corresponds to the isomorphism $G_1 \to G_s$ given by conjugation by $\mathfrak{r}_s$.*

$$\begin{array}{ccc} \mathrm{PGL}^+(2,\mathbb{R}+\mathbb{R}\tau) & \xrightarrow{\mathfrak{a}_s} & \mathrm{PGL}^+(2,\mathcal{B}_s) \\ \downarrow \cong & & \downarrow \cong \\ \mathrm{PSO}(2,2) & \xrightarrow{\mathfrak{r}_s} & G_s \end{array} \tag{4.2}$$

Recall that in the case $s = 0$, the metric on $\mathbb{X}_0$ is degenerate, so that the isometries of $\mathbb{X}_0$ ended up being too large to be of use. The half-pipe group G_{HP} was defined to be a strict subgroup giving a useful structure for the purposes of geometric transitions.

Proposition 28. *The map* $\mathrm{PGL}(2, \mathbb{R} + \mathbb{R}\sigma) \to G_0 = \mathit{Isom}(\mathbb{X}_0)$ *maps* $\mathrm{PGL}(2, \mathbb{R} + \mathbb{R}\sigma)$ *isomorphically onto* G^+_{HP}.

Proof. To begin, we think of $\mathbb{R} + \mathbb{R}\sigma$ as the cotangent bundle of $\mathbb{R}$. The element σ should be thought of as a differential quantity, whose square is zero. Similarly, $\mathrm{PGL}(2, \mathbb{R} + \mathbb{R}\sigma)$ is the cotangent bundle of $\mathrm{PGL}(2, \mathbb{R})$:

Lemma 8. *Let* $A + B\sigma$ *have determinant* ± 1. *Then* $\det A = \det(A + B\sigma) = \pm 1$ *and* $\operatorname{tr} A^{-1}B = 0$. *In other words* B *is in the tangent space at* A *of the matrices of constant determinant* ± 1.

Any element of $\mathrm{Herm}(2, \mathbb{R} + \mathbb{R}\sigma)$ can be expressed uniquely in the form $X + Y\sigma$ where $X = \begin{pmatrix} x_1 + x_2 & x_3 \\ x_3 & x_1 - x_2 \end{pmatrix} = X^T$ is symmetric and $Y = \begin{pmatrix} 0 & x_4 \\ -x_4 & 0 \end{pmatrix} = -Y^T$ is skew-symmetric. Then

$$\begin{aligned} (A + B\sigma)(X + Y\sigma)(A + B\sigma)^* &= (A + B\sigma)(X + Y\sigma)(A^T - B^T\sigma) \\ &= AXA^T + (BXA^T - AXB^T + AYA^T)\sigma \end{aligned}$$

where we note that AXA^T is symmetric and $(BXA^T - AXB^T + AYA^T)$ is skew-symmetric. The symmetric part $X \mapsto AXA^T$, written in coordinates gives the familiar isomorphism $\Phi : \mathrm{PGL}(2, \mathbb{R}) \to \mathrm{O}(2, 1)$. In (x_1, x_2, x_3, x_4) coordinates the transformation defined by $A + B\sigma$ has matrix

$$\begin{pmatrix} \Phi(A) & 0 \\ v(A, B) & c(A, B) \end{pmatrix}$$

The skew-symmetric part $X + Y\sigma \mapsto (BXA^T - AXB^T + AYA^T)\sigma$, written in (x_1, x_2, x_3, x_4) coordinates gives the bottom row of this matrix:

$$\begin{aligned} v(A, B) &= \Big((be + df - ag - ch) \quad (be - df - ag + ch) \quad (bf + de - ah - cg)\Big) \\ c(A, B) &= \det(A) = \det(\Phi(A)) = \pm 1 \end{aligned}$$

where $A = \begin{pmatrix} a & b \\ c & d \end{pmatrix}$, $B = \begin{pmatrix} e & f \\ g & h \end{pmatrix}$. To show that $\mathrm{PGL}(2, \mathbb{R}+\mathbb{R}\sigma) \to G^+_{\mathrm{HP}}$ is an isomorphism,

one must simply check that for any given A, the map $B \to v(A, B)$ is a linear isomorphism to $\mathbb{R}^3$. □

Finally, we restate the condition of *compatibility to first order* in these terms. In order to make sense of continuity and limits for paths of representations over the varying algebras $\mathcal{B}_s$, we can embed all of the $\mathcal{B}_s$ in a larger Clifford algebra $\mathcal{C}$ (see Section 5.4). For our purposes here, assume that $\kappa_s \to \kappa_0$ as $s \to 0$.

In the hyperbolic case:

Proposition 29. *Let $\rho_t : \pi_1 M \to G_{+1}$ be a path of representations, defined for $t \geq 0$, converging to a representation ρ_0 with image in the subgroup $H_0 = \begin{pmatrix} \mathrm{O}(2,1) & 0 \\ 0 & \pm 1 \end{pmatrix}$. Then the corresponding representations $\tilde{\rho}_t : \pi_1 M \to \mathrm{PGL}(2, \mathbb{C})$ limit to a representation $\tilde{\rho}_0$ into $\mathrm{PGL}(2, \mathbb{R})$. Suppose further that $\mathfrak{r}_t \rho_t \mathfrak{r}_t^{-1}$ limit to a representation ρ_{HP}. Then*

$$\mathfrak{a}_t \tilde{\rho}_t \mathfrak{a}_t^{-1} \xrightarrow[t \to 0]{} \tilde{\rho}_{\mathrm{HP}}$$

where $\tilde{\rho}_{\mathrm{HP}}$ is the representation into $\mathrm{PGL}(2, \mathbb{R} + \mathbb{R}\sigma)$ corresponding to ρ_{HP}. Further $\tilde{\rho}_{\mathrm{HP}}$ is defined by

$$\mathrm{Re}\, \tilde{\rho}_{\mathrm{HP}} = \tilde{\rho}_0 \qquad\qquad \mathrm{Im}\, \tilde{\rho}_{\mathrm{HP}} = \frac{d}{dt} \mathrm{Im}\, \tilde{\rho}_t \Big|_{t=0}.$$

Similarly, in the AdS case:

Proposition 30. *Let $\rho_t : \pi_1 M \to G_{-1}$ be a path of representations, defined for $t \leq 0$, converging to a representation ρ_0 with image in the subgroup $H_0 = \begin{pmatrix} \mathrm{O}(2,1) & 0 \\ 0 & \pm 1 \end{pmatrix}$. Then the corresponding representations $\tilde{\rho}_t : \pi_1 M \to \mathrm{PGL}(2, \mathbb{R} + \mathbb{R}\tau)$ limit to a representation $\tilde{\rho}_0$ into $\mathrm{PGL}(2, \mathbb{R})$. Suppose further that $\mathfrak{r}_t \rho_t \mathfrak{r}_t^{-1}$ limit to a representation ρ_{HP}. Then*

$$\mathfrak{a}_t \tilde{\rho}_t \mathfrak{a}_t^{-1} \xrightarrow[t \to 0]{} \tilde{\rho}_{\mathrm{HP}}$$

where $\tilde{\rho}_{\mathrm{HP}}$ is the representation into $\mathrm{PGL}(2, \mathbb{R} + \mathbb{R}\sigma)$ corresponding to ρ_{HP}. Further $\tilde{\rho}_{\mathrm{HP}}$ is defined by

$$\mathrm{Re}\, \tilde{\rho}_{\mathrm{HP}} = \tilde{\rho}_0 \qquad\qquad \mathrm{Im}\, \tilde{\rho}_{\mathrm{HP}} = \frac{d}{dt} \mathrm{Im}\, \tilde{\rho}_t \Big|_{t=0}.$$

4.9 Proof of regeneration theorem

We restate Theorem 4 in terms of $\mathrm{PGL}(2, \mathcal{B}_s)$ isometry groups.

Theorem 5. *Let (N, Σ) be a closed HP^3 three-manifold with infinitesimal cone singularity of infinitesimal angle $-\omega$ along the knot Σ. Let $M = N \setminus \Sigma$ be the smooth part and let $\rho_{\mathrm{HP}} : \pi_1 M \to \mathrm{PGL}(2, \mathbb{R} + \mathbb{R}\sigma)$ be the holonomy representation. Suppose that the real part ρ_0 of ρ_{HP} satisfies the condition $H^1(\pi_1 M, \mathfrak{sl}(2, \mathbb{R})_{Ad\rho_0}) = \mathbb{R}$. Then there exists singular geometric structures on (N, Σ) parametrized by $t \in (-\delta, \delta)$ which are*

- *hyperbolic cone structures with cone angle $2\pi - \omega t$ for $t > 0$*
- AdS *structures with a tachyon of mass $-\omega t$ for $t < 0$.*

Proof. We begin with a lemma about the representation variety $\mathscr{R}(\pi_1 M, \mathrm{SL}(2, \mathbb{R}))$ of representations modulo conjugation.

Lemma 9. *The condition $H^1(\pi_1 M, \mathfrak{sl}(2, \mathbb{R})_{Ad\rho_0}) = \mathbb{R}$ guarantees that the representation variety $\mathscr{R}(\pi_1 M, \mathrm{SL}(2, \mathbb{R}))$ is smooth at ρ_0.*

Proof. It is a standard fact that $H^1(\pi_1 M, \mathfrak{sl}(2, \mathbb{R})_{Ad\rho}) \to H^1(\pi_1 \partial M, \mathfrak{sl}(2, \mathbb{R})_{Ad\rho})$ has half-dimensional image (see for example [HK05]). In this case, $\rho_0(m) = 1$ and $\rho_0(\ell)$ is a non-trivial translation (possibly plus a rotation by π), so any nearby representation φ of $\pi_1(\partial M)$ preserves an axis and has $\dim H^1(\pi_1 \partial M, \mathfrak{sl}(2, \mathbb{R})_{Ad\varphi}) = 2$. So, $\dim H^1(\pi_1 M, \mathfrak{sl}(2, \mathbb{R})_{Ad\rho}) \geq 1$ for all ρ nearby ρ_0. It follows that ρ_0 is a smooth point of $\mathscr{R}(\pi_1 M, \mathrm{PSL}(2, \mathbb{R}))$, and that the tangent space at ρ_0 is one dimensional. □

Let m be a meridian around Σ in the direction consistent with the orientation of Σ (so that in particular, the discrete rotational part of the holonomy of m is $+2\pi$).

Hyperbolic case ($t > 0$): In order to use Proposition 23, we must produce for $t > 0$ a path of representations ρ_t into $\mathrm{PGL}(2, \mathbb{C})$ with the following properties:

1. $\rho_t \to \rho_0$
2. $\rho_t(m)$ is a rotation by $2\pi - \omega t$
3. $\mathfrak{r}_t \rho_t \mathfrak{r}_t^{-1}$ converges to ρ_{HP} as $t \to 0$. By Proposition 29 this is equivalent to

$$\frac{d}{dt} \operatorname{Im} \rho_t \Big|_{t=0} = \operatorname{Im} \rho_{\mathrm{HP}}.$$

Now, our HP representation gives a $\mathrm{PSL}(2,\mathbb{R})$ tangent vector at ρ_0 as follows: $\rho_{\mathrm{HP}}(\gamma) = \rho_0(\gamma) + Y(\gamma)\ \sigma$. Define $z(\gamma) = Y(\gamma)\rho_0(\gamma)^{-1}$. Then z is an $\mathfrak{sl}(2,\mathbb{R})_{Ad\rho_0}$ co-cycle. It spans the tangent space of $\mathscr{R}(\pi_1 M, \mathrm{PSL}(2,\mathbb{R}))$. As the structure is singular, we must have $z(m) \neq 0$. Thus the translation length of m increases (or decreases) away from zero. The complexified variety $\mathscr{R}(\pi_1 M, \mathrm{PSL}(2,\mathbb{C}))$ is also smooth at ρ_0 and $\mathscr{R}(\pi_1 M, \mathrm{PSL}(2,\mathbb{C})) \to \mathscr{R}(\pi_1 \partial M, \mathrm{PSL}(2,\mathbb{C}))$ is a local immersion at ρ_0. The variety $\mathscr{R}(\pi_1 \partial M, \mathrm{PSL}(2,\mathbb{C}))$ has complex dimension 2.

Lemma 10. *The subset*

$$S = \{\rho \in \mathscr{R}(\pi_1 \partial M, \mathrm{PSL}(2,\mathbb{C})) : \rho(m) \text{ is elliptic}\}$$

is locally a smooth real sub-manifold of dimension three. The image of $\mathscr{R}(\pi_1 M, \mathrm{PSL}(2,\mathbb{C}))$ in $\mathscr{R}(\pi_1 \partial M, \mathrm{PSL}(2,\mathbb{C}))$ is transverse to S.

Proof of lemma. That S is smooth of dimension three follows immediately from the fact that $\mathscr{R}(\pi_1 \partial M, \mathrm{PSL}(2,\mathbb{C}))$ is parameterized (near ρ_0) by the complex lengths of m, ℓ. The image of $\mathscr{R}(\pi_1 M, \mathrm{PSL}(2,\mathbb{C}))$ in $\mathscr{R}(\pi_1 \partial M, \mathrm{PSL}(2,\mathbb{C}))$ is transverse to S because z increases translation length of m away from zero. □

Now, from the lemma, we have that the $\mathrm{PSL}(2,\mathbb{C})$ representations of $\pi_1 M$ with m elliptic near ρ_0 form a smooth real one-dimensional manifold. The tangent space at ρ_0 is spanned by $iz(\cdot)$. Thus the rotation angle of m is changing along this manifold and we can choose ρ_t as desired.

AdS **case ($t < 0$):** We obtain, from the argument above, a path $\varphi_t : \pi_1 M \to \mathrm{PSL}(2,\mathbb{R})$ defined in a neighborhood of $t = 0$ with $\varphi_0 = \rho_0$, $\frac{d}{dt}\varphi_t\big|_{t=0} = \mathrm{Im}\rho_{\mathrm{HP}}$ and $z(m) = \frac{d}{dt}\varphi_t(m)$ is an infinitesimal translation by $-\omega$ along the axis $\mathfrak{L}$ of $\rho_0(\ell)$. We may assume that the axis in $\mathbb{H}^2$ preserved by $\varphi_t(\partial M)$ is also $\mathfrak{L}$ (constant). Now, define $\rho_t : \pi_1 M \to \mathrm{PSL}(2, \mathbb{R} + \mathbb{R}\tau)$ by

$$\rho_t(\cdot) = \frac{1+\tau}{2}\varphi_t(\cdot) + \frac{1-\tau}{2}\varphi_{-t}(\cdot).$$

A quick computation shows that $\frac{d}{dt}\rho_t\big|_{t=0} = \tau\frac{d}{dt}\varphi_t\big|_{t=0}$. Further, $\rho_t(m)$ is a boost around the axis $\mathfrak{L}$ by hyperbolic angle ωt. So Proposition 23 implies the result for $t < 0$.

□

4.10 Cone/Tachyon transitions

The regeneration theorem 4 can be stated as a theorem about geometric transitions.

Theorem 6. *Let N be a closed three-manifold, with Σ a knot, and let $M = N \setminus \Sigma$. Let h_t be a path of hyperbolic cone structures on (N, Σ) defined for $t > 0$. Suppose that:*

- *As $t \to 0$, the cone angle approaches 2π and h_t limits to a transversely hyperbolic foliation with holonomy $\rho : \pi_1 M \to \mathrm{O}(2,1)$.*
- *There are projective structures $\mathscr{P}_t$, defined for $t > 0$, equivalent to h_t, and which converge to an* HP *structure with an infinitesimal cone singularity.*
- $H^1(\pi_1 M, \mathfrak{so}(2,1)_{Ad\rho}) = \mathbb{R}$.

Then a transition to AdS *structures with tachyons exists: We can continue the path $\mathscr{P}_t$ to $t < 0$ so that $\mathscr{P}_t$ is projectively equivalent to an* AdS *structure with a tachyon singularity (of mass $O(t)$). The same result holds when the roles of hyperbolic and* AdS *structures are interchanged.*

Remark 24. By an argument using the Schlafli formula, collapsing hyperbolic cone manifolds must have *increasing* cone angle (see [Hod86, Por98]). So the cone manifolds in the theorem will have cone angle approaching 2π from below. Hence, the AdS tachyon manifolds produced by the theorem will have negative mass.

Remark 25. The assumption that the cone angles limit to 2π is not necessary. Indeed a similar version of theorem holds when the cone angles limit to any multiple of π. The statement of this version involves generalized tachyons (Remark 17) and generalized infinitesimal cone singularities (Remark 18). As we have not given a formal discussion of these generalized singularities, we leave this version of the theorem for a later article.

4.11 Borromean Rings Example

Here we will construct examples of transitioning structures on the Borromean rings complement M (with one boundary component required to be a parabolic cusp). In this case, the $\mathrm{SO}(2,1)$ representation variety is singular at the locus of degenerated structures, so Theorem 6 does not apply. We will see that a transitional HP structure on M can be deformed

to nearby HP structures that *do not* regenerate to hyperbolic structures. However, in this case these nearby HP structures do regenerate to AdS structures. Such examples can be constructed using ideal tetrahedra and the methods of Chapter 5 (in fact, M is the union of eight tetrahedra). However, for brevity, we observe this phenomenon only at the level of representations.

4.11.1 Representation variety

Consider the three-torus T^3 defined by identifying opposite faces of a cube. Now, define $M^3 = T^3 - \{\alpha, \beta, \gamma\}$, where α, β, γ are disjoint curves freely homotopic to the generators a, b, c of $\pi_1 T^3$ as shown in Figure 4.13. Then M is homeomorphic to the complement of the

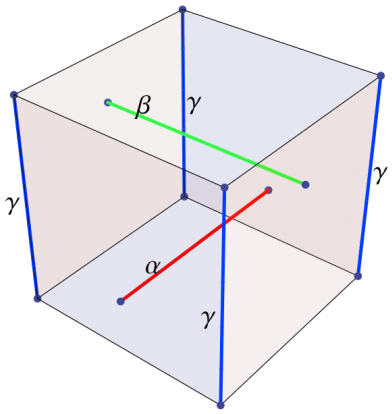

Figure 4.13: We remove the three curves α, β, γ shown in the diagram from the three-torus T^3 (opposite sides of the cube are identified). The resulting manifold M is homeomorphic to the complement of the Borromean rings in S^3.

Borromean rings in S^3 (this is stated in [Hod86]). A presentation for $\pi_1 M$ is given by:

$$\pi_1 M = \langle a, b, c : [[a, b], c] = [[c, b^{-1}], a] = 1 \rangle.$$

We study the representation variety $\mathscr{R}_{par}(M)$ of representations $\rho : \pi_1 M \to \mathrm{PSL}(2, \mathbb{R})$ up to conjugacy such that $\rho[a, b]$ is parabolic (and so $\rho(c)$ is parabolic with the same fixed point). These representations correspond to transversely hyperbolic foliations which are "cusped" at one boundary component and have Dehn surgery type singularities at the other two boundary components (see [Hod86]).

Let T denote the punctured torus, with $\pi_1 T = \langle a, b \rangle$. Then $\pi_1 T \hookrightarrow \pi_1 M$, so that

$\mathscr{R}_{par}(M) \to \mathscr{R}_{par}(T)$. The elements of $\mathscr{R}_{par}(T)$ correspond to hyperbolic punctured tori (with a cusp at the puncture). A representation $\rho : \pi_1 T \to \mathrm{PSL}_2\,\mathbb{R}$ satisfies the parabolic condition if and only if $\rho(a), \rho(b)$ are hyperbolic elements with

$$\sinh \frac{l(a)}{2} \sinh \frac{l(b)}{2} \sin \varphi = 1$$

where $l(a), l(b)$ are the translation lengths of $\rho(a), \rho(b)$ respectively and φ is the angle between the axes. To lift such a representation to a representation of $\pi_1 M$, we must assign $\rho(c)$ so that the relations of $\pi_1 M$ are satisfied. Since $\rho(c)$ must commute with the parabolic $\rho[a, b]$, $\rho(c)$ is parabolic with the same fixed point. Let x denote the amount of parabolic translation of $\rho(c)$ relative to $\rho[a, b]$, so if $\rho[a, b] = \left(\begin{smallmatrix} -1 & 1 \\ 0 & -1 \end{smallmatrix}\right)$, then $\rho(c) = \left(\begin{smallmatrix} -1 & x \\ 0 & -1 \end{smallmatrix}\right)$. It turns out (by a nice geometric argument) that there are exactly two solutions for x:

$$x = 0 \quad \text{or} \quad x = \frac{1}{2}\mathrm{sech}\frac{l(a)}{2}\mathrm{sech}\frac{l(b)}{2} \cot \varphi.$$

This describes the representation variety $\mathscr{R}_{par}$ rather explicitly as the union of two irreducible two-dimensional components $\mathscr{R}_T$ and $\mathscr{R}_R$. The first component $\mathscr{R}_T$ ('T' for Teichmuller) consists of the obvious representations with $\rho(c) = 1$ and $\rho(a), \rho(b)$ generating a hyperbolic punctured torus group. The associated transversely hyperbolic foliations are products (with two fillable singularities at α and β). The second component $\mathscr{R}_R$ ('R' for regenerate) describes transversely hyperbolic foliations with more interesting structure. This component, in fact its complexification, is the relevant one for regenerating hyperbolic structures. Note that $\mathscr{R}_T$ and $\mathscr{R}_R$ meet (transversely) exactly at the locus of "rectangular" punctured tori ($\cot \varphi = 0$).

Remark 26. If we identify $\mathscr{R}_T$ with the Teichmuller space $\mathcal{T}_{1,1}$ of the punctured torus, then the singular set of $\mathscr{R}_{par}$, given by $\mathscr{R}_T \cap \mathscr{R}_R$, is exactly the *line of minima* for the curves a and b. In other words, $\mathscr{R}_T \cap \mathscr{R}_R$ consists of the representations in $\mathscr{R}_T$ where there is a relation between the differentials $dl(a)$ and $dl(b)$. The relevance of such a relation in the context of regeneration questions is discussed in Section 3.17 of [Hod86].

4.11.2 Regenerating 3D structures

Fix a particular rectangular punctured torus $\rho_0 : \pi_1 T \to \mathrm{PSL}(2, \mathbb{R})\mathbb{R}$, and lift ρ_0 to $\pi_1 M$ by setting $\rho_0(c) = 1$ (this is the only possible lift). Let v be a tangent vector at ρ_0, tangent to

the component $\mathscr{R}_R$ but transverse to $\mathscr{R}_T$. For suitably chosen v, the representation $\rho_0+\sigma v : \pi_1 M \to \mathrm{PSL}_2(\mathbb{R}+\mathbb{R}\sigma)$ is the holonomy of a robust HP structure (which can be constructed from eight tetrahedra). Now, as the variety $\mathscr{R}_R$ is smooth, the complexified variety $\mathscr{R}_R^{\mathbb{C}}$ is smooth at ρ_0. Thus the Zariski tangent vector iv is tangent to a path $\rho_t : \pi_1 M \to \mathrm{PSL}(2,\mathbb{C})$ which is compatible to first order with $\rho_0 + \sigma v$. By Proposition 15, the HP structure regenerates to a path of hyperbolic structures with holonomy ρ_t (or alternatively, this path of hyperbolic structures can be constructed directly using tetrahedra). Similarly, the variety $\mathscr{R}_R^{\mathbb{R}+\mathbb{R}\tau}$ is smooth at ρ_0 yielding a path of holonomies $\rho_t : \pi_1 M \to \mathrm{PSL}(2,\mathbb{R}+\mathbb{R}\tau)$ with $\rho_0' = \tau v$ so that Proposition 15 then produces a regeneration to AdS structures with holonomy ρ_t. Thus, our HP structure is transitional. Actually, in the AdS case, the representations can be constructed directly. Let $\sigma_t : \pi_1 M \to \mathrm{PSL}(2,\mathbb{R})$ be a path with $\sigma_0' = v$. Then, a path ρ_t of $\mathrm{PSL}(2,\mathbb{R}+\mathbb{R}\tau)$ representations with $\rho_0' = \tau v$ is defined by

$$\rho_t = \frac{1+\tau}{2}\sigma_t + \frac{1-\tau}{2}\sigma_{-t}.$$

4.11.3 An interesting flexibility phenomenon

The transitional HP structure from the previous sub-section, with holonomy $\rho_0 + \sigma v$, can be deformed in an interesting way. By Lemma 5, nearby HP structures are determined by nearby holonomy representations. We consider a deformation of the form

$$\rho_0 + \sigma(v + \epsilon u)$$

where ϵu is a small tangent vector at ρ_0, tangent to the component $\mathscr{R}_T$ and transverse to $\mathscr{R}_R$ (see Figure 4.14). Now, $\mathscr{R}_{par}^{\mathbb{C}}(M)$ is the union of its irreducible components $\mathscr{R}_T^{\mathbb{C}}$ and $\mathscr{R}_R^{\mathbb{C}}$ (locally at ρ_0). So, as u and v are tangent to different components of $\mathscr{R}_{par}(M)$, any Zariski tangent vector of the form $w+i(v+\epsilon u)$, for w real, is not integrable. Thus, the deformed HP structure *does not* regenerate to hyperbolic structures. However, it does regenerate to AdS structures. To see this, consider paths σ_t and μ_t with derivatives $2v$ and $2\epsilon u$ respectively at $t = 0$. Then,

$$\rho_t = \frac{1+\tau}{2}\sigma_t + \frac{1-\tau}{2}\mu_{-t}$$

gives a family of $\mathrm{PSL}(2,\mathbb{R}+\mathbb{R}\tau)$ representations with $\rho_0' = (v-\epsilon u)+\tau(v+\epsilon u)$. Proposition 15 now implies that the deformed HP structure regenerates to AdS structures.

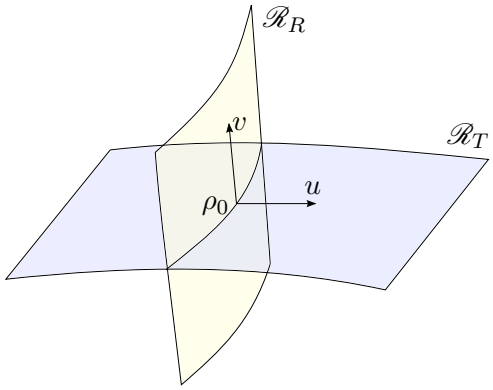

Figure 4.14: A schematic picture of the $\mathrm{PSL}(2,\mathbb{R})$ representation variety $\mathscr{R}_{par}(M)$. The variety is the union of two irreducible two-dimensional components which meet at the locus of rectangular punctured torus representations (with $c = 1$). We let ρ_0 be one such representation, with v tangent to one component, and u tangent to the other.

Remark 27. The author thanks Joan Porti for suggesting the possibility of this phenomenon.

Chapter 5

Ideal triangulations

In this chapter, we construct and deform transversely hyperbolic foliations, anti de Sitter structures, and half-pipe structures by building them out of ideal tetrahedra. This generalizes Thurston's construction of deformation spaces of triangulated hyperbolic structures (see [Thu80] or 2.2.4). Assume throughout that M^3 has a fixed topological ideal triangulation $\mathcal{T} = \{\mathcal{T}_1, \ldots, \mathcal{T}_n\}$ and that ∂M is a union of tori.

5.1 General construction of ideal tetrahedra

The following construction takes place in (real) projective space and is a bit more algebraic than the construction in $\mathbb{H}^3$ on which it is based. The generality of this construction is its main advantage. Geometric interpretations for the cases of interest will be given in the following sections.

We begin by recalling the construction from Section 4.8. Let $\mathcal{B}$ be a real two-dimensional (commutative) algebra with a (nontrivial) conjugation action:

$$z \mapsto \bar{z}$$
$$|z|^2 := z\bar{z} \ \in \ \mathbb{R}.$$

Note that we do not assume $|\cdot|^2$ is positive definite. It is easy to check that

$$\mathcal{B} \cong \mathbb{R} + \mathbb{R}\alpha$$

where α is a non-real element with square equal to -1,$+1$, or 0.

Consider the 2×2 matrices $M_2(\mathcal{B})$. There is an adjoint operation $A \mapsto A^*$ which simply takes the conjugate transpose of A. Let Herm_2 denote the 2×2 Hermitian matrices,

$$\text{Herm}_2 = \{A \in M_2(\mathcal{B}) : A^* = A\}.$$

As a real vector space, $\text{Herm}_2 \cong \mathbb{R}^4$. We define the following (real) inner product on Herm_2:

$$\left\langle \begin{bmatrix} a & z \\ \bar{z} & d \end{bmatrix}, \begin{bmatrix} e & w \\ \bar{w} & h \end{bmatrix} \right\rangle = -\frac{1}{2} tr \left(\begin{bmatrix} a & z \\ \bar{z} & d \end{bmatrix} \begin{bmatrix} h & -w \\ -\bar{w} & e \end{bmatrix} \right).$$

The signature of this metric depends on $\mathcal{B}$. The following defines a convex region in projective space:

$$\mathbb{X} = \{X \in \text{Herm}_2 : \langle X, X \rangle < 0\} / \sim$$

where $\sim$ represents the equivalence $X \sim \lambda X$ with $\lambda \in \mathbb{R}^*$. Note that $\langle X, X \rangle = -\det(X)$.

The ideal boundary $\partial^\infty \mathbb{X}$, given by the projectivized light cone with respect to this metric, is exactly the projectivized rank one Hermitian matrices, where for a Hermitian matrix X, rank one means $\det(X) = 0$, $X \neq 0$. Any rank one Hermitian matrix X can (up to $\pm$) be decomposed uniquely as

$$X = vv^*$$

where $v \in \mathcal{B}^2$ is a two-dimensional column vector with entries in $\mathcal{B}$ (and v^* denotes the transpose conjugate). Further v must satisfy that $\lambda v = 0$ for $\lambda \in \mathcal{B}$ if and only if $\lambda = 0$. This gives the identification

$$\partial^\infty \mathbb{X} = \mathbb{P}^1\mathcal{B} = \left\{ \begin{bmatrix} x \\ y \end{bmatrix} : \alpha x = \alpha y = 0 \text{ for } \alpha \in \mathcal{B} \iff \alpha = 0 \right\} / \sim$$

$$\text{where } \begin{bmatrix} x \\ y \end{bmatrix} \sim \begin{bmatrix} \lambda x \\ \lambda y \end{bmatrix} \text{ for } \lambda \in \mathcal{B}^\times.$$

The orientation preserving isometries of $\mathbb{X}$ are described by $\text{PGL}^+(2, \mathcal{B})$ (see Definition 22), which we think of as determinant ± 1 matrices with entries in $\mathcal{B}$, acting as follows:

$$A \cdot X := AXA^* \quad \text{where } X \in \mathbb{X} \text{ and } det(A) = \pm 1.$$

We also note that $\text{PGL}^+(2, \mathcal{B})$ acts by Mobius transformations on $\partial^\infty \mathbb{X} = \mathbb{P}^1\mathcal{B}$.

5.1.1 ideal tetrahedra

Now consider four points in the ideal boundary represented by rank one hermitian matrices Z_1, Z_2, Z_3, Z_4. From this data we define the following region in $\mathrm{Herm}_2(\mathcal{B})$:

$$T = \{t_1 Z_1 + t_2 Z_2 + t_3 Z_3 + t_4 Z_4 : \text{ all } t_i \text{ have the same sign and not all } t_i = 0\}.$$

Definition 23. T defines an *ideal tetrahedron* in $\mathbb{X}$ if T projects (under $\sim$) to a region contained in $\mathbb{X} \cup \partial\mathbb{X}$ whose intersection with $\partial\mathbb{X}$ is exactly the four ideal points $[Z_1], [Z_2], [Z_3], [Z_4]$.

Proposition 31. *T defines an ideal tetrahedron if and only if the following condition is met:*

$$\langle Z_i, Z_j \rangle < 0 \text{ for all } i \neq j \tag{5.1}$$

Remark 28. In the case $\mathcal{B} = \mathbb{C}$, $\mathbb{X} = \mathbb{H}^3$, the signs of the Z_i can always be chosen to satisfy condition 5.1. This is achieved by choosing the Z_i to have positive trace.

5.1.2 shape parameters

Let T be a tetrahedron defined by the rank one hermitian matrices Z_1, Z_2, Z_3, Z_4. Let the corresponding $\mathbb{P}^1\mathcal{B}$ elements be z_1, z_2, z_3, z_4.

Proposition 32. *If z_1, z_2, z_3, z_4 define an ideal tetrahedron, then using an element of* $\mathrm{PGL}^+(2, \mathcal{B})$*, these points can be put in* standard position *so that*

$$z_1 = \infty := \begin{bmatrix} 1 \\ 0 \end{bmatrix}, z_2 = 0 := \begin{bmatrix} 0 \\ 1 \end{bmatrix}, z_3 = 1 := \begin{bmatrix} 1 \\ 1 \end{bmatrix} \text{ and } z_4 = z.$$

Proof. Without loss in generality, we may assume $z_1 = \begin{bmatrix} 1 \\ 0 \end{bmatrix}$. Then, if $z_2 = \begin{bmatrix} x_2 \\ y_2 \end{bmatrix}$, we have

$$\langle Z_1, Z_2 \rangle = \left\langle \begin{bmatrix} 1 & 0 \\ 0 & 0 \end{bmatrix}, \begin{bmatrix} |x_2|^2 & x_2\bar{y}_2 \\ \bar{x}_2 y_2 & |y_2|^2 \end{bmatrix} \right\rangle = \frac{-|y_2|^2}{2}$$

So, $\langle Z_1, Z_2 \rangle < 0$ implies that $|y_2|^2 > 0$ so that $\begin{bmatrix} x_2 \\ y_2 \end{bmatrix} \sim \begin{bmatrix} x_2' \\ 1 \end{bmatrix}$. Using an element of

$\mathrm{PGL}^+(2,\mathcal{B})$ that fixes ∞, we move z_2 to $0 := \begin{bmatrix} 0 \\ 1 \end{bmatrix}$. Next, if $z_3 = \begin{bmatrix} x_3 \\ y_3 \end{bmatrix}$, then

$$\begin{aligned} \langle Z_1, Z_3 \rangle &= \frac{-|y_3|^2}{2} \\ \langle Z_2, Z_3 \rangle &= \frac{-|x_3|^2}{2} \end{aligned}$$

So, $\begin{bmatrix} x_3 \\ y_3 \end{bmatrix} \sim \begin{bmatrix} x_3' \\ 1 \end{bmatrix}$ with $|x_3'|^2 > 0$. We can now solve for a $\mathrm{PGL}^+(2,\mathcal{B})$ element that fixes $0, \infty$ and moves z_3 to 1:

$$\begin{bmatrix} \pm a & 0 \\ 0 & 1/a \end{bmatrix} \begin{bmatrix} x_3' \\ 1 \end{bmatrix} \sim \begin{bmatrix} 1 \\ 1 \end{bmatrix}$$

using the following easy lemma:

Lemma 11. *Let $c \in \mathcal{B}$. Then if $|c|^2 > 0$, the equation $x^2 = c$ or $x^2 = -c$ can be solved over $\mathcal{B}$.*

□

Definition 24. The parameter z determines the geometry of the tetrahedron, so it is called the *shape parameter*.

Remark 29. The shape parameter is a generalized cross ratio $z = (z_1 : z_2; z_3 : z_4)$. Some care is needed in defining such a cross ratio, as $\mathbb{P}^1\mathcal{B} \setminus \mathcal{B}$ contains more than just the point ∞ in general.

Proposition 33. *z_1, z_2, z_3, z_4 define an ideal tetrahedron in $\mathbb{X}$ if and only if the shape parameter z lies in $\mathcal{B} \subset \mathbb{P}^1\mathcal{B}$ and satisfies:*

$$|z|^2, |1-z|^2 > 0 \tag{5.2}$$

Proof. Assume the z_i are in standard position, and choose representatives

$$\begin{aligned} Z_1 &= \begin{bmatrix} 1 \\ 0 \end{bmatrix} \begin{bmatrix} 1 & 0 \end{bmatrix} = \begin{bmatrix} 1 & 0 \\ 0 & 0 \end{bmatrix} \\ Z_2 &= \begin{bmatrix} 0 \\ 1 \end{bmatrix} \begin{bmatrix} 0 & 1 \end{bmatrix} = \begin{bmatrix} 0 & 0 \\ 0 & 1 \end{bmatrix} \\ Z_3 &= \begin{bmatrix} 1 \\ 1 \end{bmatrix} \begin{bmatrix} 1 & 1 \end{bmatrix} = \begin{bmatrix} 1 & 1 \\ 1 & 1 \end{bmatrix} \\ Z_4 &= \begin{bmatrix} a \\ b \end{bmatrix} \begin{bmatrix} \bar{a} & \bar{b} \end{bmatrix} = \begin{bmatrix} |a|^2 & a\bar{b} \\ \bar{a}b & |b|^2 \end{bmatrix} \end{aligned}$$

where we are free to change the signs (or even multiply by a non-zero real number). We desire the Z_i to satisfy condition 5.1. First, note that

$$\langle Z_1, Z_2 \rangle, \langle Z_1, Z_3 \rangle, \langle Z_2, Z_3 \rangle = -\frac{1}{2} < 0$$

so it will not be fruitful to change the signs of Z_1, Z_2 or Z_3. Next,

$$\begin{aligned} \langle Z_1, Z_4 \rangle &= -\frac{|b|^2}{2} \\ \langle Z_2, Z_4 \rangle &= -\frac{|a|^2}{2} \\ \langle Z_3, Z_4 \rangle &= -\frac{1}{2}(|a|^2 + |b|^2 - a\bar{b} - \bar{a}b) = |a - b|^2. \end{aligned}$$

Condition 5.1 is satisfied if and only if $|a|^2, |b|^2$ and $|a - b|^2 > 0$, which is true if and only if

$$\begin{bmatrix} a \\ b \end{bmatrix} \sim \begin{bmatrix} z \\ 1 \end{bmatrix}$$

with $|z|^2, |z - 1|^2 > 0$. □

Remark 30. Using the language of Lorentzian geometry, we say that z and $z - 1$ are *space-like*. In fact, all facets of an ideal tetrahedron are space-like and totally geodesic with respect to the metric induced by $\langle \cdot, \cdot \rangle$ on $\mathbb{X}$.

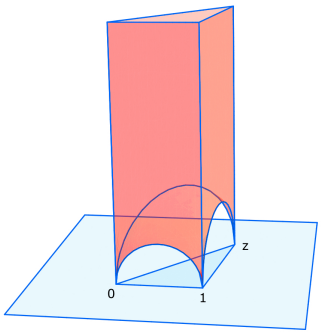

Figure 5.1: The ideal tetrahedron defined by the ideal points $0, 1, \infty, z \in \mathcal{B}$. In this picture $\mathcal{B} = \mathbb{C}$ and $\mathbb{X} = \mathbb{H}^3$.

The ordering of the vertices determines an orientation of the tetrahedron. Any face of the tetrahedron, which is determined by three vertices, inherits an orientation from the order of the z_i according to the familiar rules from (simplicial/singular) homology. Specifically: $\triangle z_1 z_2 z_3, \triangle z_1 z_3 z_4, \triangle z_2 z_4 z_3, \triangle z_1 z_4 z_2$ are given the orientation coming from the cyclic order of the vertices.

Definition 25. The ideal tetrahedron T determined by z_1, z_2, z_3, z_4 is *positively oriented* if the induced orientation on the faces is such that the normal to each face points toward the exterior of the tetrahedron.

Proposition 34. *The ideal tetrahedron T determined by z_1, z_2, z_3, z_4 is positively oriented if and only if its shape parameter z has positive imaginary part.*

Proof. We orient $\partial^\infty \mathbb{X}$ so that the direction pointing toward $\mathbb{X}$ is positive. Then $\mathcal{B} \subset \partial \mathbb{X}$ inherits an orientation allowing us to make sense of the notion of positive imaginary part (use any oriented basis $\{1, v\}$). The proof of the proposition is straightforward. □

Definition 26. The ideal tetrahedron T determined by z_1, z_2, z_3, z_4 is called a *degenerate* $\mathbb{H}^2$ tetrahedron if T is contained in a hyperbolic plane.

Proposition 35. *The ideal tetrahedron T determined by z_1, z_2, z_3, z_4 is degenerate if and only if its shape parameter z is real.*

The shape parameter z determines the isometry type of T. We think of the shape parameter of $T(z_1, z_2, z_3, z_4)$ as corresponding to the edge $z_1 z_2$. In other words, if we switch the ordering of the z_i (but maintain the orientation of T), and consider for example

$T(z_1, z_3, z_4, z_2)$, we get a different shape parameter, the one corresponding to $z_1 z_3$, which is $\frac{1}{1-z}$. Figure 5.2 summarizes the relationship between the shape parameters of the six edges of an ideal tetrahedron. There is a geometric interpretation of this, familiar from

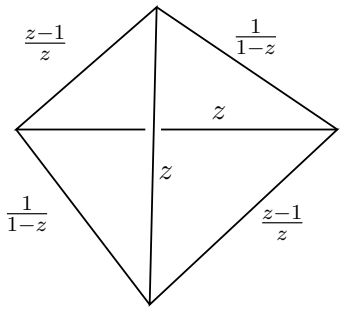

Figure 5.2: The shape parameters corresponding to the six edges of an ideal tetrahedron.

Thurston's notes. Let us assume $z_1 = \infty$ and $z_2, z_3, z_4 \in \mathcal{B} \subset \mathbb{P}^1\mathcal{B}$. Think of $\mathcal{B}$ as a plane with metric induced by $|\cdot|^2$ and with origin at z_2. The edge $z_1 z_2$ is a line connecting z_2 to ∞, drawn as a vertical line emanating from the origin of $\mathcal{B}$. The elements of $\mathrm{PGL}^+(2, \mathcal{B})$ that preserve this edge are described exactly by the group of space-like elements of $\mathcal{B}$, which can be thought of as similarities of $(\mathcal{B}, |\cdot|^2)$ which fix z_2. The shape parameter z should be thought of as the element of this group which transforms the edge $z_2 z_3$ to $z_2 z_4$. It can be be computed by

$$z = \frac{z_4 - z_2}{z_3 - z_2}.$$

If we instead focus on the edge $z_1 z_3$, so that z_3 is the origin, the new shape parameter is given by

$$\frac{z_2 - z_3}{z_4 - z_3} = \frac{1}{1 - z}$$

and similarly the shape parameter corresponding to the edge $z_1 z_4$ is given by

$$\frac{z_3 - z_4}{z_2 - z_4} = \frac{z - 1}{z}.$$

5.1.3 Glueing tetrahedra together

The faces of an ideal tetrahedron are hyperbolic ideal triangles. Given two tetrahedra T, S and a face $\triangle v_1 v_2 v_4, \triangle w_1 w_2 w_3$ on each such that the orientations are opposite, there is a

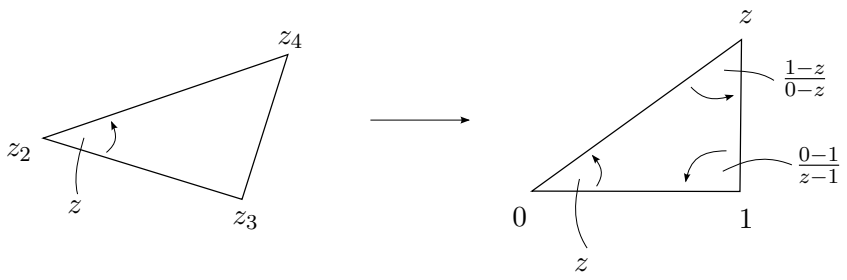

Figure 5.3: calculation of shape parameters corresponding to the various edges of T.

unique isometry $A \in \mathrm{PGL}^+(2, \mathcal{B})$ mapping

$$\begin{aligned} w_1 &\mapsto v_1 \\ w_2 &\mapsto v_2 \\ w_3 &\mapsto v_4 \end{aligned}$$

that glues S to T along the given faces. Suppose T, S are in standard position so that $v_1 = w_1 = \infty$, $v_2 = v_2 = 0$, $v_3 = w_3 = 1$ and $v_4 = z$. Then the glueing map A fixes ∞ and 0 and acts as a (linear) similarity of $(\mathcal{B}, |\cdot|^2)$. This similarity is exactly multiplication by the shape parameter z associated to the edge v_1v_2 of T. Composition of glueing maps for tetrahedra $T_1, T_2, \ldots, T_n$ in standard position about the common edge 0∞ is described by the product of shape parameters $z_1 z_2 \ldots z_{n-1}$ (this describes the map that glues T_n on to the other $n-1$ tetrahedra which have already been glued together). Hence, in order for the geometric structure to extend over an interior edge e of a union of tetrahedra, our shape parameters must satisfy:

$$\prod_{T_i \text{ meets edge } e} z_i = 1 \tag{5.3}$$

where z_i is the shape parameter of T_i with respect to the edge of T_i being identified to e. In fact we need that the development of the tetrahedra around the edge e winds around the edge exactly once (in other words $\prod z_i$ is a rotation by 2π rather than $2\pi n$ for some $n \neq 1$). The terminology we will use for this condition is the following:

Definition 27. Given ideal tetrahedra $T_1, \ldots, T_n$ glued together around and edge e, we say that the edge e has *total dihedral angle* 2π if the development of the tetrahedra in $\mathbb{X} \setminus e$ has

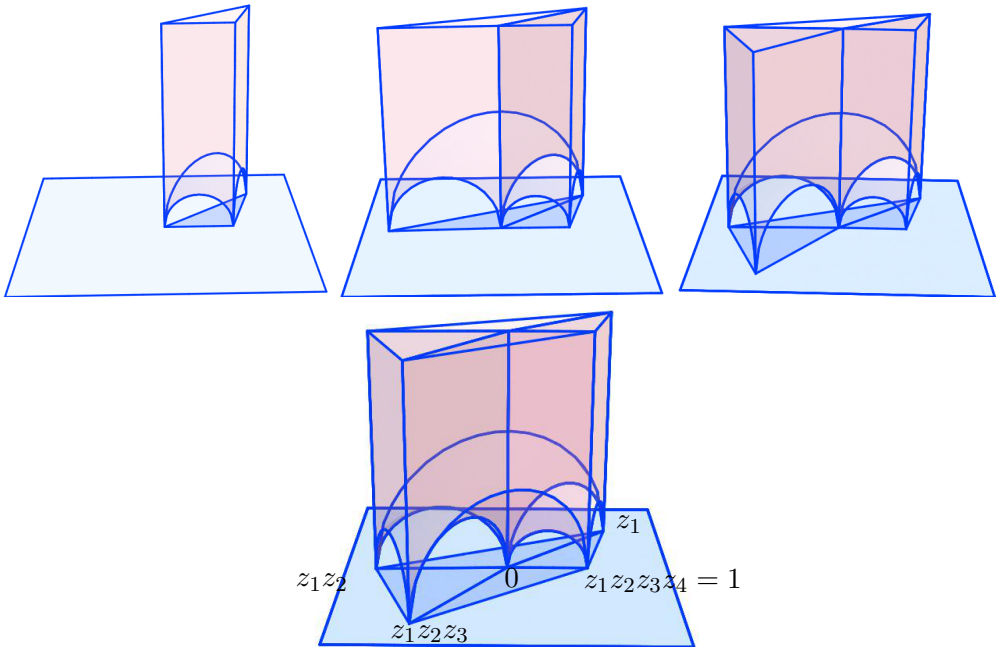

Figure 5.4: Glueing tetrahedra together around an edge.

rotational part exactly 2π. Note that in some cases, $\mathbb{X}$ will not have a continuous group of isometries which rotate around e. Nonetheless, rotations by multiples of π are always defined in $\mathbb{X} \setminus e$.

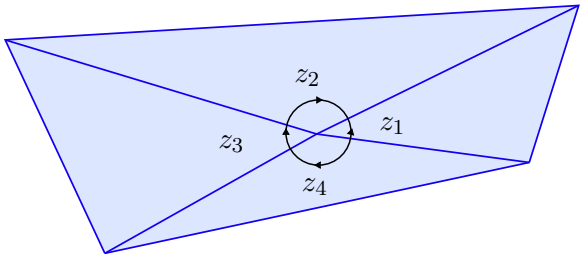

Figure 5.5: The shape parameters going around an edge must have product one and total dihedral angle 2π.

Let M be a three-manifold with a fixed topological ideal triangulation $\mathcal{T} = \{\mathcal{T}_1, \ldots, \mathcal{T}_n\}$, that is M is the union of tetrahedra $\mathcal{T}_i$ glued together along faces, with vertices removed. A triangulated $\mathbb{X}$ structure on M is a realization of all the tetrahedra comprising M as geometric tetrahedra so that the structure extends over all interior edges of the triangulation. This

amounts to assigning each tetrahedron $\mathcal{T}_i$ a shape parameter z_i. For each interior edge e of our union of tetrahedra, we get an equation of the form 5.3. All of these equations together make up *Thurston's equations* (also commonly called the *edge consistency equations*). The solutions of these equations (with total dihedral angle 2π around each edge) make up the *deformation variety* of triangulated $\mathbb{X}$ structures on M.

5.2 Triangulated geometric structures

We apply the general construction just described to build triangulated geometric structures for the cases $\mathbb{X} = \mathbb{H}^3, \mathbb{H}^2, \mathrm{AdS}^3, \mathrm{HP}^3$.

5.2.1 tetrahedra in $\mathbb{H}^3$

Assume that our algebra $\mathcal{B} = \mathbb{C}$. In this case, the inner product $\langle \cdot, \cdot \rangle$ on $\mathrm{Herm}_2(\mathbb{C})$ is of type $(3, 1)$ and $\mathbb{X}$ is the projective model for $\mathbb{H}^3$. Since $|z|^2 \geq 0$ holds for any z with equality if and only if $z = 0$, Proposition 33 gives the well-known fact that any $z \in \mathbb{C} \setminus \{0, 1\}$ is a valid shape parameter defining an ideal tetrahedron in $\mathbb{H}^3$.

Thus, if M is a three-manifold with fixed ideal triangulation $\mathcal{T} = \{\mathcal{T}_1, \ldots, \mathcal{T}_n\}$, hyperbolic structures on $(M, \mathcal{T})$ are obtained by solving Thurston's equations (5.3) over $\mathbb{C}$ with all shape parameters z_i having positive imaginary part.

Cone manifolds

Consider a triangulated manifold $(M, \mathcal{T})$. Let us assume that there is only one ideal vertex v in $\mathcal{T}$ (after identification). Then ∂M, which is naturally identified with $L(v)$, has only one component. Assume that ∂M is a torus and that M has a fixed hyperbolic structure determined by a positively oriented solution to Thurston's equations. Let $\mathcal{N}(v)$ be a deleted neighborhood of v in M. The hyperbolic structure on M induces a Euclidean similarity structure on $L(v)$. In [Thu80], it is shown that the geodesic completion of $\mathcal{N}(v)$ can be understood in terms of this similarity structure. We briefly recall the main idea here. Let $D_\partial : \widetilde{L(v)} \to \mathbb{C}$ be the developing map for the similarity structure on $L(v)$. If M is not complete near v, then the holonomy H of the similarity structure on $L(v)$ fixes a point, which we may assume to be the origin. Then $H : \pi_1 L(v) \to \mathbb{C}^*$ is the *exponential complex length* function restricted to $\pi_1 \partial M$. The lift $\widetilde{H}$ of this representation to $\widetilde{\mathbb{C}^*} = \mathbb{C}$ via analytic

continuation of log gives the *complex length* of $\pi_1\partial M$ elements:

$$\widetilde{H}(\gamma) = \log|H(\gamma)| + i\tilde{\mathcal{R}}(\gamma)$$

where $\tilde{\mathcal{R}}(\gamma)$ is the *total rotational part* of the holonomy of γ (see Definition 17 of Section 4.2), which measures the total angle around 0 swept out by developing along γ. Now, some curves $\gamma \in \pi_1 L(v)$ have a non-trivial dilation component $|H(\gamma)|$ and some others have a non-trivial rotational part $\tilde{\mathcal{R}}(\gamma)$ (this follows from the more general theory of affine structures on the torus [NY74]). It follows that the image of D_∂ is all of $\mathbb{C}^*$. In the upper half-space model, the developing map D_∂ is the "shadow" of the developing map $D : \widetilde{\mathcal{N}(v)} \to \mathbb{H}^3$. So the image of D is $I \setminus \mathfrak{L}$, where I is a neighborhood of the geodesic $\mathfrak{L}$ with endpoints $0, \infty$. The completion of $\widetilde{\mathcal{N}(v)}$ is then given by adjoining a copy of $\mathfrak{L}$. So the completion of $\mathcal{N}(v)$ is

$$\begin{aligned}\overline{\mathcal{N}(v)} &= \left(\widetilde{I \setminus \mathfrak{L}} \cup \mathfrak{L}\right) / \widetilde{H}(\pi_1\partial M) \\ &= \mathcal{N}(v) \cup (\mathfrak{L}/H(\pi_1\partial M)).\end{aligned}$$

In particular, if the moduli $|H(\pi_1\partial M)|$ form a discrete subgroup of the multiplicative group $\mathbb{R}^+$, then $\mathfrak{L}/H(\pi_1\partial M)$ is a circle and $\overline{\mathcal{N}(v)}$ is a manifold. This is the case if and only if there exists a generator α of $\pi_1\partial M$ such that $\widetilde{H}(\alpha)$ is a rotation. In this case the completion $\overline{M}$ (which is given near the boundary by $\overline{\mathcal{N}(v)}$) is topologically the Dehn filled manifold M_α, gotten by Dehn filling along the curve α. The cone angle is the total rotation angle $\tilde{\mathcal{R}}(\alpha)$ of α.

Remark 31. If the moduli $|H(\pi_1\partial M)|$ are dense in $\mathbb{R}^+$, the geodesic completion of M near v has a topological singularity, called a Dehn surgery type singularity. We do not address this case here.

Example 1. (Figure eight knot complement) Let M be the figure eight knot complement. Let $\mathcal{T}$ be the decomposition of M into two ideal tetrahedra (four faces, two edges, and one ideal vertex) well-known from [Thu80]. The edge consistency equations reduce to the following:

$$z_1(1-z_1)z_2(1-z_2) = 1. \tag{5.4}$$

The exponential complex length of the longitude ℓ and the meridian m, which can be read

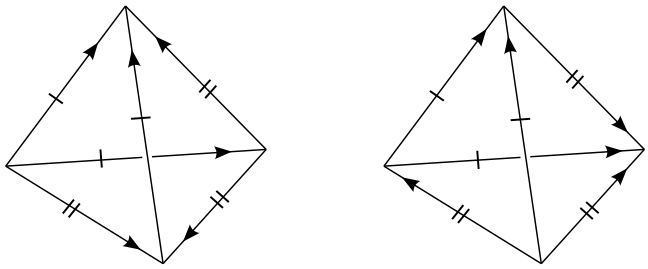

Figure 5.6: The figure eight knot complement is the union of two ideal tetrahedra. In the diagram, identify two faces if the boundary edges and their orientations match.

off from the triangulation of ∂M (see Figure 5.7), are given by

$$H(\ell) = z_1^2(1-z_1)^2$$
$$H(m) = z_2(1-z_1).$$

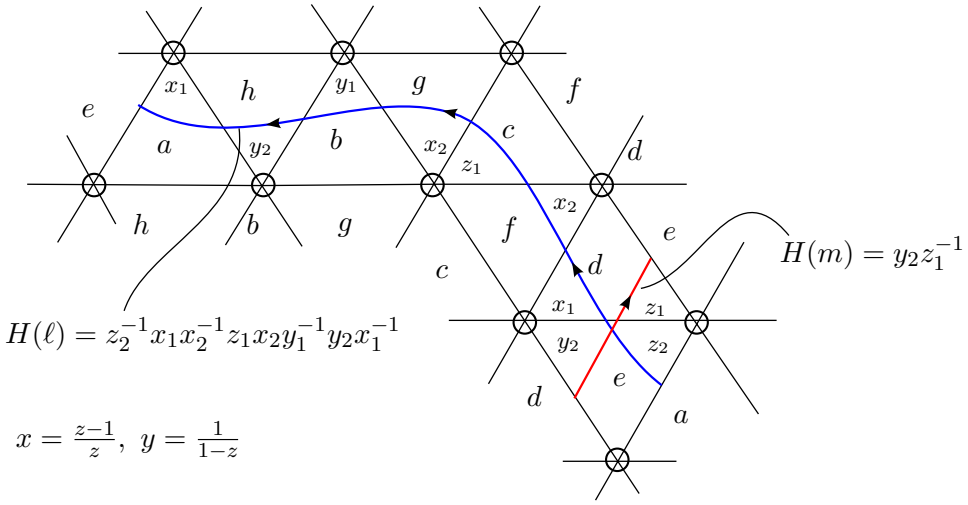

Figure 5.7: The exponential complex lengths of ℓ and m can be read off from a picture of the tessellation of ∂M. The triangles are labeled as in [Thu80, Ch. 4]

Let $\theta \in (0, 2\pi)$ and consider solutions to the Equation (5.4) with the added condition that

$$H(\ell) = z_1^2(1-z_1)^2 = e^{i\theta}.$$

A positively oriented solution is given by

$$z_1 = \frac{1 \pm \sqrt{1 - 4e^{i\theta/2}}}{2}$$

$$z_2 = \frac{1 \pm \sqrt{1 - 4e^{-i\theta/2}}}{2}$$

where we may choose the root with positive imaginary part. The solution gives a hyperbolic structure whose completion $\bar{M}$ is topologically the manifold M_ℓ gotten by Dehn filling M along ℓ. The completed hyperbolic structure has a cone singularity with cone angle θ. Note that $\bar{M}$ is a torus bundle over the circle with monodromy $\begin{pmatrix} 2 & 1 \\ 1 & 1 \end{pmatrix}$ and the singular locus is a curve running once around the circle direction.

5.2.2 Flattened tetrahedra and transversely hyperbolic foliations

Consider the degenerate case $\mathcal{B} = \mathbb{R}$. Then $\mathrm{Herm}_2(\mathbb{R})$ is the symmetric real matrices (which is $\mathbb{R}^3$ as a vector space) and $\langle \cdot, \cdot \rangle$ is of signature $(2, 1)$. The resulting geometry is $\mathbb{X} = \mathbb{H}^2$. Proposition 33 gives that any $z \in \mathbb{R} \setminus \{0, 1\}$ is a valid shape parameter defining an ideal tetrahedron in $\mathbb{H}^2$. Such tetrahedra are *degenerate*. However, we may still think of the faces as being oriented, so that we can tell which side of a given triangle faces outward from the tetrahedron. In figure 5.8, edge crossings are drawn in such a way as to indicate which faces are in front and which faces are in back.

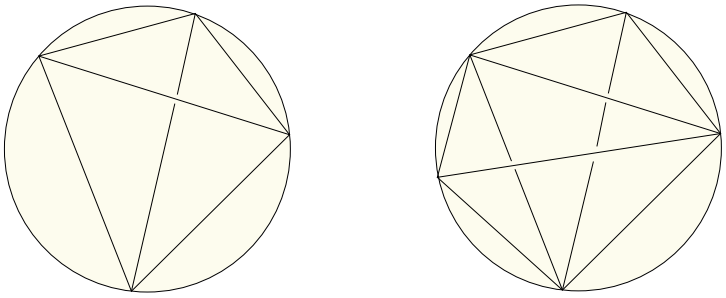

Figure 5.8: A degenerate tetrahedron drawn in the Klein model on the left. Two degenerate tetrahedra glued together along faces with opposite orientation on the right.

Proposition 36. *A solution to Thurston's equations (5.3) over* $\mathbb{R}$ *defines a transversely hyperbolic foliation on* M*. Such a structure will be referred to as a* triangulated transversely

hyperbolic foliation *on* $(M, \mathcal{T})$. *The deformation variety* $\mathscr{D}_{\mathbb{R}}$ *of these structures is called the* real deformation variety*.*

Proof. A degenerate tetrahedron $T(\infty, 0, 1, z)$, with $z \in \mathbb{R}$, should be thought of as map from a topological ideal tetrahedron $\mathcal{T}_j$ into $\mathbb{H}^2$ which is a local submersion and sends facets of $\mathcal{T}_j$ to the corresponding geodesic facets of the degenerate ideal tetrahedron $T(\infty, 0, 1, z)$. Such local submersions of the topological tetrahedra $\mathcal{T}_j \in \mathcal{T}$ can be developed to produce a globally defined local submersion

$$D : \widetilde{M} \to \mathbb{H}^2$$

which is equivariant with respect to a representation

$$\rho : \pi_1 M \to \mathrm{PGL}(2, \mathbb{R}).$$

That the shape parameters satisfy Thurston's equations guarantees that the map D can be made a local submersion at the edges of the triangulation. The map D can be thought of as a degenerate developing map defining a transversely hyperbolic foliation on M. □

Note that, in this case, the condition that the development of tetrahedra around an edge be of winding number one is equivalent to requiring that exactly two of the z_i at that edge be negative. Such negative real shape parameters are thought of as having dihedral angle π, while positive real shape parameters have dihedral angle zero.

Remark 32. In the case of non-positively oriented solutions to Thurston's equations over $\mathbb{C}$ (which do not directly determine $\mathbb{H}^3$ structures), it is possible for the dihedral angle at an edge of some tetrahedron, defined via analytic continuation, to lie outside the range $(0, \pi)$. In the case that a path of such solutions converges to a real solution, each dihedral angle converges to $k\pi$ for some k, possibly with $k \neq 0, 1$. We ignore these real solutions; there are no positively oriented solutions nearby.

Example 2. (Figure eight knot complement) Let M be the complement of the figure eight knot as defined in Example (1). To find transversely hyperbolic foliations on M, we solve the edge consistency equations

$$z_1(1 - z_1)z_2(1 - z_2) = 1. \tag{5.5}$$

over $\mathbb{R}$. The variety of solutions to (5.5) has four (topological) components:

1. $z_1 < 0$ and $z_2 < 0$
2. $z_1 < 0$ and $z_2 > 1$
3. $z_1 > 1$ and $z_2 < 0$
4. $z_1 > 1$ and $z_2 > 1$

Cases 1 and 4 determine solutions with angular holonomy 4π around one edge and zero around the other edge. So these solutions are discarded. Cases 2 and 3 are symmetric under switching z_1 and z_2. So, the transversely hyperbolic structures on $(M, \mathcal{T})$ are parametrized by $z_1 < 0$ (which determines $z_2 > 1$). It follows that the structures are also parametrized by $H(\ell) = z_1^2(1 - z_1)^2$. This is a special case of Theorem 7.

5.2.3 tetrahedra in AdS^3

Let $\mathcal{B}$ be the real algebra generated by an element τ, with $\tau^2 = +1$. As a vector space $\mathcal{B} = \mathbb{R} + \mathbb{R}\tau$ is two dimensional over $\mathbb{R}$. The conjugation operation is given by

$$a + b\tau \longmapsto \overline{a + b\tau} = a - b\tau.$$

In this case, the form $\langle \cdot, \cdot \rangle$ on $\mathrm{Herm}_2(\mathcal{B})$ is of signature $(2, 2)$ and $\mathbb{X} = \mathrm{AdS}^3$. Before constructing triangulated AdS structures, we discuss some important properties of the algebra $\mathcal{B} = \mathbb{R} + \mathbb{R}\tau$.

The algebra $\mathcal{B} = \mathbb{R} + \mathbb{R}\tau$

First, note that $\mathcal{B}$ is not a field as e.g.

$$(1 + \tau) \cdot (1 - \tau) = 0.$$

The square-norm defined by the conjugation operation

$$|a + b\tau|^2 = (a + b\tau)\overline{(a + b\tau)} = a^2 - b^2,$$

comes from the $(1, 1)$ Minkowski inner product on $\mathbb{R}^2$ (with basis $\{1, \tau\}$). The space-like elements of $\mathcal{B}$ (i.e. square-norm > 0), acting by multiplication on $\mathcal{B}$ form a group and can be thought of as the similarities of the Minkowski plane that fix the origin. Note that if

$|a+b\tau|^2 = 0$ then $b = \pm a$ and multiplication by $a+b\tau$ collapses all of $\mathcal{B}$ onto the light-like line spanned by $a+b\tau$.

The elements $\frac{1+\tau}{2}$ and $\frac{1-\tau}{2}$ are two spanning idempotents which annihilate one another:

$$\left(\frac{1\pm\tau}{2}\right)^2 = \frac{1\pm\tau}{2}, \quad \text{and} \quad \left(\frac{1+\tau}{2}\right)\cdot\left(\frac{1-\tau}{2}\right) = 0.$$

Thus $\mathcal{B} \cong \mathbb{R}\oplus\mathbb{R}$ as $\mathbb{R}$ algebras via the isomorphism

$$a\left(\frac{1+\tau}{2}\right) + b\left(\frac{1-\tau}{2}\right) \longmapsto (a,b). \tag{5.6}$$

We have a similar splitting for $M_2(\mathcal{B})$:

$$\left(\frac{1+\tau}{2}A + \frac{1-\tau}{2}B\right)\cdot\left(\frac{1+\tau}{2}C + \frac{1-\tau}{2}D\right) = \left(\frac{1+\tau}{2}AC + \frac{1-\tau}{2}BD\right)$$

and also

$$\det\left(\frac{1+\tau}{2}A + \frac{1-\tau}{2}B\right) = \frac{1+\tau}{2}\det(A) + \frac{1-\tau}{2}\det(B).$$

Therefore $\mathrm{PSL}(2,\mathcal{B}) \cong \mathrm{PSL}(2,\mathbb{R})\times\mathrm{PSL}(2,\mathbb{R})$. $\mathrm{Isom}^+\,\mathrm{AdS}^3 = \mathrm{PGL}^+(2,\mathcal{B})$ is the subgroup of $\mathrm{PGL}(2,\mathbb{R})\times\mathrm{PGL}(2,\mathbb{R})$ such that the determinant has the same sign in both factors.

Proposition 37. *$\mathbb{P}^1\mathcal{B} \cong \mathbb{P}^1\mathbb{R}\times\mathbb{P}^1\mathbb{R}$ and the isomorphism (given below) identifies the action of $\mathrm{PGL}(2,\mathcal{B})$ on $\mathbb{P}^1\mathcal{B}$ with that of $\mathrm{PGL}(2,\mathbb{R})\times\mathrm{PGL}(2,\mathbb{R})$ on $\mathbb{P}^1\mathbb{R}\times\mathbb{P}^1\mathbb{R}$.*

Proof. The isomorphism $\mathbb{P}^1\mathbb{R}\times\mathbb{P}^1\mathbb{R} \to \mathbb{P}^1\mathcal{B}$ is given by

$$\begin{bmatrix}a\\b\end{bmatrix}, \begin{bmatrix}c\\d\end{bmatrix} \longmapsto \frac{1+\tau}{2}\begin{bmatrix}a\\b\end{bmatrix} + \frac{1-\tau}{2}\begin{bmatrix}c\\d\end{bmatrix}$$

□

Now, $\mathbb{P}^1\mathcal{B}$ is the *Lorentz compactification* of $\mathcal{B} = \left\{\begin{bmatrix}x\\1\end{bmatrix} : x\in\mathcal{B}\right\}$. The added points make up a wedge of circles, so that $\mathbb{P}^1\mathcal{B}$ is topologically a torus. The square-norm $|\cdot|^2$ on $\mathcal{B}$ induces a flat conformal Lorentzian structure on $\mathbb{P}^1\mathcal{B}$ that is preserved by $\mathrm{PGL}^+(2,\mathcal{B})$. We refer to $\mathrm{PGL}^+(2,\mathcal{B})$ as the *Lorentz Mobius transformations*. With its conformal structure $\mathbb{P}^1\mathcal{B}$ is the $(1+1)$-dimensional Einstein universe $\mathrm{Ein}^{1,1}$ (see e.g. [BCD+08]).

Thurston's equations for AdS^3

We think of $\mathbb{R} + \mathbb{R}\tau$ as the Lorentzian plane equipped with the metric induced by $|\cdot|^2$. Proposition 33 immediately implies:

Proposition 38. *The following are equivalent:*

1. *The ideal tetrahedron $T(z_1, z_2, z_3, z_4)$ is defined.*
2. *The shape parameter z of the edge z_1z_2 of T satisfies $|z|^2, |1-z|^2 > 0$.*
3. *The shape parameters $z, \frac{1}{1-z}, \frac{z-1}{z}$ of all edges of T are each space-like.*
4. *Placing z_1 at ∞, the triangle $\triangle z_2z_3z_4$ has space-like edges in the Lorentzian plane.*

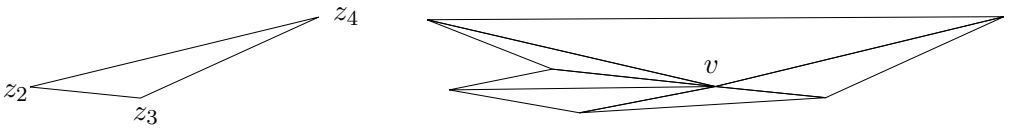

Figure 5.9: left: Placing one vertex z_1 at infinity, the other three vertices z_2, z_3, z_4 determine a *spacelike* triangle in the Lorentzian plane: $|z_2 - z_3|^2, |z_3 - z_4|^2, |z_4 - z_2|^2 > 0$. right: if tetrahedra are glued together along an interior edge (connecting ∞ to v), the corresponding space-like triangles must fit together around the vertex v.

Similar to the case of degenerate tetrahedra, the total dihedral angle condition is discrete for AdS tetrahedra:

Proposition 39. *The condition of Definition 27, that the total dihedral angle around an interior edge be 2π, is equivalent to the condition that exactly two of the z_i at that edge have negative real part.*

Using the isomorphism (5.6), a shape parameter $z \in \mathbb{R} + \mathbb{R}\tau$ can be described as a pair (λ, μ) of real numbers:

$$z = \frac{1+\tau}{2}\lambda + \frac{1-\tau}{2}\mu$$

Proposition 40. *z is the shape parameter for an ideal tetrahedron in* AdS *if and only if λ, μ lie in the same component of $\mathbb{R} \setminus \{0, 1\}$.*

Proof. We have

$$|z|^2 = \lambda\mu,$$
$$|1-z|^2 = (1-\lambda)(1-\mu).$$

Hence $|z|^2, |1-z|^2 > 0$ if and only if λ and μ have the same sign and $1-\lambda$ and $1-\mu$ have the same sign. □

Proposition 41. *A tetrahedron with shape parameter z is positively oriented if and only $\lambda > \mu$.*

Proof. The imaginary part of z is $\frac{\lambda-\mu}{2}$. □

These propositions combine to give:

Proposition 42. *The shape parameters $z_i = \frac{1+\tau}{2}\lambda_i + \frac{1-\tau}{2}\mu_i$, for $i = 1, \ldots, n$, define positively oriented ideal tetrahedra that glue together compatibly around an edge in* AdS^3 *if and only if:*

- $\prod_{i=1}^n \lambda_i = 1 \quad$ *and* $\quad \prod_{i=1}^n \mu_i = 1$.
- *λ_i, μ_i lie in the same component of $\mathbb{R} \setminus \{0, 1\}$ for each $i = 1, \ldots, n$,*
- *$\lambda_i > \mu_i$ for each $i = 1, \ldots, n$.*
- *For exactly two $i \in \{1, \ldots, n\}$, we have $\lambda_i, \mu_i < 0$.*

Thus a triangulated AdS structure on $(M, \mathcal{T})$ is determined by two triangulated transversely hyperbolic foliations on $(M, \mathcal{T})$ whose shape parameters (λ_i) and (μ_i) obey the conditions set out in the above Propositions. This gives a concrete method for regenerating AdS structures from transversely hyperbolic foliations:

Corollary. *Let (λ_i) be shape parameters defining a transversely hyperbolic foliation on $(M, \mathcal{T})$. Suppose this structure can be deformed to a new one with shape parameters $\lambda_i' > \lambda_i$. Then $z_i = \frac{1+\tau}{2}\lambda_i + \frac{1-\tau}{2}\lambda_i'$ defines an* AdS *structure on $(M, \mathcal{T})$.*

Question. When and how do two transversely hyperbolic foliations on M determine an AdS structure in the absence of an ideal triangulation?

Tachyons

Consider a triangulated manifold $(M, \mathcal{T})$. Let us assume that there is only one ideal vertex v in $\mathcal{T}$ (after identification). Then ∂M, which is naturally identified with $L(v)$, has only one component. Assume that ∂M is a torus and that M has a fixed AdS structure determined

by a positively oriented solution to Thurston's equations over $\mathcal{B} = \mathbb{R} + \mathbb{R}\tau$. Let $\mathcal{N}(v)$ be a deleted neighborhood of v in M. Similar to the hyperbolic case, the AdS structure on M induces a structure on $L(v)$ modeled on the similarities of the Minkowski plane $\mathbb{R}^{1,1}$ which we identify with $\mathcal{B}$. The similarities of $\mathcal{B}$ that fix the origin are exactly the space-like elements $\mathcal{B}^+$ (i.e. the elements with positive square-norm). Just as in the hyperbolic case, the geodesic completion of $\mathcal{N}(v)$ can be understood in terms of this similarity structure. Let $D_\partial : \widetilde{L(v)} \to \mathcal{B}$ be the developing map. If M is not complete near v, then the holonomy H of the similarity structure on $L(v)$ fixes a point, which we may assume to be the origin. Then $H : \pi_1 L(v) \to \mathcal{B}^+$ is the *exponential $\mathcal{B}$-length* function restricted to $\pi_1 \partial M$. The image of D_∂ does not contain the origin, so D_∂ determines a lift $\widetilde{H}$ of H to the similarities $\widetilde{\mathcal{B}}^+$ of $\widetilde{\mathbb{R}^{1,1} \setminus 0}$:

$$\begin{aligned} \widetilde{H}(\gamma) &= \log|H(\gamma)| + \tau\varphi(\gamma) + i\tilde{\mathcal{R}}(\gamma) \\ &\in \quad \mathbb{R} + \tau\mathbb{R} + i\pi\mathbb{Z} \end{aligned}$$

where $\varphi(\gamma)$ is the hyperbolic angle of the boost part of $H(\gamma)$ and $\tilde{\mathcal{R}}(\gamma)$ is the *total rotational part* of the holonomy of γ (see Definition 17 of Section 4.2), which is an integer multiple of π measuring the number of half rotations around 0 swept out by developing along γ. Assume that there is some element of $\pi_1 \partial M$ with non-zero discrete rotational part. Then D_∂ is a covering map onto $\mathcal{B} \setminus 0$ (this follows from the more general theory of affine structures on the torus [NY74]). In the half-space model for AdS (see Appendix A), the developing map D_∂ is the "shadow" of the developing map $D : \widetilde{\mathcal{N}(v)} \to \mathrm{AdS}^3$. So the image of D is $I \setminus \mathfrak{L}$, where I is a neighborhood of the geodesic $\mathfrak{L}$ with endpoints $0, \infty$ (note that I is no longer a cone as it was in the hyperbolic case). The completion of $\widetilde{\mathcal{N}(v)}$ is then given by adjoining a copy of $\mathfrak{L}$. So the completion of $\mathcal{N}(v)$ is

$$\begin{aligned} \overline{\mathcal{N}(v)} &= \left(\widetilde{I \setminus \mathfrak{L}} \cup \mathfrak{L}\right) / \widetilde{H}(\pi_1 \partial M) \\ &= \mathcal{N}(v) \cup (\mathfrak{L}/H(\pi_1 \partial M)). \end{aligned}$$

In particular, if the moduli $|H(\pi_1 \partial M)|$ form a discrete subgroup of the multiplicative group $\mathbb{R}^+$, then $\mathfrak{L}/H(\pi_1 \partial M)$ is a circle and $\overline{\mathcal{N}(v)}$ is a manifold. This is the case if and only if there exists a generator α of $\pi_1 \partial M$ such that $\widetilde{H}(\alpha)$ is a rotation by $k\pi \neq 0$ plus a boost. In this case, the completion $\overline{M}$ (which is given near the boundary by $\overline{\mathcal{N}(v)}$) is topologically

the manifold M_α obtained by Dehn filling M along the curve α. If the discrete rotational part $\tilde{\mathcal{R}}(\alpha) = 2\pi$, then $\overline{M}$ has a *tachyon* singularity (see Section 4.4) with mass equal to the hyperbolic angle $\varphi(\alpha)$ of the boost part of $H(\alpha)$.

Remark 33. If the moduli $|H(\pi_1 \partial M)|$ are dense in $\mathbb{R}^+$, the geodesic completion of M near v has a topological singularity that resembles a Dehn surgery type singularity in hyperbolic geometry. This more general singularity has not yet been studied to the knowledge of the author.

Example 3. (figure eight knot complement) Let M be the complement of the figure eight knot from Examples 1 and 2. We use Proposition 42 and the analysis in Example 2 to build AdS structures on $(M, \mathcal{T})$. Consider the connected component of real solutions to the edge consistency Equation (5.5) with $z_1 < 0$ and $z_2 > 1$. Taking the differential of log of Equation (5.5), we obtain

$$\frac{2z_1}{z_1(1-z_1)}dz_1 + \frac{2z_2}{z_2(1-z_2)}dz_2 = 0 \tag{5.7}$$

which implies that $\frac{dz_2}{dz_1} > 0$ at any point of (this connected component) of the variety. Thus, any two distinct solutions (λ_1, λ_2) and (μ_1, μ_2) satisfy (up to switching the λ's with the μ's)

$$\lambda_1 > \mu_1 \quad \text{and} \quad \lambda_2 > \mu_2$$

and give a positively oriented solution

$$z_1 = \frac{1+\tau}{2}\lambda_1 + \frac{1-\tau}{2}\mu_1$$

$$z_2 = \frac{1+\tau}{2}\lambda_2 + \frac{1-\tau}{2}\mu_2$$

to the edge consistency equations over $\mathbb{R} + \mathbb{R}\tau$ determining AdS structures on M. It is straight forward to show that the discrete rotational part of the holonomy of ℓ is $\tilde{\mathcal{R}}(\ell) = +2\pi$.

Now impose the additional condition

$$H(\ell) = z_1^2(1-z_1)^2 \quad = \quad e^{\tau\varphi}$$

which is equivalent to

$$\begin{aligned} \lambda_1^2(1-\lambda_1)^2 &= \cosh(\varphi)+\sinh(\varphi) = e^{\varphi} \\ \mu_1^2(1-\mu_1)^2 &= \cosh(\varphi)-\sinh(\varphi) = e^{-\varphi}. \end{aligned}$$

The geodesic completion of the AdS structure determined by (z_1, z_2) is an AdS tachyon structure on the Dehn filled manifold M_ℓ. Note that as $\mu_1 < \lambda_1 < 0$, we must have that the tachyon mass $\varphi < 0$.

5.2.4 Triangulated HP structures

Next let $\mathcal{B} = \mathbb{R} + \mathbb{R}\sigma$ where $\sigma^2 = 0$. The conjugation action is given by

$$a + b\sigma \longmapsto \overline{a+b\sigma} = a - b\sigma.$$

Then the form $\langle \cdot, \cdot \rangle$ on $\mathrm{Herm}_2(\mathcal{B})$ is degenerate (with the eigenvalue signs being $+, +, -, 0$). In this case, $\mathbb{X} = \mathrm{HP}^3$ and $\mathrm{PGL}^+(2, \mathbb{R}+\mathbb{R}\sigma) \cong G_{\mathrm{HP}}$ acts by half-pipe isometries.

The algebra $\mathbb{R}+\mathbb{R}\sigma$ should be thought of as the cotangent bundle of $\mathbb{R}$: Letting x be the standard coordinate function on $\mathbb{R}$, the element σ can be thought of as a differential quantity dx whose square is zero. This point of view is particularly appropriate for the purposes of constructing geometric transitions. For example, given collapsing hyperbolic structures with holonomy representations $\rho_t : \pi_1 M \to \mathrm{PSL}(2, \mathbb{C})$ converging to $\rho_0 : \pi_1 M \to \mathrm{PGL}(2, \mathbb{R})$, then the rescaling process described in Section 3.2 produces an HP representation

$$\rho_{\mathrm{HP}}(\cdot) = \rho_0(\cdot) + \sigma A(\cdot)$$

where $A(\gamma) \in T_{\rho_0(\gamma)} \mathrm{PSL}(2, \mathbb{R})$ is the imaginary part of the derivative of ρ_t

$$A(\cdot) = \mathrm{Im}\frac{d}{dt}\rho_t(\cdot)$$

and satisfies the product rule: $A(\gamma_1\gamma_2) = A(\gamma_1)\rho_0(\gamma_2) + \rho_0(\gamma_1)A(\gamma_2)$. The exact same interpretation is possible in the context of collapsing AdS structures with holonomy representations $\rho_t : \pi_1 M \to \mathrm{PGL}^+(2, \mathbb{R}+\mathbb{R}\tau)$ whose imaginary parts are going to zero.

We equip $\mathbb{R}+\mathbb{R}\sigma$ with the degenerate metric induced by $|\cdot|^2$. Proposition 33 immediately implies:

Proposition 43. *The following are equivalent:*

1. *The ideal tetrahedron $T(z_1, z_2, z_3, z_4)$ is defined.*
2. *The shape parameter z of the edge z_1z_2 of T satisfies Re $z \neq 0, 1$.*
3. *The shape parameters $z, \frac{1}{1-z}, \frac{z-1}{z}$ of all edges of T have real parts not equal to $0, 1$.*
4. *Placing z_1 at ∞, $\triangle z_2z_3z_4$ is a triangle in the $\mathbb{R} + \mathbb{R}\sigma$ plane that has non-degenerate edges.*

The real part a of $z = a + b\sigma$ describes a degenerate tetrahedron in $\mathbb{H}^2$, while the imaginary part $b\sigma$ describes an infinitesimal "thickness". If $b > 0$, then the tetrahedron is positively oriented; In this case z is thought of as being tangent to a path of complex (resp. $\mathbb{R}+\mathbb{R}\tau$) shape parameters describing a degenerating family of positively oriented hyperbolic (resp. AdS) tetrahedra.

Proposition 44. *The shape parameters $z_i = a_i+b_i\sigma$, for $i = 1, \ldots, n$, define ideal tetrahedra that glue together compatibly around an edge in* HP^3 *if and only if:*

- *$(a_1, \ldots, a_n) \in \mathbb{R}^n$ satisfy the equation $\prod_{i=1}^n a_i = 1$,*
- *$(b_1, \ldots, b_n) \in T_a\mathbb{R}^n$ satisfy the differential of that equation*

$$d(\prod_{i=1}^{n} z_i)\Big|_{z_i=a_i}(b_1, \ldots, b_n) = 0,$$

- *and exactly two of the a_i are negative.*

Thus the real part of a solution to Thurston's equations over $\mathbb{R} + \mathbb{R}\sigma$ defines a triangulated transversely hyperbolic foliation, and the imaginary (σ) part defines an infinitesimal deformation of this structure.

5.3 Regeneration of $\mathbb{H}^3$ and AdS^3 structures

In [Hod86], Hodgson studies the problem of regenerating hyperbolic structures from transversely hyperbolic foliations. In the context of ideal triangulations, the problem of regenerating hyperbolic and AdS structures from transversely hyperbolic foliations becomes more straight-forward, especially in the presence of smoothness assumptions.

Proposition 45. *If the real deformation variety $\mathscr{D}_{\mathbb{R}}$ is smooth at a point $(z_j) \in \mathbb{R}^N$, then any positive tangent vector $(v_j) \in \mathbb{R}^N$ determines regenerations to robust hyperbolic and anti de Sitter structures.*

Proof. The imaginary tangent vector (iv_j) can be integrated to give a path of complex solutions to the edge consistency equations. Similarly, the imaginary tangent vector (τv_j) can be integrated to give a path of $\mathbb{R} + \mathbb{R}\tau$ solutions. In both cases the solutions have positive imaginary part, so they determine robust structures. □

In light of this proposition, we ask the following question:

Question. Given a triangulated three-manifold $(M, \mathcal{T})$, which points of the real deformation variety $\mathscr{D}_{\mathbb{R}}$ are smooth with positive tangent vectors?

We give a partial answer to this question in the case that M is a punctured torus bundle.

Theorem 7. *Let M^3 be a punctured torus bundle with anosov monodromy and let $\mathcal{T}$ be the monodromy ideal triangulation on M. Let $\mathscr{D}_{\mathbb{R}}$ be the deformation variety of of transversely hyperbolic foliations on $(M, \mathcal{T})$. Then, there are two canonical smooth, one dimensional, connected components $\mathscr{V}_+$ of $\mathscr{D}_{\mathbb{R}}$ with positive tangent vectors at every point. Further, each component of $\mathscr{V}_+$ is parameterized by the (signed) length of the puncture curve.*

Chapter 6 is dedicated to the proof of this theorem.

Corollary. *Any transversely hyperbolic foliation on $(M, \mathcal{T})$ belonging to $\mathscr{V}_+$ regenerates to both hyperbolic and anti de Sitter structures.*

Corollary. *The deformation variety of anti de Sitter structures on $(M, \mathcal{T})$ contains a smooth one $\mathbb{R} + \mathbb{R}\tau$ dimensional component parametrized by the $\mathbb{R} + \mathbb{R}\tau$ length of the puncture curve. In particular, tachyon structures are parametrized by their (negative) tachyon mass and the mass can be decreased without bound.*

Remark 34. The $\mathbb{R} + \mathbb{R}\tau$ length, referred to in the above corollary, of an AdS^3 isometry is defined analogously to the complex length of a hyperbolic isometry. See the discussion of Tachyons in Section 5.2.3

5.4 Triangulated transitions

The shape parameter algebra of hyperbolic tetrahedra intersects that of AdS tetrahedra exactly in the shape parameter algebra of degenerate $\mathbb{H}^2$ tetrahedra: $\mathbb{C} \cap (\mathbb{R} + \mathbb{R}\tau) = \mathbb{R}$. In some sense, this intersection is tranverse. In order to construct smooth transitions on $(M, \mathcal{T})$, we enlarge the shape parameter coefficient algebra to the *generalized Clifford algebra* $\mathcal{C}$ generated by i and τ:

$$\mathcal{C} = \langle 1, i, \tau : i^2 = -1,\ \tau^2 = +1,\ i\tau = -\tau i \rangle.$$

Consider the following path in $\mathcal{C}$ (defined for $t \neq 0$):

$$\mathfrak{I}(t) = \frac{(1 + t|t|)i + (1 - t|t|)\tau}{2|t|}.$$

Note that for $t > 0$, $\mathfrak{I}^2 = -1$, while for $t < 0$, $\mathfrak{I}^2 = +1$. We define the following $\mathscr{C}^1$ path of two dimensional sub-algebras:

$$\mathcal{B}_t = \mathbb{R} + \mathbb{R}|t|\mathfrak{I}(t).$$

The path $\mathcal{B}_t$ satisfies the following properties:

- If $t > 0$ then $\mathcal{B}_t \cong \mathbb{C}$ via the isomorphism $\mathfrak{I}(t) \mapsto i$.
- If $t < 0$ then $\mathcal{B}_t \cong \mathbb{R} + \mathbb{R}\tau$ via the isomorphism $\mathfrak{I}(t) \mapsto \tau$.
- $\mathcal{B}_0 = \mathbb{R} + \mathbb{R}\sigma$, where $\sigma = \frac{i+\tau}{2}$. Note that $\sigma^2 = 0$.

To describe geometric transitions of triangulated structures, one constructs a smooth path of solutions to the edge consistency equations over the varying algebra $\mathcal{B}_t$. A solution for some $t \neq 0$ is interpreted as an assignment of shape parameters for either hyperbolic (if $t > 0$) or anti de Sitter (if $t < 0$) ideal tetrahedra via the isomorphisms given above. The transitional shape parameter algebra $\mathcal{B}_0 = \mathbb{R} + \mathbb{R}\sigma$ describes shape parameters for half-pipe ideal tetrahedra or HP tetrahedra (see Section 5.2.4).

We formalize the discussion of transitioning shape parameters with the following definition:

Definition 28. A *geometric transition on* $(M, \mathcal{T})$ is described by a $\mathscr{C}^1$ path of shape parameters $(z_j(t))$ that solve the edge consistency equations over the varying algebra $\mathcal{B}_t$

such that for $t > 0$, $(z_j(t))$ determines a hyperbolic structure, for $t < 0$, $(z_j(t))$ determines an AdS structure, and $(z_j(0))$ determines an HP structure.

Proposition 46. *A geometric transition on $(M, \mathcal{T})$ determines a transition on M in the sense of Theorem 6, except that the singularities at the boundary may lie in the more general class of Dehn surgery singularities (see [Thu80, Hod86]).*

Proof. Applying the formalism of Section 5.1, a solution to Thurston's equations over $\mathcal{B}_t$ determines a three-dimensional real projective structure. Choose a base tetrahedron in $(\widetilde{M}, \widetilde{\mathcal{T}})$, and for each t build a developing map D_t into $\mathbb{RP}^3$ by placing the base tetrahedron in standard position and developing from there. The construction of D_t depends smoothly on the shape parameters $z_j(t)$. Thus we get a smooth path of projective structures transitioning from hyperbolic to AdS geometry passing through HP geoemtry. □

Proposition 47. *The data of a geometric transition on $(M, \mathcal{T})$ is equivalent to the following:*

1. *A path of hyperbolic structures on $(M, \mathcal{T})$, defined for $t > 0$, determined by shape parameters $z_j(t) = c_j(t) + d_j(t)i$.*
2. *A path of* AdS *structures on $(M, \mathcal{T})$, defined for $t < 0$, determined by shape parameters $z_j(t) = c_j(t) - d_j(t)\tau$.*
3. *An* HP *structure determined by shape parameters $z_j(0) = c_j(0) + d'_j(0)\sigma$*

where, for all j, c_j and d_j are $\mathscr{C}^1$ functions on a neighborhood of $t = 0$ with $d_j(0) = 0$.

Proof. To convert from the data given in the proposition to a $\mathscr{C}^1$ geometric transition, simply replace i (resp. τ) with $\mathfrak{I}(t)$ when $t > 0$ (resp. $t < 0$). □

The above proposition and proposition 45 give the following corollary.

Corollary. *If the real deformation variety is smooth at a point $(z_j) \in \mathbb{R}^N$, then any positive tangent vector $(v_j) \in \mathbb{R}^N$ determines a geometric transition on $(M, \mathcal{T})$.*

5.4.1 Example: figure eight knot complement

Let M be the figure eight knot complement, discussed in Examples 1, 2, and 3. Let $\mathcal{T}$ be the decomposition of M into two ideal tetrahedra (four faces, two edges, and one ideal

vertex) well-known from [Thu80] (see Figure 5.6). The edge consistency equations reduce to the following:

$$z_1(1-z_1)z_2(1-z_2) = 1. \tag{5.8}$$

In Example 2, we showed that the variety of real solutions to (5.8) (with total dihedral angle 2π around each edge) is a smooth one-dimensional variety with positive tangent vectors. Thus, any transversely hyperbolic foliation on $(M, \mathcal{T})$ regenerates to robust hyperbolic and AdS structures by Proposition 45. As M is a punctured torus bundle, this is a special case of Theorem 7.

Next, we consider hyperbolic cone structures on M, with singular meridian being the longitude ℓ of the knot (this is also the curve around the puncture in a torus fiber). Recall from Example 1 that such a structure, with cone angle $\theta < 2\pi$, is constructed by solving the equations

$$\begin{aligned} H(\ell) = z_1^2(1-z_1)^2 &= e^{i\theta} \\ &= e^{-i(2\pi-\theta)} \end{aligned} \tag{5.9}$$

over $\mathbb{C}$. Recall from Example 3 that AdS tachyon structures with mass $\varphi < 0$ are constructed by solving the equations

$$\begin{aligned} H(\ell) = z_1^2(1-z_1)^2 &= e^{\tau\varphi} \\ &= e^{-\tau(-\varphi)} \end{aligned} \tag{5.10}$$

over $\mathbb{R}+\mathbb{R}\tau$. In order to construct a smooth transition between these two types of structures, we consider a generalized version of these equations defined over the transitioning family $\mathcal{B}_t$ of sub-algebras of $\mathcal{C}$. The idea is to replace i in (5.9) (resp. τ in (5.10)) by the algebraically equivalent elements $\mathfrak{I}(t)$. The generalized version of (5.9) and (5.10) that we wish to solve is

$$H(\ell) = z_1^2(1-z_1)^2 = -e^{-\mathfrak{I}(t)|t|}. \tag{5.11}$$

Note that the right hand side (which can be defined in terms of Taylor series) is a smooth function of t. In fact, solving (5.11) over the varying algebra $\mathcal{B}_t = \mathbb{R} + \mathbb{R}|t|\mathfrak{I}(t)$ for small t, gives a smooth path $(z_1(t), z_2(t))$ of shape parameters for transitioning structures. For

$t > 0$, (z_1, z_2) determines a hyperbolic cone structure with cone angle $\theta = 2\pi - |t|$. For $t < 0$, (z_1, z_2) determines a AdS tachyon structure with hyperbolic angle $\varphi = -|t|$. At $t = 0$, interpreting $|t|\Im(t)$ as $\sigma = \frac{i+\tau}{2}$, we get shape parameters for a half-pipe structure:

$$z_1(0) = \tfrac{1-\sqrt{5}}{2} + \tfrac{1}{2\sqrt{5}}\sigma, \quad z_2(0) = \tfrac{1+\sqrt{5}}{2} + \tfrac{1}{2\sqrt{5}}\sigma.$$

The exponential $\mathbb{R} + \mathbb{R}\sigma$-length of the curve ℓ around the singular locus is

$$\begin{aligned} H(\ell) = z_1^2(1-z_1)^2 &= \left(\tfrac{1-\sqrt{5}}{2} + \tfrac{1}{2\sqrt{5}}\sigma\right)^2 \left(\tfrac{1+\sqrt{5}}{2} - \tfrac{1}{2\sqrt{5}}\sigma\right)^2 \\ &= (-1 + \tfrac{1}{2}\sigma)^2 \\ &= 1 - \sigma \ = e^{-1\cdot\sigma}. \end{aligned}$$

In fact, the solution $(z_1(0), z_2(0))$ defines an HP structure whose completion has an infinitesimal cone singularity of infinitesimal cone angle $\omega = -1$ (see Section 4.5).

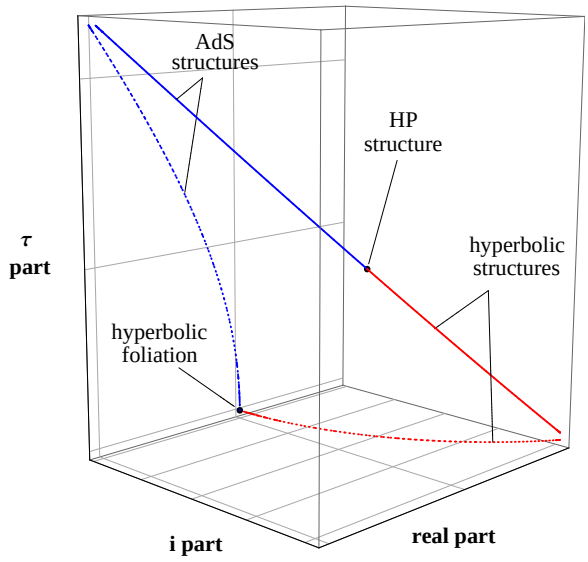

Figure 5.10: The $\mathcal{C}$-length of the singular curve is plotted as hyperbolic cone structures (red) transition to AdS tachyon structures (blue). After rescaling (solid lines), the transition is realized as a $\mathscr{C}^1$ path passing through a half-pipe structure.

Chapter 6

Punctured Torus Bundles

In this chapter we prove:

Theorem 7. *Let M^3 be a punctured torus bundle with Anosov monodromy and let $\mathcal{T}$ be the monodromy ideal triangulation on M. Let $\mathscr{D}_{\mathbb{R}}$ be the deformation variety of transversely hyperbolic foliations on $(M, \mathcal{T})$. Then, there are two canonical smooth, one dimensional, connected components $\mathscr{V}_+$ of $\mathscr{D}_{\mathbb{R}}$ with positive tangent vectors at every point. Further, each component of $\mathscr{V}_+$ is parameterized by the (signed) length of the puncture curve.*

Via the discussion in Section 5.3, this theorem gives a large class of examples of geometric transitions.

We begin with a brief description of the monodromy triangulation (sometimes referred to as the Floyd-Hatcher triangulation) and Gueritaud's convenient description of Thurston's equations. See [Ga06] for an elegant and self-contained introduction to this material.

6.1 The monodromy triangulation

We think of the punctured torus T as $\mathbb{R}^2 \setminus \mathbb{Z}^2$ quotiented out by the lattice of integer translations $\mathbb{Z}^2$. Any element of $\mathrm{SL}(2, \mathbb{Z})$ acts on T since it normalizes the lattice $\mathbb{Z}^2$. An element $\varphi \in \mathrm{SL}(2, \mathbb{Z})$ with distinct real eigenvalues λ_+, λ_- is called *Anosov*. We focus on the case that φ has positive eigenvalues. If φ has negative eigenvalues, then the following construction can be performed using $-\varphi$ in place of φ with some small modifications; the resulting edge consistency equations will be the same. The following is a well-known fact.

Proposition 48. *An Anosov $\varphi \in \mathrm{SL}(2,\mathbb{Z})$ with positive eigenvalues can be conjugated to have the following form:*

$$A\varphi A^{-1} = R^{m_1}L^{n_1}R^{m_2}L^{n_2}\cdots R^{m_k}L^{m_k}$$

where $m_1, n_1 \ldots, m_k, n_k$ are positive integers and R, L are the standard transvection matrices

$$R = \begin{pmatrix} 1 & 1 \\ 0 & 1 \end{pmatrix} \quad \textit{and} \quad L = \begin{pmatrix} 1 & 0 \\ 1 & 1 \end{pmatrix}.$$

This form is unique up to cyclic permutation of the factors.

This fact gives a canonical triangulation of the mapping torus $M = T\times I/(x,0) \sim (\varphi x, 1)$ as follows. Since φ and $A\varphi A^{-1}$ produce homeomorphic mapping tori, we will henceforth assume φ is given exactly by the form described in the proposition. Further we think of φ as a word W of length $N = m_1 + n_1 + \ldots + m_k + n_k$ in the letters L and R. Now, we begin with the standard ideal triangulation τ_0 of T having edges $(1,0),(0,1),(-1,1)$ (see figure below). Apply the first (left-most) letter of the word, which is R, to τ_0 to get a new ideal triangulation $\tau_1 = R\tau_0$. These triangulations differ by a *diagonal exchange*. Realize this diagonal exchange as an ideal tetrahedron as follows. Let $\mathcal{T}_1$ be an affine ideal tetrahedron in $T^2 \times \mathbb{R}$ with two bottom faces that project to the ideal triangles of τ_0 in T^2 and two top faces that project to the ideal triangles of τ_1 in T^2.

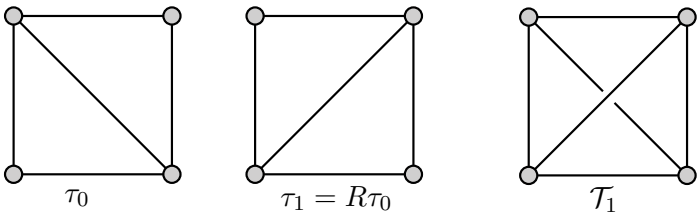

Figure 6.1: A diagonal exchange determines an ideal tetrahedron.

Next, we apply the first (left-most) two letters of W to τ_0 in order to get another ideal triangulation τ_2. We note that τ_1 and τ_2 differ by a diagonal exchange and we let $\mathcal{T}_2$ be the ideal tetrahedron with bottom faces τ_1 and top faces τ_2. The bottom faces of $\mathcal{T}_2$ are glued to the top faces of $\mathcal{T}_1$. We proceed in this way to produce a sequence of $N+1$ ideal triangulations $\tau_0, \ldots, \tau_N$ with $\tau_k = W_k\tau_0$, where W_k are the first (left-most) k letters of W.

It is easy to see that τ_k and τ_{k+1} differ by a diagonal exchange: for example if $W_{k+1} = W_k R$, then $W_{k+1}\tau_0$ and $W_k\tau_0$ differ by a diagonal exchange because $R\tau_0$ and τ_0 differ by a diagonal exchange. For consecutive τ_k, τ_{k+1} define a tetrahedron $\mathcal{T}_{k+1}$ which has τ_k as its bottom faces and τ_{k+1} as its top faces. $\mathcal{T}_{k+1}$ is glued to $\mathcal{T}_k$ along τ_k. Note that the top ideal triangulation τ_N of the top tetrahedron $\mathcal{T}_N$ is given exactly by $\tau_N = \varphi\tau_0$. So we glue $\mathcal{T}_N$ along its top faces τ_N to $\mathcal{T}_1$ along its bottom faces τ_0 using the Anosov map φ. The resulting manifold is readily seen to be M, the mapping torus of φ. This decomposition into ideal tetrahedra is called the *monodromy triangulation* or the *monodromy tetrahedralization*.

We note that the ideal triangulation τ_k of T^2 is naturally realized as a pleated surface inside M, at which the tetrahedra $\mathcal{T}_k$ and $\mathcal{T}_{k+1}$ are glued together. Further, we may label each τ_k with the k^{th} letter of W. Hence, each tetrahedron $\mathcal{T}_{k+1}$ can be labeled with two letters, the letter corresponding to its bottom pleated surface τ_k followed by the letter corresponding to its top pleated surface τ_{k+1}. If $\mathcal{T}_k$ is labeled RL or LR it is called a *hinge* tetrahedron. Consecutive LL tetrahedra make up an *LL-fan*, while consecutive RR tetrahedra make up an *RR-fan*.

In order to build geometric structures using the monodromy triangulation, we assign shape parameters to the edges of the tetrahedra as follows: For tetrahedron $\mathcal{T}_i$, we assign the shape parameter z_i to the (opposite) edges corresponding to the diagonal exchange taking τ_i to τ_{i+1}. The shape parameters $x_i = \frac{z_i - 1}{z_i}$ and $y_i = \frac{1}{1-z_i}$ are assigned to the other edges according to the orientation of the tetrahedron.

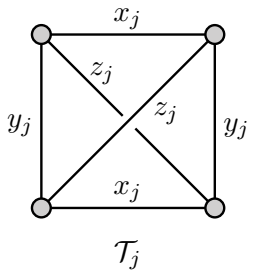

Figure 6.2: The edges corresponding to the diagonal exchange are labeled z.

The reader should note that throughout this chapter indices that are out of range will be interpreted cyclically. For example $z_{N+1} := z_1$ and $z_0 := z_N$. This convention allows for a much more efficient description of the equations.

Thurston's Equations

Many of the edges in the monodromy tetrahedralization meet exactly four faces. This happens when a given edge in T^2 lies in two consecutive triangulations τ_{j-1}, τ_j, but does not lie in either τ_{j-2} or τ_{j+1}. This will be the case if $W_j = W_{j-2}RR$, in other words if $\mathcal{T}_j$ is labeled RR.

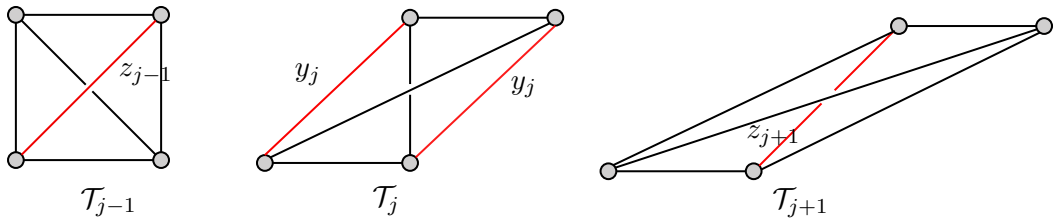

Figure 6.3: A four-valent edge.

In this case, the holonomy around the given edge takes the form

$$g_j = z_{j-1}z_{j+1}y_j^2 \tag{6.1}$$

For every j such that $W_j = W_{j-2}RR$, the corresponding edge holonomy g_j has the form (6.1). Similarly, for every k such that $W_k = W_{k-2}LL$, the corresponding edge holonomy has the form

$$g_j = z_{j-1}z_{j+1}x_j^2 = 1 \tag{6.2}$$

The other edge holonomies can be read off from the hinge tetrahedra. A *hinge edge* is an edge e that occurs in more than two consecutive triangulations $\tau_{j-1}, \ldots, \tau_k$, where we take $p = k - j + 2$ to be the maximal number of consecutive τ_i containing the edge e. In this case, $\mathcal{T}_j$ and $\mathcal{T}_k$ are both hinge tetrahedra. Note also that each hinge tetrahedron contains two distinct hinge edges. The edge e is common to the tetrahedra $\mathcal{T}_{j-1}, \mathcal{T}_j, \ldots, \mathcal{T}_k, \mathcal{T}_{k+1}$. In $\mathcal{T}_{j-1}$, e corresponds to the top edge of the diagonal exchange. In $\mathcal{T}_{k+1}$, e corresponds to the bottom edge of the diagonal exchange. In the case $\mathcal{T}_j$ is an LR hinge, we have

$$W_k = W_{j-2}LRRR\ldots RL$$

and the edge holonomy for e is given by

$$g_j = z_{j-1}x_j^2x_{j+1}^2\dots x_k^2z_{k+1}. \tag{6.3}$$

For example, if $p = k - j + 2 = 4$ the picture is as shown in Figure 6.4.

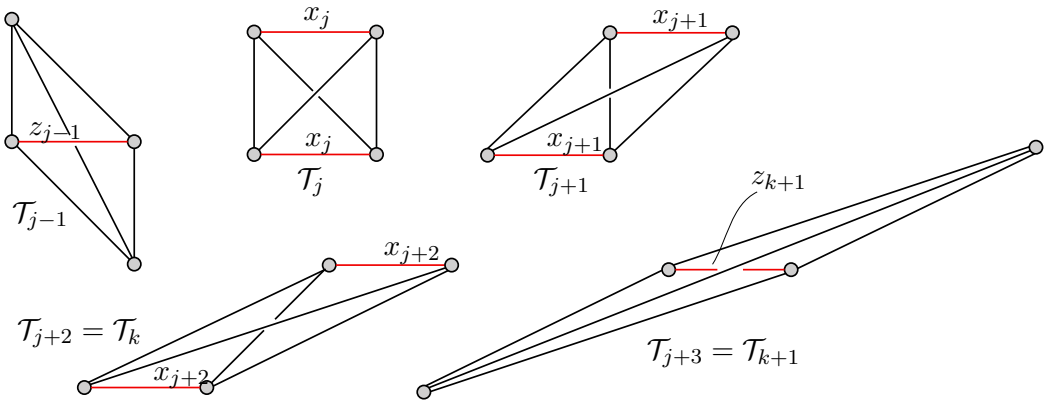

Figure 6.4: A hinge edge.

If $\mathcal{T}_j$ is an RL hinge, then we have

$$W_k = W_{j-2}RLLL\dots LR$$

and the edge holonomy for e is given by

$$g_j = z_{j-1}y_j^2y_{j+1}^2\dots y_k^2z_{j+1} = 1. \tag{6.4}$$

Every edge in the monodromy tetrahedralization has an edge holonomy expression which is either of the form (6.1), (6.2) if the edge is valence four or of the form (6.3), (6.4) if the edge is hinge.

All ideal vertices of the tetrahedra $\mathcal{T}_k$ are identified with one another. The link of the ideal vertex gives a triangulation of ∂M. The edge consistency equations can be read off directly from a picture of this triangulation. Vertices in ∂M correspond to edges in M. The interior angles of the triangles in ∂M are labeled with the shape parameters corresponding to the edges of the associated tetrahedra in M. Figure 6.5 gives a picture of the combinatorics of ∂M in the case that $W = R^4L^5$.

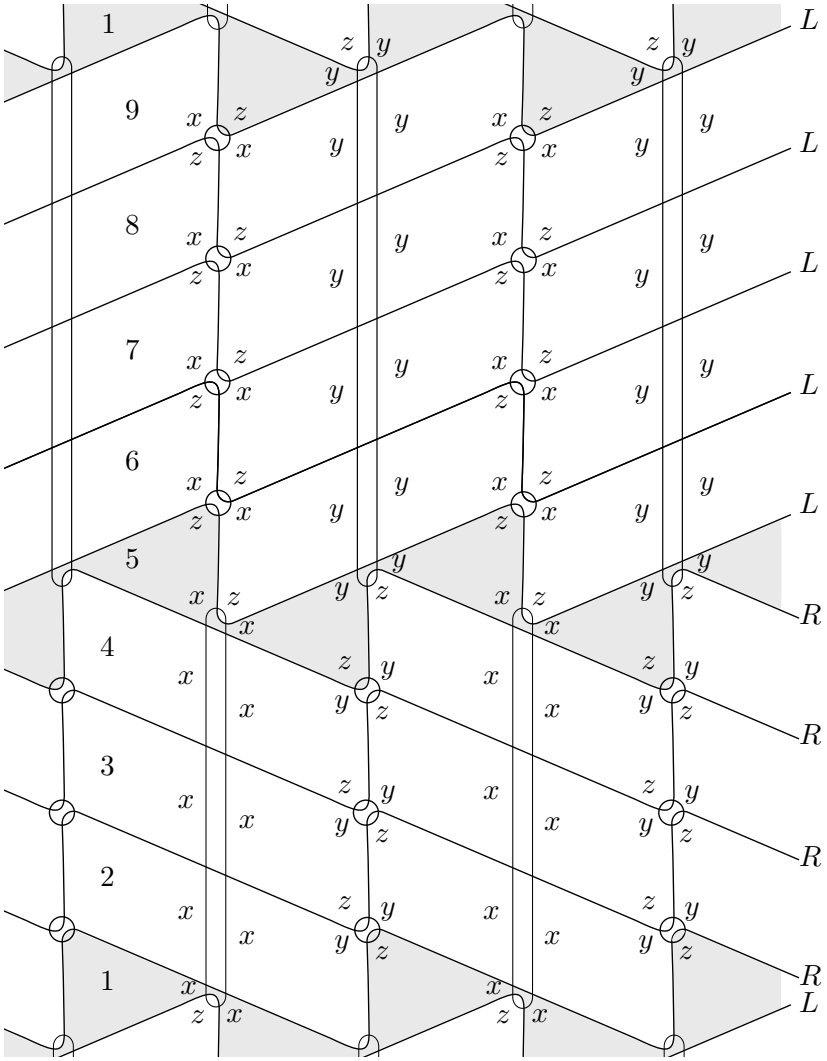

Figure 6.5: The edge consistency equations can be read off from a picture of the induced triangulation of ∂M. This figure, drawn in the style of Segerman [Seg11], depicts the case $W = R^4L^5$. The circles and long ovals each represent a vertex of the triangulation. One should imagine the long ovals collapsed down to a point, so that the adjacent quadrilaterals become a fan of triangles around the vertex. The picture is four-periodic going left to right. At any given level of this diagram, the four triangles that touch all come from the same tetrahedron.

To conclude this section we summarize the edge consistency equations as follows:

Proposition 49. *Let $\varphi : T^2 \to T^2$ be an Anosov map which is decomposed as*

$$\varphi = W = R^{m_1}L^{n_1}R^{m_2}L^{n_2}\cdots R^{m_k}L^{m_k}.$$

Then Thurston's edge consistency equations for the canonical ideal triangulation of M_φ associated to W are described as follows:

Thinking of W as a string of R's and L's, let $\{j, \ldots, k = j + m_p - 1\}$ be the indices of a maximal string of m_p R's. The corresponding m_p equations are:

$$g_j = z_{j-1}x_j^2x_{j+1}^2\cdots x_{k+1}^2z_{k+2} = 1 \qquad \textit{(R-fan)}$$

and for each $q = j+1, \ldots, k$ $\qquad g_q = z_{q-1}y_q^2z_{q+1} = 1 \qquad$ *(R-4-valent).*

Let $\{j, \ldots, k = j + n_p - 1\}$ be the indices of a maximal string of n_p L's. The corresponding n_p equations are:

$$g_j = z_{j-1}y_j^2y_{j+1}^2\cdots y_{k+1}^2z_{k+2} = 1 \qquad \textit{(L-fan)}$$

and for each $q = j+1, \ldots, k$ $\qquad g_q = z_{q-1}x_q^2z_{q+1} = 1 \qquad$ *(L-4-valent).*

For notation purposes, we write these equations in terms of $\{x_j, y_j, z_j\}$. However, we remind the reader that for each $j = 1, \ldots, N$, $x_j = \frac{z_j - 1}{z_j}$, and $y_j = \frac{1}{1-z_j}$. Thus, we think of these equations as depending on the N variables $\{z_j\}$.

6.2 The real deformation variety

We look for solutions to the equations of Proposition 49 over $\mathbb{R}$ that represent transversely hyperbolic foliations. Requiring that the total dihedral angle around each edge be 2π amounts to requiring that exactly two of the shape parameters appearing in each equation be negative (see Section 5.2.2). Recall that in the equations of Proposition 49, $x_j = \frac{z_j - 1}{z_j}$ and $y_j = \frac{1}{1-z_j}$, so that in particular $x_jy_jz_j = -1$ and exactly one of x_j, y_j, z_j lies in each of the components of $\mathbb{R} \setminus \{0, 1\}$. A real shape parameter which is negative is said to have dihedral angle π, while a positive shape parameter is said to have dihedral angle 0.

The construction of the monodromy triangulation involved stacking tetrahedra in $T^2 \times \mathbb{R}$, with each tetrahedron corresponding to a diagonal exchange. From this picture, it would

be natural to guess that the edges with dihedral angle π should be the edges corresponding to diagonal exchanges, which are labeled z_j. This, however, is not the case.

Proposition 50. *There is no solution to the equations of Proposition 49 with all $z_j < 0$.*

Proof. Suppose all $z_j < 0$. Then for all j, $x_j > 1$ and $0 < y_j < 1$. Take all the equations involving x_j's and multiply them together. The result is the following:

$$\prod_{j=1}^{N} x_j^2 \cdot \prod_{j=1}^{N} z_j^{\epsilon_j} = 1$$

where each $\epsilon_j = 0, 1$, or 2. This implies that

$$\prod_{j=1}^{N} x_j^{2-\epsilon_j} = \pm \prod_{j=1}^{N} y_j^{\epsilon_j}$$

which is a contradiction, since the left hand side must be greater than one, while the right hand side must be less than one. □

Due to the structure of the equations, having one of the z_j positive actually implies that many other z_j's will be positive as well. In many cases, it can be shown that *all* z_j must be positive. Therefore, a natural subset of solutions to consider is:

$$\mathscr{V}_+ = \{ \text{ real solutions to the equations of Proposition 49 with } z_j > 0 \text{ for all } j \} \qquad (6.5)$$

This set is a union of connected components of the deformation variety. It is also a semi-algebraic set. There are only two possible assignments of dihedral angles (signs) for $\mathscr{V}_+$:

Proposition 51. *Consider an element $(z_1, \ldots, z_N)$ of $\mathscr{V}_+$. Then $y_j < 0$ if $\mathcal{T}_j$ is RR, and $x_k < 0$ if $\mathcal{T}_k$ is LL. If $\mathcal{T}_j$ is a hinge tetrahedron, then one of the following two cases holds:*

1. *$x_j < 0$ if $\mathcal{T}_j$ is an LR hinge tetrahedron. $y_k < 0$ if $\mathcal{T}_k$ is an RL hinge tetrahedron.*

2. *$x_j < 0$ if $\mathcal{T}_j$ is an RL hinge tetrahedron. $y_k < 0$ if $\mathcal{T}_k$ is an LR hinge tetrahedron.*

Proof. Begin with the tetrahedron $\mathcal{T}_1$ which is an LR hinge tetrahedron. Since z_1 is not negative, we must have $x_1 < 0$ or $y_1 < 0$. Assume, as in case 1, that $x_1 < 0$. Since x_1

appears twice in the first fan equation, choosing $x_1 < 0$ forces all other terms in the first R-fan equation,

$$z_N x_1^2 x_2^2 \cdots x_{m_1+1}^2 z_{m_1+2} = 1,$$

to be positive (by the 2π total dihedral angle condition). In particular, $x_{m_1+1} > 0$. Thus, as $z_{m_1+1} > 0$, we must have $y_{m_1+1} < 0$. Note that $\mathcal{T}_{m_1+1}$ is the second hinge tetrahedron, of type RL. Examining the second fan equation (this one is an L-fan),

$$z_{m_1} y_{m_1+1}^2 \cdots y_{m_1+m_2+1}^2 z_{m_1+m_2+2} = 1,$$

we find that $y_{m_1+1} < 0$. This implies in particular that $y_{m_1+m_2+1} > 0$. So, we get that $x_{m_1+m_2+1} < 0$. Note that $\mathcal{T}_{m_1+m_2+1}$ is the third hinge tetrahedron, of type LR. This process continues to determine the sign of all hinge shape parameters to be as in case 1. It then follows that the signs of all shape parameters for RR and LL tetrahedra are determined as specified in the Proposotion as well.

Similarly, if we begin by choosing $y_1 < 0$, the signs of all other shape parameters are determined to be as in case 2. □

We will focus on the behavior of the variety $\mathscr{V}_+$. Over the course of the next four sub-sections, we show the following

1. $\mathscr{V}_+$ is smooth of dimension one.
2. All tangent vectors to $\mathscr{V}_+$ have positive entries (or negative entries).
3. $\mathscr{V}_+$ is non-empty. In particular $\mathscr{V}_+$ contains a canonical solution corresponding to the Sol geometry of the torus bundle gotten by Dehn filling the puncture curve in M.
4. $\mathscr{V}_+$ is locally parameterized by the exponential length of the puncture curve.

The particularly nice form of the equations allows us to prove these properties with relatively un-sophisticated methods.

6.2.1 $\mathscr{V}_+$ is smooth of dimension one.

We assume case 1 of Proposition 51. The other case is symmetric. So, we have

- $x_j < 0$ if and only if either $\mathcal{T}_j$ is an LR hinge tetrahedron or $\mathcal{T}_j$ is LL.
- $y_k < 0$ if and only if either $\mathcal{T}_k$ is an RL hinge tetrahedron or $\mathcal{T}_k$ is RR.

Recall that the edge holonomy expressions, described in Proposition 49, are enumerated according to the index of the first x_j^2 or y_j^2 term appearing in the equation:

$$\begin{aligned}
g_1(z_1,\ldots,z_N) &:= z_N x_1^2 x_2^2 \ldots x_{m_1+1}^2 z_{m_1+2} \\
g_2(z_1,\ldots,z_N) &:= z_1 y_2^2 z_3 \\
&\vdots \\
g_{m_1}(z_1,\ldots,z_N) &:= z_{m_1} y_{m_1+1}^2 y_{m_1+2}^2 \cdots y_{m_1+m_2+1}^2 z_{m_1+m_2+2} \\
g_{m_1+1}(z_1,\ldots,z_N) &:= z_{m_1} x_{m_1+1}^2 z_{m_1+2} \\
&\vdots
\end{aligned}$$

The edge consistency equations are given by $g_j = 1$ for all $j = 1,\ldots,N$. In order to determine smoothness and the local dimension, we work with the differentials dg_j of these expressions. Actually, it will be more convenient to work with $d\log g_j = dg_j/g_j$. For convenience we note the differential relationship between x, y, z (leaving off the indices):

$$\begin{aligned}
d\log z &= -\frac{1}{y} d\log x = -x d\log y \\
d\log y &= -z d\log x.
\end{aligned}$$

We choose the following convenient basis for the cotangent space $\mathbb{R}^{N*}$ at our point $(z_1,\ldots,z_N) \in \mathscr{V}_+$. For indices j such that $x_j < 0$, define $\xi_j = d\log x_j$, $c_j = z_j$, and $t_j = (1 - z_j)$ so that

$$\begin{aligned}
d\log x_j &= \xi_j \\
d\log y_j &= -c_j \xi_j \\
d\log z_j &= -t_j \xi_j.
\end{aligned}$$

For indices j such that $y_j < 0$, define $\xi_j = d\log y_j$, $c_j = 1/z_j$, and $t_j = (1 - z_j)$ so that

$$\begin{aligned} d\log x_j &= -c_j\xi_j \\ d\log y_j &= \xi_j \\ d\log z_j &= -t_j\xi_j. \end{aligned}$$

Note that in both cases $0 < c_j, t_j < 1$. The differential of a fan equation is given by

$$d\log g_j = -t_{j-1}\xi_{j-1} + 2\xi_j - 2(c_{j+1}\xi_{j+1} + \ldots + c_{k+1}\xi_{k+1}) - t_{k+2}\xi_{k+2} \tag{6.6}$$

while the differential of a 4-valent equation is given by

$$d\log g_q = -t_{q-1}\xi_{q-1} + 2\xi_q - t_{q+1}\xi_{q+1}. \tag{6.7}$$

We think of $(d\log g_1, \ldots, d\log g_N)$ as a map $\mathbb{R}^N \to \mathbb{R}^N$. The kernel of this (linear) map is the Zariski tangent space to $\mathscr{V}_+$. Using the dual basis to $\{\xi_j\}$ for the domain we let A be the matrix of this map. The matrix A is nearly block diagonal, having a block for each string of R's and a block for each string of L's in the word W. A block corresponding to m_p R's will be $m_p \times (m_p + 3)$. It overlaps with the following $n_p \times (n_p + 3)$ L-block in three columns.

$A =$

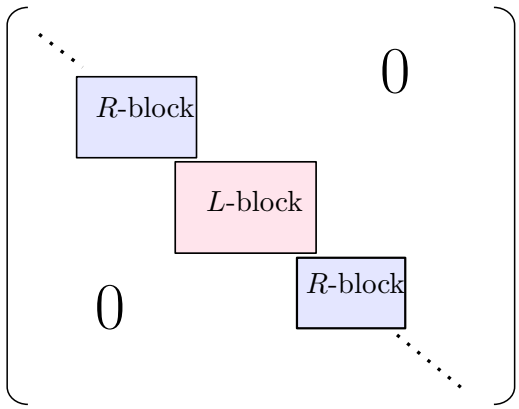

Both R-blocks and L-blocks have the same form. Indexing the variables to match Proposition 49, each block is described as follows:

$$\begin{pmatrix} -t_{j-1} & 2 & -2c_{j+1} & -2c_{j+2} & -2c_{j+3} & \dots & -2c_k & -2c_{k+1} & -t_{k+2} \\ 0 & -t_j & 2 & -t_{j+2} & 0 & \dots & 0 & 0 & 0 \\ 0 & 0 & -t_{j+1} & 2 & -t_{j+3} & \dots & 0 & 0 & 0 \\ 0 & 0 & 0 & -t_{j+2} & 2 & \dots & 0 & 0 & 0 \\ & \vdots & & & & \ddots & & \vdots & \\ 0 & 0 & 0 & 0 & 0 & \dots & 2 & -t_{k+1} & 0 \end{pmatrix}$$

where the 2's lie on the diagonal of A.

Example: $W = R^4L^5$

If we take $W = R^4L^5$ as in Figure 6.5, the matrix A is made up of two blocks, an R-block of size 3×6 and an L-block of size 5×8 (note: in general the first and last blocks "spill" over to the other side of the matrix).

$$A = \begin{pmatrix} 2 & -2c_2 & -2c_3 & -2c_4 & -2c_5 & -t_6 & 0 & 0 & -t_9 \\ -t_1 & 2 & -t_3 & 0 & 0 & 0 & 0 & 0 & 0 \\ 0 & -t_2 & 2 & -t_4 & 0 & 0 & 0 & 0 & 0 \\ 0 & 0 & -t_3 & 2 & -t_5 & 0 & 0 & 0 & 0 \\ -2c_1 & -t_2 & 0 & -t_4 & 2 & -2c_6 & -2c_7 & -2c_8 & -2c_9 \\ 0 & 0 & 0 & 0 & -t_5 & 2 & -t_7 & 0 & 0 \\ 0 & 0 & 0 & 0 & 0 & -t_6 & 2 & -t_8 & 0 \\ 0 & 0 & 0 & 0 & 0 & 0 & -t_7 & 2 & -t_9 \\ -t_1 & 0 & 0 & 0 & 0 & 0 & 0 & -t_8 & 2 \end{pmatrix}$$

The crucial things to notice about A are:

- All diagonal entries are equal to 2.
- All entries away from the diagonal are non-positive.
- The entries one off of the diagonal are strictly negative.
- Each column sums to zero. This is the differential version of the fact that the product of all g_j's is identically equal to one.

Proposition 52. *The matrix A has one dimensional kernel.*

Proof. It will be more convenient to work with the transpose A^T, which also has the properties listed above, except that the rows sum to zero rather than the columns. We write

$$A^T = 2I - B - C$$

where I is the $N \times N$ identity matrix, B is a matrix with positive entries one off the diagonal and zeros otherwise, and C is a matrix with non-negative entries that is zero within one place of the diagonal. That is $b_{ij}, c_{ij} \geq 0$ for all indices, $b_{ij} > 0$ if and only if $|i-j| = 1$, and $c_{ij} = 0$ if $|i-j| \leq 1$. Now, since the rows of A^T sum to zero, we have that

$$v = \begin{pmatrix} 1 \\ \vdots \\ 1 \end{pmatrix} \in \ker A^T.$$

Suppose w is another non-zero vector with $w \in \ker A^T$. Then, let $u = w - \min(w)v \in \ker A^T$. Note that all entries of u are non-negative and at least one entry $u_p = 0$. Next, consider the p^{th} entry of $A^T u$:

$$\begin{aligned} 0 = -(A^T u)_p &= -2u_p + (Bu)_p + (Cu)_p \\ &= 0 + b_{p,p-1}u_{p-1} + b_{p,p+1}u_{p+1} + (Cu)_p \\ &\geq b_{p,p-1}u_{p-1} + b_{p,p+1}u_{p+1}. \end{aligned}$$

This implies that $u_{p-1} = u_{p+1} = 0$. It follows by induction that $u = 0$ and so w is a multiple of v. Thus A^T has one dimensional kernel and so does A. □

6.2.2 Positive tangent vectors

Actually, we can spiff up the proof of Proposition 52 to get the following:

Proposition 53. *The kernel of A is spanned by a vector with strictly positive entries.*

Proof. Again, we work with A^T. We will make use of the following:

Lemma 12. *The range of A^T does not contain any vectors with non-negative entries (other than the zero vector).*

Proof. Let $h \in \mathbb{R}^N$ have non-negative entries and suppose there is $w \in \mathbb{R}^N$ such that $A^T w = h$. Set $u = w - \min(w)v$, where $v \in \ker A^T$ is, as above, the vector of all 1's. Then all entries of u are non-negative, $A^T u = h$, and at least one $u_p = 0$. Following the same argument from above, we have

$$\begin{aligned} 0 \;=\; -(A^T u - h)_p &= -2u_p + (Bu)_p + (Cu)_p + h_p \\ &= 0 + b_{p,p-1}u_{p-1} + b_{p,p+1}u_{p+1} + (Cu)_p + h_p \\ &\geq b_{p,p-1}u_{p-1} + b_{p,p+1}u_{p+1} + h_p. \end{aligned}$$

which shows u_{p-1}, u_{p+1}, and h_p are equal to zero. Proceeding inductively, we get that each entry of u and each entry of h is zero. □

The lemma implies that $\ker A$ is spanned by a vector with positive components. One way to see this is as follows. The the reduced row echelon form R for A is (possibly after relabeling indices in the domain):

$$R = UA = \begin{pmatrix} 1 & 0 & \dots & 0 & \alpha_1 \\ 0 & 1 & \dots & 0 & \alpha_2 \\ \vdots & & \ddots & & \vdots \\ 0 & 0 & \dots & 1 & \alpha_{N-1} \\ 0 & 0 & \dots & 0 & 0 \end{pmatrix}$$

Each row of R is in the range of A^T. So the lemma implies that each $\alpha_i < 0$. It is now easy to see that $\ker A$ is spanned by a vector with strictly positive components. □

We have (nearly) shown:

Theorem 8. *The deformation variety is smooth with dimension equal to one at all points of $\mathscr{V}_+$. Further, the tangent space at a point of $\mathscr{V}_+$ is spanned by a vector with positive components (with respect to z_j-coordinates).*

Proof. The smoothness follows from Proposition 52. Proposition 53 gives that the tangent space to the deformation variety is spanned by a vector u in $\mathbb{R}^N$, whose coordinates with respect to the basis dual to $\{\xi_j\}$ are positive. Recall that $\xi_j = d\log x_j$ if $x_j < 0$, or

$\xi_j = d\log y_j$ if $y_j < 0$. Hence, if $x_j < 0$, then

$$dx_j(u) = x_j\xi_j(u) < 0$$

and if $y_j < 0$, then

$$dy_j(u) = y_j\xi_j(u) < 0.$$

Let $v = -u$. We remind the reader that

$$dx = d\left(\frac{z-1}{z}\right) = \frac{1}{z^2}dz$$

and similarly

$$dy = d\left(\frac{1}{1-z}\right) = \frac{1}{(1-z)^2}dz$$

so that $dz_j(v) > 0$ if and only if $dx_j(v) > 0$ if and only if $dy_j(v) > 0$. That is, z_j increases in the direction of v if and only if x_j increases in the direction of v if and only y_j increases in the direction of v. Hence v has positive coordinates in the standard (z_j) basis. □

6.2.3 $\mathscr{V}_+$ is non-empty

In this section we construct two "canonical" solutions to the edge consistency equations which lie in different (connected) components of $\mathscr{V}_+$, showing in particular that $\mathscr{V}_+$ is non-empty. These solutions correspond to certain projections of the Sol geometry of the torus bundle associated to φ. We construct them directly from the natural affine $\mathbb{R}^2$ structure of the layered triangulations used to construct the monodromy tetrahedralization of M.

By construction, the punctured torus bundle M comes equipped with a projection map $\pi : \widetilde{M} \to \mathbb{R}^2$ which induces a one dimensional foliation of M with a transverse affine linear structure. Think of π as a developing map for the transverse structure. The holonomy $\sigma : \pi_1 M \to \mathrm{Aff}^+\mathbb{R}^2$ can be described as follows:

$$\begin{aligned}
\sigma(\alpha) &: (x,y) \mapsto (x+1, y) \\
\sigma(\beta) &: (x,y) \mapsto (x, y+1) \\
\sigma(\gamma) &: (x,y) \mapsto \varphi(x,y)
\end{aligned}$$

where α, β generate the fiber $\pi_1 T^2$ and γ is a lift of the base circle. We can use π to

project our tetrahedra onto parallelograms in $\mathbb{R}^2$. Begin by choosing a lift $\tilde{\mathcal{T}}_1$ of the first tetrahedron. We can choose the lift that projects onto the square P_1 with bottom left corner at the origin. We then "develop" consecutive tetrahedra into $\mathbb{R}^2$ along a path in $\widetilde{M}$. The result is a sequence of parallelograms P_j, with each consecutive pair overlapping in a triangle.

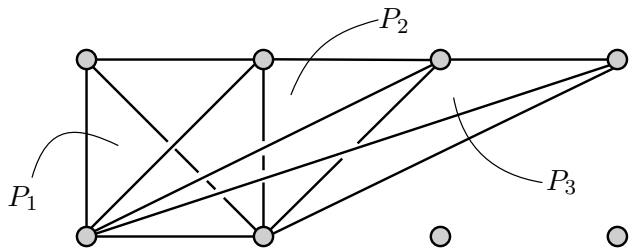

Figure 6.6: The development of tetrahedra into $\mathbb{R}^2$ is a union of parallelograms.

The bottom faces of $\tilde{\mathcal{T}}_j$ map to triangles of $\tilde{\tau}_{j-1}$ and the top faces map to triangles of $\tilde{\tau}_j$, where $\tilde{\tau}_j$ is the lift of the triangulation τ_j to $\mathbb{R}^2$. The face glueing maps are realized in $\mathbb{R}^2$ as combinations of the affine linear transformations $\sigma(\alpha), \sigma(\beta)$, and $\sigma(\gamma)$.

We now construct $\mathbb{H}^2$ tetrahedra as follows. Let v_+, v_- be the eigenvectors of φ corresponding to the eigenvalues $\lambda_+ > 1$, and $\lambda_- < 1$ respectively. Let $r_+, r_- : \mathbb{R}^2 \to \mathbb{R}$ be the coordinate functions with respect to the basis $\{v_+, v_-\}$. For each j, project the vertices of P_j to $\mathbb{R}$ using, e.g., r_+. The vertices project to four distinct real numbers which we use to build an $\mathbb{H}^2$ tetrahedron. Orient the resulting $\mathbb{H}^2$ ideal tetrahedron compatibly with the original tetrahedron. It is an easy exercise to show that this process always produces $\mathbb{H}^2$ tetrahedra that are folded along the z-edges corresponding to diagonal exchanges (i.e. the shape parameter z has zero dihedral angle). See Figure 6.7.

Next, note that r_+ takes translations in $\mathbb{R}^2$ to translations in $\mathbb{R}$ and r_+ converts the action of φ into scaling by λ_+ on $\mathbb{R}$. Hence, the map $r_+ \circ \pi : \widetilde{M} \to \mathbb{R}$ is equivariant, converting covering transformations to similarities of $\mathbb{R}$. In other words, the face glueing maps for our $\mathbb{H}^2$ tetrahedra are realized by hyperbolic isometries which fix ∞. Hence, the shape parameters for these $\mathbb{H}^2$ tetrahedra are well-defined. Using r_- in place of r_+ we get a different set of $\mathbb{H}^2$ shape parameters. The following proposition shows that the condition on dihedral angles is satisfied so that the r_+ and r_- shape parameters each determine a solution to Thurston's equation lying in $\mathscr{V}_+$. It is a corollary of the proof that these solutions

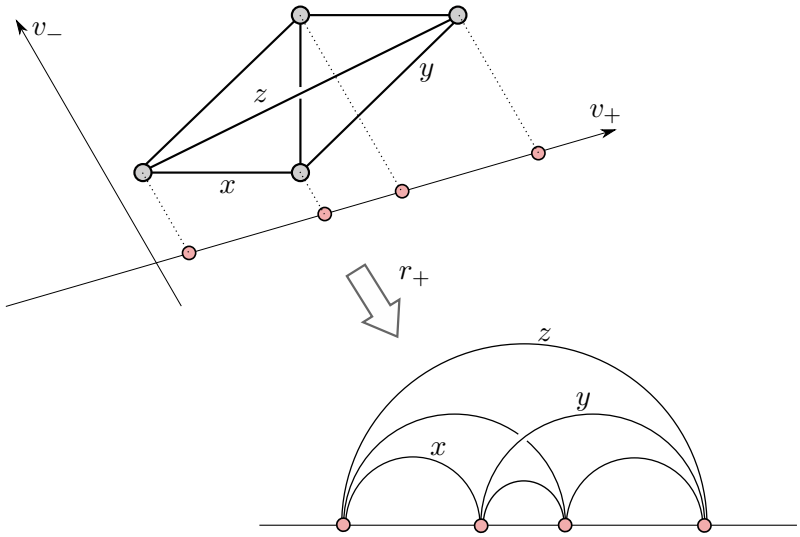

Figure 6.7: The projection r_+ determines flattened tetrahedra in $\mathbb{H}^2$.

lie in distinct components of $\mathscr{V}_+$.

Proposition 54. *The $\mathbb{H}^2$ tetrahedralizations determined by r_+, r_- have total dihedral angle 2π around each edge in $\mathcal{T}$.*

Proof. Let e be an edge of the triangulation $\mathcal{T}$. Recall that e is an edge of consecutive tetrahedra $\mathcal{T}_{j-1}, \ldots, \mathcal{T}_{k+1}$, for $k \geq j$ (with $k = j$ if e is 4-valent, and $k > j$ if e is a hinge edge). In $\widetilde{M}$, (a lift of) e is bordered by one lift each of $\mathcal{T}_{j-1}, \mathcal{T}_{k+1}$, and two lifts of each $\mathcal{T}_i$ for $i = j, \ldots, k$. The tetrahedra are represented by $2(k-j+2)$ parallelograms P_i which are layered around the corresponding edge e' in $\mathbb{R}^2$. We number the parallelograms in cyclic order around e' so that P_1 is the image of $\mathcal{T}_{j-1}$, and P_{k-j+3} is the image of $\mathcal{T}_{k+1}$. For $i = j, \ldots, k$, the two lifts of $\mathcal{T}_i$ that border e map to P_{i-j+2} and $P_{2k-j+4-i}$, which are translates of one another. Let the endpoints of e' be $p, q \in \mathbb{Z}^2$. For each $s = 1, \ldots, 2(k-j+2)$, let e'_s be the edge opposite e' in P_s with endpoints p_s, q_s. Note that in the cases $s = 1$ and $s = k - j + 3$, the edges e', e'_s are diagonals of P_s. Let e_+ (resp. e_-) be the geodesic in $\mathbb{H}^2$ connecting $r_+(p)$ to $r_+(q)$ (resp. $r_-(p)$ to $r_-(q)$). For each s, the $\mathbb{H}^2$ ideal tetrahedron T_s^+ with vertices $r_+(p), r_+(q), r_+(p_s), r_+(q_s)$ has dihedral angle π at e'' if and only if the intervals $r_+(e')$ and $r_+(e'_s)$ overlap *partially* (with neither one contained in the other). We will use this characterization to show that the total dihedral angle around e_+ is 2π (and similarly for e_-).

The union of the e'_s is a closed polygonal loop in $\mathbb{R}^2$ with a particularly nice structure. The three edges e', e'_1, e'_{k-j+3} share a common midpoint. The edges $e'_2, \ldots, e'_{k-j+2}$ are each parallel to e'; their union forms a straight line segment $I_1 \subset \mathbb{R}^2$. Similarly, the edges $e'_{k-j+4}, \ldots, e'_{2(k-j+2)}$ are each parallel to e' and their union forms a straight line segment I_2. Orienting I_1, I_2 in the direction of increasing s, we have that I_2 is a translate of I_1 with the same orientation. Hence the union of the e'_s is a closed polygonal loop with four straight sides $e'_1, I_1, e'_{k-j+3}, I_2$. In light of this, the proof will be complete after demonstrating the following lemma.

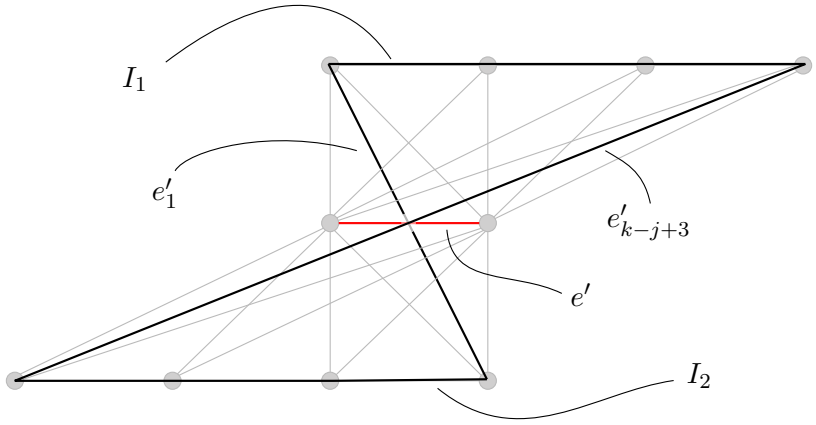

Figure 6.8: The development of tetrahedra around an edge.

Lemma 13. *The images of the edges e'_1, e', e'_{k-j+3} are nested as follows:*

$$r_+(e'_1) \subset r_+(e') \subset r_+(e'_{k-j+3})$$
$$r_-(e'_{k-j+3}) \subset r_-(e') \subset r_-(e'_1).$$

Proof. Let P_0 be the base parallelogram (actually a square) with vertices $(0,0)$, $(1,0)$, $(1,1)$, and $(0,1)$. By construction, the parallelogram P_1, which corresponds to $\mathcal{T}_{j-1}$ is given by a translate of $W_{j-2}P_0$ where W_s is the product of the first (left-most) s letters in the word W describing φ. The edge e'_1 is the bottom diagonal of P_1, which is a translate of the vector $W_{j-2}\begin{pmatrix}1\\-1\end{pmatrix}$ and the edge e' is the top diagonal of P_1, which is a translate of the vector $W_{j-2}\begin{pmatrix}1\\1\end{pmatrix}$. Similarly, P_{k-j+3}, which corresponds to $\mathcal{T}_{k+1}$ is a translate of W_kP_0. So e',

which is the bottom diagonal of P_{k-j+3}, is a translate of $W_k \begin{pmatrix} 1 \\ -1 \end{pmatrix}$ and e'_{k-j+3}, which is the top diagonal of P_{k-j+3}, is a translate of $W_k \begin{pmatrix} 1 \\ 1 \end{pmatrix}$. Recall that either $W_k = W_{j-2}RL^{k-j}R$ or $W_k = W_{j-2}LR^{k-j}L$. From this it is easy to check that $W_{j-2} \begin{pmatrix} 1 \\ 1 \end{pmatrix} = \pm W_k \begin{pmatrix} 1 \\ -1 \end{pmatrix}$, so they determine the same line segment up to translation in $\mathbb{R}^2$.

Next, we may assume that v_+ lies in the positive quadrant and that v_- has negative first coordinate and positive second coordinate (this is easy to check). Hence $W_s \begin{pmatrix} 0 \\ 1 \end{pmatrix}$ and $W_s \begin{pmatrix} 1 \\ 0 \end{pmatrix}$, which lie in the positive quadrant, have $r_+ > 0$. Thus we have that for any s,

$$\begin{aligned} r_+ W_s \begin{pmatrix} 1 \\ 1 \end{pmatrix} - r_+ W_s \begin{pmatrix} 1 \\ -1 \end{pmatrix} &= 2r_+ W_s \begin{pmatrix} 0 \\ 1 \end{pmatrix} && > 0 \\ r_+ W_s \begin{pmatrix} 1 \\ 1 \end{pmatrix} + r_+ W_s \begin{pmatrix} 1 \\ -1 \end{pmatrix} &= 2r_+ W_s \begin{pmatrix} 1 \\ 0 \end{pmatrix} && > 0. \end{aligned}$$

This implies that

$$\left| r_+ W_s \begin{pmatrix} 1 \\ 1 \end{pmatrix} \right| > \left| r_+ W_s \begin{pmatrix} 1 \\ -1 \end{pmatrix} \right|.$$

Applying this fact with $s = j-2$ and $s = k$ implies that the lengths of the intervals $r_+(e')$, $r_+(e'_1)$, and $r_+(e'_{k-j+3})$ are ordered as follows:

$$|r_+(e'_{k-j+3})| > |r_+(e')| > |r_+(e'_1)|.$$

Thus, as e',e'_1, and e'_{k-j+3} share a common midpoint, the r_+ statement of the Lemma follows.

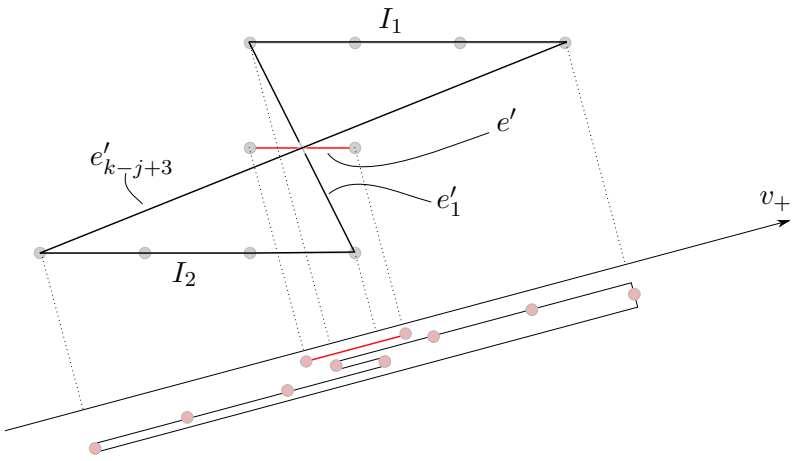

Figure 6.9: The r_+ projection of the edges opposite e'.

The r_- statement is similar. In this case $r_- W_s \begin{pmatrix} 0 \\ 1 \end{pmatrix} > 0$ while $r_- W_s \begin{pmatrix} 1 \\ 0 \end{pmatrix} < 0$. Thus

$$r_- W_s \begin{pmatrix} 1 \\ 1 \end{pmatrix} - r_- W_s \begin{pmatrix} 1 \\ -1 \end{pmatrix} = 2 r_- W_s \begin{pmatrix} 0 \\ 1 \end{pmatrix} \qquad > 0$$

$$r_- W_s \begin{pmatrix} 1 \\ 1 \end{pmatrix} + r_- W_s \begin{pmatrix} 1 \\ -1 \end{pmatrix} = 2 r_- W_s \begin{pmatrix} 1 \\ 0 \end{pmatrix} \qquad < 0.$$

It follows that for any s,

$$\left| r_- W_s \begin{pmatrix} 1 \\ 1 \end{pmatrix} \right| < \left| r_- W_s \begin{pmatrix} 1 \\ -1 \end{pmatrix} \right|.$$

So the lengths of the intervals $r_-(e')$, $r_-(e'_1)$, and $r_-(e'_{k-j+3})$ are ordered like so:

$$|r_-(e'_{k-j+3})| < |r_-(e')| < |r_-(e'_1)|.$$

The r_- part of the Lemma now follows.

□

By the Lemma, and the above characterization of the edges e'_s, we must have that $r_+(e'_s)$ partially overlaps $r_+(e')$ if and only if $s = 2$ or $s = 2(k - j + 2)$. Hence the $\mathbb{H}^2$ tetrahedron T_s^+ has dihedral angle π at e_+ if and only if $s = 2$, or $s = 2(k - j + 2)$. Similarly, the $\mathbb{H}^2$ tetrahedron T_s^- in the r_- tetrahedralization has dihedral angle π if and only if $s = k - j + 2$

or $s = k-j+4$. Note that this shows that r_+ produces a solution in case 1 of Proposition 51, while r_- produces a solution in case 2. □

We note that $r_+ \circ \pi$ and $r_- \circ \pi$ give maps to $\mathbb{R} \subset \mathbb{RP}^1$ which are invariant under representations $\rho_+, \rho_- : \pi_1 M \to \mathrm{PSL}(2,\mathbb{R})$ which fix ∞ (so ρ_+, ρ_- are reducible). The tetrahedra construction just performed determines (degenerate) developing maps D_+, D_- for two transversely hyperbolic foliations with respective holonomies ρ_+, ρ_-. These two transversely hyperbolic foliations correspond to projecting the Sol geometry of M onto the two vertical hyperbolic planes in Sol.

6.2.4 A local parameter

Let ϵ represent the curve encircling the puncture in $T^2 \subset M$. We show in this section that the length of ϵ is a local parameter for $\mathscr{V}_+$. This will follow, after some calculation, from the fact that the tangent direction to $\mathscr{V}_+$ must increase all shape parameters. As the general calculation is notationally cumbersome, we start with an example.

Example: $W = R^4L^5$

Let $W = R^4L^5$ as in Figure 6.5. The puncture curve ϵ is the curve going across the diagram from left to right (see Figure 6.10). The exponential length of ϵ can be read off from the diagram:

$$H(\epsilon) = (z_9 x_1 z_2^{-1} y_1^{-1})^2.$$

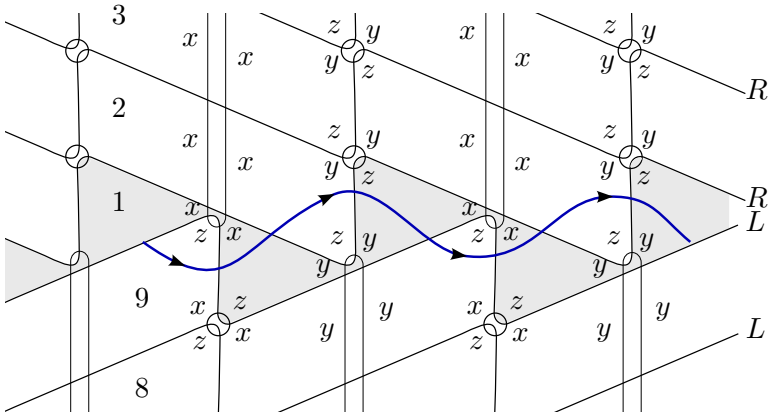

Figure 6.10: The puncture curve ϵ is drawn in blue

We assume (as the other case is similar) that we are in case 1 of Proposition 51. That is, $x_1 < 0$, $y_2, \ldots, y_5 < 0$ and $x_6, \ldots, x_9 < 0$. We adopt the following notation:

$$\alpha_j = \begin{cases} x_j & \text{if } x_j < 0, \\ y_j & \text{if } y_j < 0. \end{cases}$$

$$\beta_j = \begin{cases} x_j & \text{if } x_j > 0, \\ y_j & \text{if } y_j > 0. \end{cases}$$

Note that, in either case, we have $\alpha_j \beta_j z_j = -1$. Using this notation, $H(\epsilon) = (z_9 \alpha_1 z_2^{-1} \beta_1^{-1})^2$, and the edge consistency equations are given by

$$\begin{aligned}
1 = \ & g_1 = z_9 \alpha_1^2 \beta_2^2 \beta_3^2 \beta_4^2 \beta_5^2 z_6 & \qquad 1 = \ & g_5 = z_4 \alpha_5^2 \beta_6^2 \beta_7^2 \beta_8^2 \beta_9^2 \beta_1^2 z_2 \\
1 = \ & g_2 = z_1 \alpha_2^2 z_3 & 1 = \ & g_6 = z_5 \alpha_6^2 z_7 \\
1 = \ & g_3 = z_2 \alpha_3^2 z_4 & 1 = \ & g_7 = z_6 \alpha_7^2 z_8 \\
1 = \ & g_4 = z_3 \alpha_4^2 z_5 & 1 = \ & g_8 = z_7 \alpha_8^2 z_9 \\
& & 1 = \ & g_9 = z_8 \alpha_9^2 z_1
\end{aligned}$$

The following trick produces a useful description of $H(\epsilon)$. We remind the reader to interpret the indices cyclically, e.g. $z_{10} := z_1$.

$$\begin{aligned}
\prod_{i=1}^{8} g_{i+1}^i &= \left(\prod_{i=1}^{8} (z_i \alpha_{i+1}^2 z_{i+2})^i \right) z_6^{-4} z_2^4 \prod_{i=6}^{10} \beta_i^8 \\
&= z_9^{-9} z_1^9 \left(\prod_{i=1}^{8} \alpha_{i+1}^{2i} z_{i+1}^{2i} \right) z_6^{-4} z_2^4 \prod_{i=6}^{10} \beta_i^8 \\
&= z_9^{-9} z_1^9 z_6^{-4} z_2^4 \prod_{i=2}^{9} \beta_i^{-2i+2} \prod_{i=6}^{10} \beta_i^8 \\
&= z_9^{-9} z_1^9 z_6^{-4} z_2^4 \beta_1^{18} \prod_{i=2}^{5} \beta_i^{-2i+2} \prod_{i=6}^{10} \beta_i^{-2i+10} \\
&= (z_9^{-9} \alpha_1^{-9} z_2^9 \beta_1^9) z_6^{-4} z_2^{-5} \prod_{i=2}^{5} \beta_i^{-2i+2} \prod_{i=6}^{10} \beta_i^{-2i+10}.
\end{aligned}$$

and therefore a solution to the glueing equations satisfies

$$H(\epsilon)^{9/2} = \left(\prod_{i=1}^{4} \beta_{i+1}^{-2i}\right)\left(\prod_{i=5}^{9} \beta_{i+1}^{-2i+8}\right) z_2^{-5} z_6^{-4}.$$

This shows that $H(\epsilon)$ is a product of negative powers of β_j's and z_j's. Now, by Theorem 8, the tangent direction to $\mathscr{V}_+$ increases all β_j's and z_j's and so it decreases $H(\epsilon)$. Hence, $H(\epsilon)$ is a local parameter for $\mathscr{V}_+$. In fact, $H(\epsilon)$ can be made arbitrarily small or increased to infinity. The argument will be given below.

Remark 35. The trick of considering $\prod_{i=1}^{8} g_{i+1}^i$ seems to come out of nowhere. Indeed, the author knows of no geometric interpretation of the quantity that would suggest it has any importance. However, the trick readily extends to give a (relatively) succinct proof in the general case.

The general case. Recall that our Anosov map φ is decomposed as:

$$A\varphi A^{-1} = W = R^{s_1} L^{s_2} R^{s_3} L^{s_4} \cdots R^{s_{K-1}} L^{s_K}.$$

Note that we have changed notation slightly in order to ease the upcoming computation. Let M_p denote the index of the p^{th} hinge tetrahedron:

$$M_p = 1 + \sum_{j=1}^{p-1} s_j,$$

where we define $M_{K+1} = N + 1$ where $N = \sum s_j$ is the total length of the word W. Note, as usual, that indices i of the α_i, β_i, z_i are interpreted cyclically so that, for example, $\beta_{N+1} := \beta_1$. Then,

Proposition 55. *$H(\epsilon)$ can be expressed in the following form (generalizing the form in the above example):*

$$H(\epsilon)^{N/2} = \prod_{p=1}^{K} \left(z_{1+M_{p+1}}^{-s_p} \prod_{j=1+M_p}^{M_{p+1}} \beta_j^{-2j+2M_p} \right). \tag{6.8}$$

In particular, $H(\epsilon)$ is a local parameter for $\mathscr{V}_+$.

Proof. We follow the same general procedure as in the above example:

$$\begin{aligned}
\prod_{i=1}^{N-1} g_{i+1}^i &= \prod_{i=1}^{N-1} (z_i \alpha_{i+1}^2 z_{i+2})^i \prod_{p=2}^{K} \left(z_{1+M_p}^{-(M_p-1)} z_{1+M_{p+1}}^{(M_p-1)} \prod_{j=1+M_p}^{M_{p+1}} \beta_j^{2(M_p-1)} \right) \\
&= z_1^N z_N^{-N} \prod_{i=1}^{N-1} \left(z_{i+1}^{2i} \alpha_{i+1}^{2i} \right) \left(\prod_{p=2}^{K} z_{1+M_p}^{1-M_p} \prod_{j=1+M_p}^{M_{p+1}} \beta_j^{2M_p-2} \right) \prod_{p=3}^{K+1} \left(z_{1+M_p}^{-1+M_{p-1}} \right) \\
&= z_1^N z_N^{-N} \prod_{i=1}^{N-1} \beta_{i+1}^{-2i} \left(\prod_{p=2}^{K} \prod_{j=1+M_p}^{M_{p+1}} \beta_j^{2M_p-2} \right) z_2^N \prod_{p=2}^{K+1} \left(z_{1+M_p}^{M_{p-1}-M_p} \right) \\
&= z_1^N z_N^{-N} z_2^N \beta_1^{2N} \left(\prod_{p=1}^{K} \prod_{j=1+M_p}^{M_{p+1}} \beta_j^{-2(j-1)+2M_p-2} \right) \prod_{p=2}^{K+1} \left(z_{1+M_p}^{-s_{p-1}} \right) \\
&= (z_N^{-1} \alpha_1^{-1} z_2 \beta_1)^N \prod_{p=1}^{K} \left(z_{1+M_{p+1}}^{-s_p} \prod_{j=1+M_p}^{M_{p+1}} \beta_j^{-2j+2M_p} \right).
\end{aligned}$$

So, as $H(\epsilon) = (z_N \alpha_1 z_2^{-1} \beta_2^{-1})^2$, we have the result:

$$H(\epsilon)^{N/2} = \prod_{p=1}^{K} \left(z_{1+M_{p+1}}^{-s_p} \prod_{j=1+M_p}^{M_{p+1}} \beta_j^{-2j+2M_p} \right).$$

□

Corollary. *The exponential length of the puncture curve, $H(\epsilon)$, can be made arbitrarily small or arbitrarily large .*

Proof. We show that $H(\epsilon)$ can be made arbitrarily small; the second statement is similar. By Theorem 8, any point $(z_1, \ldots, z_N) \in \mathscr{V}_+$ is a smooth point of the deformation variety, and all shape parameters can be increased locally. They can be increased globally until some of them go to infinity. Consider such a path. Recall that for some j, $\beta_j = x_j$ while for other k, $\beta_k = y_k$. We show that one of the β_i must approach infinity. Assume not. Then some $z_j \to \infty$, for recall that all $\alpha_j < 0$. Examining the $(j+1)^{st}$ glueing equation, we see that $\alpha_{j+1} \to 0$ as all other terms are positive and increasing. If $\beta_{j+1} > 1$ ($\iff$ $\beta_j = y_j$), then we must have $\beta_{j+1} \to \infty$. If not then $z_{j+1} > 1$ and $z_{j+1} \to \infty$. We continue inductively and eventually reach an index i such that $\beta_i > 1$ and $\beta_i \to \infty$. It is clear from the expression (6.8) that $H(\epsilon) \to 0$. □

Remark 36. It is straightforward to check that the discrete rotational part of the holonomy of ϵ must be $+2\pi$. Hence by the argument from Example 3 in Chapter 5, AdS tachyon structures regenerated from the canonical solution in $\mathscr{V}_+$ must have negative mass. The corollary implies that the mass of these structures can be decreased to $-\infty$.

Appendix A

A half-space model for AdS^3

In [Ahl85] Ahlfors describes a general construction of n-dimensional hyperbolic space as a half-space inside a Clifford algebra $\mathcal{C}_n$. The isometries in this model are Mobius transformations with coefficients in a sub-algebra $\mathcal{C}_{n-1}$. In the case $n = 3$, $\mathcal{C}_3$ is the Hamiltonian quaternions, $\mathcal{C}_2$ is the complex numbers and the construction gives the standard upper half-space model of $\mathbb{H}^3$. Following Ahlfors, we construct a half-space model of AdS^3 using generalized Clifford numbers. The isometries in this model will be $\mathrm{PSL}(2, \mathbb{R} + \mathbb{R}\tau)$ acting by Mobius transformations. This construction can (surely) be extended to higher anti de Sitter spaces.

A.1 AdS^3 via Clifford numbers

Starting with our algebra $\mathcal{B} = \mathbb{R} + \mathbb{R}\tau$ from Sections 4.8 and 5.2.3, we add an element j with $j^2 = -1$ and $j\tau = -\tau j$. This defines a Clifford algebra $\mathcal{A}$ that is four dimensional over the reals. In fact, in this low dimensional case $\mathcal{A}$ is isomorphic to the algebra of real two-by-two matrices. There are many different copies of $\mathbb{C}$ lying inside $\mathcal{A}$, one distinguished copy being $\mathbb{R} + \mathbb{R}j$, just as there are many isomorphic copies of $\mathcal{B}$. There is a conjugation operation on $\mathcal{A}$, $z \mapsto \overline{z}$ defined by

$$\overline{1} = 1, \quad \overline{j} = -j, \quad \overline{\tau} = -\tau, \text{ and } \overline{(zw)} = \overline{w}\,\overline{z}.$$

The conjugation defines a square-norm

$$|z|^2 = z\overline{z} = \overline{z}z \ \in \mathbb{R}.$$

Let $V = \text{span}\{1, j, \tau\}$ be the subspace of elements of $\mathcal{A}$ having degree ≤ 1, the so-called *vectors* of $\mathcal{A}$. The square-norm restricted to V comes from the $(2,1)$ Minkowski product on $\mathbb{R}^{2,1}$ (with basis $\{1, j, \tau\}$). In Section 5.2.3, we showed that $\text{SL}(2, \mathcal{B})$ acts on the compactification $\mathbb{P}^1\mathcal{B}$ of $\mathcal{B}$. Our goal here is to extend to a suitable compactification of V in a way that allows $\text{SL}(2, \mathcal{B})$ to act naturally.

Define $\mathbb{P}^1 V$ as follows:

$$\mathbb{P}^1 V = \left\{ \begin{pmatrix} x \\ y \end{pmatrix} \in \mathcal{A}^2 : \ x\overline{y} \in V, \ x\alpha = 0 \text{ and } y\alpha = 0 \text{ for } \alpha \in \mathcal{A} \iff \alpha = 0 \right\} / \sim$$

$$\text{where } \begin{pmatrix} x \\ y \end{pmatrix} \sim \begin{pmatrix} x\lambda \\ y\lambda \end{pmatrix} \text{ for } \lambda \in A^\times.$$

Note that when y is invertible we have $xy^{-1} = x\overline{y}/|y|^2$, so that the condition $x\overline{y} \in V$ allows us to think of $\begin{pmatrix} x \\ y \end{pmatrix} \sim \begin{pmatrix} xy^{-1} \\ 1 \end{pmatrix}$ as the vector xy^{-1} in $V \subset \mathbb{P}^1 V$. Let us examine the extra points in $\mathbb{P}^1 V$. Consider $\left[\begin{pmatrix} x \\ y \end{pmatrix} \right] \in \mathbb{P}^1 V$ with y not invertible (so $y\overline{y} = 0$). There are several cases

1. $y = 0$, and so x is invertible. Thus $\begin{pmatrix} x \\ y \end{pmatrix} \sim \begin{pmatrix} 1 \\ 0 \end{pmatrix} = \infty$.

2. x is invertible and $y \neq 0$. Then $\begin{pmatrix} x \\ y \end{pmatrix} \sim \begin{pmatrix} a \\ \frac{e^{j\theta}+\tau}{2} \end{pmatrix}$ for some $a \in \mathbb{R}$ and some $e^{j\theta} = \cos\theta + j\sin\theta$ on the unit circle in $\mathbb{R} + \mathbb{R}j$.

3. x is not invertible ($\implies y \neq 0$). Then $\begin{pmatrix} x \\ y \end{pmatrix} \sim \begin{pmatrix} 1 - e^{-j\theta}\tau \\ e^{j\theta} + \tau \end{pmatrix} \sim \begin{pmatrix} e^{-j\theta} - \tau \\ 1 + e^{j\theta}\tau \end{pmatrix}$.

These added points are all endpoints of lines in V. Space-like and time-like lines all limit to ∞. Light-like lines limit to the points described in cases 2 and 3. Indeed, any light-like

line can be written in orthogonal coordinates as

$$r(t) = bje^{j\theta} + a\ \frac{e^{j\theta}+\tau}{2} + t\frac{e^{j\theta}-\tau}{2}$$

where $a, b \in \mathbb{R}$. If $a \neq 0$, then in $\mathbb{P}^1V$

$$\begin{aligned} r(t) &= \begin{pmatrix} bje^{j\theta} + a\ \frac{e^{j\theta}+\tau}{2} + t\frac{e^{j\theta}-\tau}{2} \\ 1 \end{pmatrix} \left(\frac{e^{-j\theta}-\tau}{2} \cdot \frac{a-bj}{t} + \frac{e^{-j\theta}+\tau}{2} \right) \\ &= \begin{pmatrix} \frac{1+e^{j\theta}\tau}{2} \cdot \frac{abj+b^2}{t} + \frac{1-e^{j\theta}}{2}bj + \frac{1+e^{j\theta}}{2}a + \frac{1-e^{j\theta}}{2}(a-bj) \\ \frac{e^{-j\theta}-\tau}{2} \cdot \frac{a-bj}{t} + \frac{e^{-j\theta}+\tau}{2} \end{pmatrix} \\ &\longrightarrow \begin{pmatrix} a \\ \frac{e^{-j\theta}+\tau}{2} \end{pmatrix} \qquad \text{as } t \to \pm\infty \end{aligned}$$

and we see that we are in case 2. If $a = 0$ a similar calculation shows that

$$r(t) \longrightarrow \begin{pmatrix} 1 - e^{j\theta}\tau \\ e^{-j\theta} + \tau \end{pmatrix} \qquad \text{as } t \to \pm\infty$$

which is of the form in case 3. In fact $\mathbb{P}^1V$ is the conformal compactification of V, the so called *Einstein universe* Ein^{2,1} (see [BCD$^+$08]).

The description of Ein^{2,1} as $\mathbb{P}^1V$ is nice because we can easily see that $\mathrm{SL}(2,\mathcal{B})$ acts on $\mathbb{P}^1V$ (and indeed $\mathrm{PSL}(2,\mathcal{B})$ acts faithfully). For consider $\begin{pmatrix} a & b \\ c & d \end{pmatrix} \in \mathrm{SL}(2,\mathcal{B})$ and $\begin{pmatrix} x \\ y \end{pmatrix}$ with $x\overline{y} = e + \alpha j$ where $e \in \mathbb{R} + \mathbb{R}\tau$ and $\alpha \in \mathbb{R}$. Then $y\overline{x} = \overline{x\overline{y}} = \overline{e} - \alpha j$ and so

$$\begin{pmatrix} a & b \\ c & d \end{pmatrix} \begin{pmatrix} x \\ y \end{pmatrix} = \begin{pmatrix} ax + by \\ cx + dy \end{pmatrix}$$

has

$$\begin{aligned} (ax+by)\overline{(cx+dy)} &= (ax+by)(\overline{x}\ \overline{c} + \overline{y}\ \overline{d}) \\ &= |x|^2 a\overline{c} + |y|^2 b\overline{d} + a(e+\alpha j)\overline{d} + b(\overline{e}-\alpha j)\overline{c} \\ &= |x|^2 a\overline{c} + |y|^2 b\overline{d} + ae\overline{d} + b\overline{e}\ \overline{c} + \alpha(ad-bc)j \\ &= (\text{ something in } \mathbb{R} + \mathbb{R}\tau\ ) + \alpha j \quad \in V. \end{aligned}$$

Though $\mathbb{P}^1\mathcal{B}$ sits inside $\mathbb{P}^1V$, $\mathbb{P}^1\mathcal{B}$ does not divide $\mathbb{P}^1V$ into two components. In fact points in the upper half of V (i.e. j component > 0) can easily be sent to points in the lower half (i.e. j component < 0) by an element of $\mathrm{SL}(2,\mathcal{B})$. The Einstein universe $\mathbb{P}^1V$ is actually a non-orientable three manifold, homeomorphic to the mapping torus of the antipodal map of the two sphere. So, breaking from the analogy to the hyperbolic upper half-space model, we will define our model for AdS^3 as the quotient of $\mathbb{P}^1V$ by an involution fixing $\mathbb{P}^1\mathcal{B}$.

Define the algebra homomorphism $\mathcal{I}$ on $\mathcal{A}$ by $\mathcal{I}(1) = 1$, $\mathcal{I}(\tau) = \tau$, $\mathcal{I}(j) = -j$. It is clear that $\mathcal{I}$ is an involution whose fixed set is $\mathcal{B}$. $\mathcal{I}$ also defines an involution of $\mathbb{P}^1V$ by

$$\mathcal{I}\left[\begin{pmatrix} x \\ y \end{pmatrix}\right] = \left[\begin{pmatrix} \mathcal{I}(x) \\ \mathcal{I}(y) \end{pmatrix}\right]$$

which has fixed set $\mathbb{P}^1\mathcal{B}$. It is easy to check that the action of $\mathrm{PSL}(2,\mathcal{B})$ commutes with $\mathcal{I}$, so $\mathrm{PSL}(2,\mathcal{B})$ acts on the quotient $X = \mathbb{P}^1V/\mathcal{I}$. It is an entertaining exercise to check the following proposition.

Proposition 56. *$X = \mathbb{P}^1V/\mathcal{I}$ is a solid torus with boundary $\mathbb{P}^1\mathcal{B}$.*

Note that after taking the quotient by $\mathcal{I}$, many of the added points in $\mathbb{P}^1V - V$ lie in the *interior* of X. A line ℓ in V has closure in $\mathbb{P}^1V$ given by a circle $\ell \cup q$. If ℓ is, for example, light-like with non-constant j-component then q descends to a point in the interior of X.

A.2 The AdS metric

For simplicity, we will work out the metric aspects in the space $V - \mathcal{B}$. We let x_1, x_2, x_3 be real coordinates for V by the formula $x = x_1 + x_2\tau + x_3 j$. Consider the metric obtained by rescaling the $(2,1)$ Lorentzian metric on V by $1/|x_3|$:

$$ds^2 = \frac{|dx|^2}{x_3^2} = \frac{dx_1^2 - dx_2^2 + dx_3^2}{x_3^2}.$$

Now consider a transformation $g = \begin{pmatrix} a & b \\ c & d \end{pmatrix} \in \mathrm{SL}(2,\mathcal{B})$. Assume that x is in a neighborhood where $cx + d$ is invertible so that

$$g(x) = (ax + b)(cx + d)^{-1} \quad \in V.$$

Differentiating the expression $g(x)(cx+d) = ax+b$ and applying it to a tangent vector $u \in V$ we obtain

$$\begin{aligned} Dg(x)u(cx+d) &= (a - g(x)c)u \\ &= (ac^{-1}(cx+d) - (ax+b))(cx+d)^{-1}cu \\ &= c^{-1}(ad-bc)(cx+d)^{-1}cu \\ &= (x\overline{c}+\overline{d})^{-1}u \end{aligned}$$

where we've assumed c invertible (to avoid a more painful calculation). Anyway, we get the formula

$$Dg(x)\cdot u = (x\overline{c}+\overline{d})^{-1}u(cx+d)^{-1} \tag{A.1}$$

from which we see that g is conformal (with respect to the Minkowski $(2,1)$ metric on V) with rate of magnification $(|cx+d|^2)^{-2}$. Next, writing $g(x) = g_1 + g_2\tau + g_3 j$, a quick computation shows

$$g_3 = \frac{x_3}{|cx+d|^2}$$

which gives that the metric ds^2 is preserved by g:

$$\frac{|Dg\cdot u|^2}{g_3^2} = \frac{|u|^2}{x_3^2}.$$

The curvature of our metric ds^2 is -1 (the calculation should be the same as in the hyperbolic case).

Proposition 57. *$X = \mathbb{P}^1V/\mathcal{I}$ with the metric ds^2 is isometric to* $\mathrm{PSL}(2,\mathbb{R})$ *with the* AdS *metric.*

Proof. We now know X is locally isometric to AdS. In fact, X is geodesically complete (geodesics will be explicitly computed in the next section). The proposition follows by calculating the length of a time-like geodesic. □

A.3 Geodesics

Let P be the (closure of the) plane spanned by $\{1, j\}$ passing through the origin. The (euclidean) reflection about P is clearly an isometry of our metric ds^2. It follows that P

is a totally geodesic plane in X. Of course, P is the upper half-plane model of $\mathbb{H}^2$, so in particular the curve $\gamma_0(t) = e^t j$ is a unit speed space-like geodesic. We translate γ_0 around by $\mathrm{SL}(2,\mathcal{B})$ to obtain a description of all space-like geodesics in this model. Given $A = \begin{pmatrix} a & b \\ c & d \end{pmatrix} \in \mathrm{SL}(2,\mathcal{B})$, consider

$$\gamma(t) = A\gamma_0(t) = (ae^t j + b)(ce^t j + d)^{-1}.$$

For ease of demonstration, we will assume here and in the subsequent computation that c, d are invertible and that t is such that $ce^t j + d$ is invertible (this is true for all except possibly one value of t). Then

$$\gamma(t) = \frac{a\bar{c}e^t + b\bar{d}e^{-t} + j}{|c|^2 e^t + |d|^2 e^{-t}}$$

and we note that the endpoints of γ are $\gamma(-\infty) = bd^{-1}$ and $\gamma(\infty) = ac^{-1}$. Now, by analogy with the hyperbolic case we expect γ to be some sort of conic section in V perpendicular to the boundary with midpoint equal to $\frac{1}{2}(ac^{-1} + bd^{-1})$. In fact, a calculation shows that

$$\gamma(t) - \frac{ac^{-1} + bd^{-1}}{2} = \left(\frac{|c|^2 e^t - |d|^2 e^{-t}}{|c|^2 e^t + |d|^2 e^{-t}}\right)\frac{1}{2cd} + \left(\frac{1}{|c|^2 e^t + |d|^2 e^{-t}}\right) j$$

and so we see that $\gamma(t)$ lies in the affine plane centered at $\frac{ac^{-1}+bd^{-1}}{2}$ and spanned by the directions j and $1/(2cd) = (ac^{-1} - bd^{-1})/2$. Further $\gamma(t)$ satisfies

$$\left|\gamma(t) - \frac{ac^{-1} + bd^{-1}}{2}\right|^2 = \frac{1}{4|c|^2|d|^2}$$

showing that γ parametrizes an ellipse if $|c|^2, |d|^2$ have the same sign, or a hyperbola if $|c|^2, |d|^2$ have opposite sign. Note that in the latter case γ is still a smooth path through $\mathbb{P}^1 V/\mathcal{I}$ though it appears discontinuous when we draw it in V. We have demonstrated the following:

Proposition 58 (Space-like geodesics)**.** *Let $p_1, p_2 \in \mathcal{B}$ such that the displacement $\Delta = (p_1 - p_2)/2$ is not light-like. Let p be the midpoint $p = (p_1 + p_2)/2$. Then the* AdS *geodesic γ connecting p_1 to p_2 is the conic lying in the affine plane $p + \mathrm{span}\{\Delta, j\}$ defined by the*

equation

$$|\gamma - p|^2 = |\Delta|^2.$$

If $|\Delta|^2 > 0$ *then* γ *is a (euclidean) ellipse, and if* $|\Delta|^2 < 0$ *then* γ *is a hyperbola. In either case,* γ *meets the* $\mathbb{R} + \mathbb{R}\tau$ *plane at right angles.*

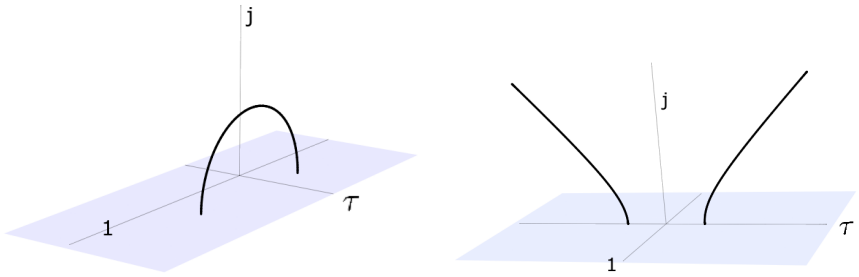

Figure A.1: A space-like geodesic is either an ellipse or a hyperbola depending on the displacement between its endpoints. In the hyperbola case, the geodesic comes out from the boundary along one branch of the hyperbola, passes though an "added" point of $\mathbb{P}^1 V$ and then returns to the boundary along the other branch.

Time-like geodesics have a similar description, though we won't give a detailed proof:

Proposition 59 (Time-like geodesics)**.** *Let* $p, \Delta \in \mathcal{B}$ *with* $|\Delta|^2 < 0$*. Then, the locus of points* γ *in the affine plane* $p + \mathrm{span}\{\Delta, j\}$ *satisfying*

$$|\gamma - p|^2 = -|\Delta|^2$$

defines a time-like geodesic. All time-like geodesics are described in this way.

We note that each time-like geodesic closes up after passing through exactly one "added" point in $\mathbb{P}^1 V$.

Proposition 60 (Light-like geodesics)**.** *The parametrized light-like geodesics are described by*

$$\gamma(t) = p + \frac{1}{t}\ell$$

where $p \in \mathbb{R} + \mathbb{R}\tau$*, and* ℓ *is a lightlike vector in* V*.*

Note that in this light-like case $\gamma(\infty) = \gamma(-\infty)$ and that after performing the quotient by $\mathcal{I}$, the two ends of γ appear to meet at an angle at the boundary. This is in contrast

with the projective model of AdS in $\mathbb{RP}^3$ in which lightlike geodesics are tangent to the boundary.

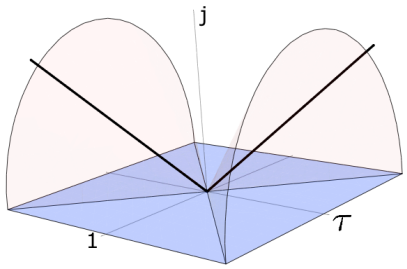

Figure A.2: A light-like geodesic. The light cone is drawn (in red) for reference.

Proposition 61 (Space-like Planes)**.** *Both of the following are space-like planes in this model:*

1. *A two-sheeted hyperboloid in V meeting the boundary $\mathcal{B}$ at right angles, described by an equation of the form*
$$|x - p|^2 = -R^2$$
where $p \in \mathcal{B}$. Note that the two components of the hyperboloid actually meet up in $\mathbb{P}^1 V$.

2. *a vertical affine plane of the form $p + \mathrm{span}\{v, j\}$ where $p, v \in R + \mathbb{R}\tau$ with v space-like.*

A.4 AdS ideal tetrahedra

Let z_1, z_2, z_3, z_4 be four points in the ideal boundary $\mathbb{P}^1\mathcal{B}$ of AdS. Recalling the isomorphism $\mathbb{P}^1\mathcal{B} \cong \mathbb{RP}^1 \times \mathbb{RP}^1$, we write each z_i as

$$z_i = \lambda_i \frac{1+\tau}{2} + \mu_i \frac{1-\tau}{2}$$

where $\lambda_i, \mu_i \in \mathbb{RP}^1$. If the λ_i are distinct and the μ_i are distinct, then taking the z_i three at a time, we get four space-like hyperbolic ideal triangles $\triangle_1, \triangle_2, \triangle_3, \triangle_4$. If further $(\lambda_1, \lambda_2, \lambda_3, \lambda_4)$ and $(\mu_1, \mu_2, \mu_3, \mu_4)$ have the same cyclic order in $\mathbb{RP}^1$, then the $\triangle_i$ bound an AdS *ideal tetrahedron*.

Every AdS ideal tetrahedron can be put into *standard position*, with ideal vertices $0, 1, \infty, z$ where z satisfies $|z|^2 > 0, |1-z|^2 > 0$ so that in particular all of the $\mathbb{R} + \mathbb{R}\tau$ ratios

$$z, \quad \frac{1}{1-z}, \quad \frac{z-1}{z}$$

assigned to the edges are defined and space-like (see Section 5.2.3). We describe this ideal tetrahedron in our half-space model. The three faces containing ∞ are vertical planes, while the fourth bottom face is a hyperboloid $|x-p|^2 = -R^2$. Writing $z = a + b\tau$, a simple calculation gives

$$p = \frac{1}{2} + \frac{a - |z|^2}{2b}\tau$$

$$R^2 = \frac{|z|^2\ |1-z|^2}{b^2}.$$

Note that in the case $b \to 0$, our tetrahedron degenerates and all four faces lie in a common plane.

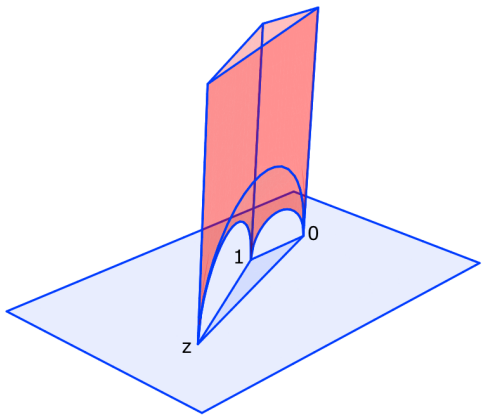

Figure A.3: The ideal AdS tetrahedron defined by the points $0, 1, \infty, z \in \mathbb{P}^1\mathcal{B} = \partial\,\mathrm{AdS}$. Each of the three side faces lies in an affine plane in V, while the bottom face lies in a hyperboloid. Each face is a totally geodesic ideal triangle isometric to an ideal triangle in the hyperbolic plane.

Bibliography

[ABB+07] Lars Andersson, Thierry Barbot, Riccardo Benedetti, Francesco Bonsante, William M. Goldman, Francois Labourie, Kevin P. Scannell, and Jean-Marc Schlenker, *Notes on a paper of Mess*, Geometriae Dedicata **126** (2007), no. 1, 47–70.

[Ahl85] Lars V. Ahlfors, *Mobius transformations and clifford numbers*, Differential Geometry and Complex Analysis, H.E. Rauch Memorial Volume (1985), 65–73.

[BB09] Riccardo Benedetti and Francesco Bonsante, *Canonical wick rotations in 3-dimensional gravity*, Memoirs of the American Mathematical Society, 2009.

[BBS09] Thierry Barbot, Francesco Bonsante, and Jean-Marc Schlenker, *Collisions of particles in locally AdS spacetimes*, preprint (2009).

[BCD+08] Thierry Barbot, Virginie Charette, Todd A. Drumm, William M. Goldman, and Karin Melnick, *A primer on the* $(2+1)$ *Einstein universe*, Recent developments in pseudo-Riemannian geometry (Dmitri V. Alekseevsky and Helga Baum, eds.), ESI Lectures in Mathematics and Physics, 2008, pp. 179–229.

[BEE96] John K. Beem, Paul E. Ehrlich, and Kevin L. Easley, *Global lorentzian geometry, 2nd ed.*, Marcel Dekker, New York, 1996.

[Ber60] Lipman Bers, *Simultaneous uniformization*, Bull. Amer. Math. Soc. **66** (1960), 94–97.

[BLP05] Michel Boileau, Bernhard Leeb, and Joan Porti, *Geometrization of 3-dimensional orbifolds*, Annals of Math **162** (2005), no. 1, 195–250.

[Bro07] Ken Bromberg, *Projective structures with degenerate holonomy and the bers density conjecture*, Annals of Math **166** (2007), 77–93.

[CG97] Suhyoung Choi and William M. Goldman, *The classification of real projective structures on surfaces*, Bulletin of the American Math Society **34** (1997), 161–171.

[CHK00] Daryl Cooper, Craig Hodgson, and Steven Kerckhoff, *Three-dimensional orbifolds and cone manifolds*, MSJ Memoirs, vol. 5, Mathematical Society of Japan, Tokyo, 2000.

[CLT07] Daryl Cooper, Darren D. Long, and Morwin B. Thistlethwaite, *Flexing closed hyperbolic structures*, Geometry and topology **11** (2007), 2413–2440.

[Ehr36] Charles Ehresmann, *Sur les espaces localement homogenes*, L'Enseignement Mathmatique **35** (1936), 317–333.

[FG07] V.V. Fock and A.B. Goncharov, *Moduli spaces of convex projective structures on surface*, Advances in Mathematics **208** (2007), no. 1, 249–273.

[Ga06] Francois Gueritaud and David Futer (appendix), *On canonical triangulations of once punctured torus bundles and two-bridge link complements*, Geometry and Topology **10** (2006), 1239–1284.

[Gol85] William M. Goldman, *Nonstandard lorentz space forms*, Journal of Differential Geometry **21** (1985), 301–308.

[Gol90] ———, *Convex real projective structures on compact surfaces*, Journal of Differential Geometry **31** (1990), 791–845.

[Gol10] ———, *Locally homogeneous geometric manifolds*, Proceedings of the International Congress of Mathematicians, Hyderabad, India (2010).

[HK98] Craig Hodgson and Steven Kerckhoff, *Rigidity of hyperbolic cone manifolds and hyperbolic dehn surgery*, Journal of Differential Geometry **48** (1998), 1–60.

[HK05] ———, *Universal bounds for hyperbolic dehn surgery*, Annals of Mathematics **162** (2005), no. 1, 367–421.

[Hod86] Craig Hodgson, *Degeneration and regeneration of hyperbolic structures on three-manifolds*, Ph.D. thesis, Princeton University, 1986.

[HPS01] Michel Huesener, Joan Porti, and Eva Suárez, *Regenerating singular hyperbolic structures from sol*, Journal of Differential Geometry **59** (2001), 439–478.

[Lab97] Francois Labourie, $\mathbb{RP}^2$*-structures et differentielles cubiques holomorphes*, Proceedings of the GARC Conference on Differential Geometry, Seoul National University (1997).

[Lac00] Marc Lackenby, *Word hyperbolic Dehn surgery*, Inventiones mathematicae **140** (2000), 243–282.

[Luo10] Feng Luo, *Volume optimization, normal surfaces and Thurston's equation on triangulated 3-manifolds*, preprint (2010).

[Mal99] Juan Martín Maldacena, *The large N limit of superconformal field theories and supergravity*, International Journal of Theoretical Physics **38** (1999), no. 4, 1113–1133.

[Mes07] Geoffrey Mess, *Lorentz spacetimes of constant curvature*, Geometriae Dedicata **126** (2007), no. 1, 3–45.

[NY74] Tadashi Nagano and Katsumi Yagi, *The affine structures on the real two-torus. i.*, Osaka Journal of Mathematics **11** (1974), 181–210.

[NZ85] Walter Neumann and Don Zagier, *Volumes of hyperbolic three-manifolds*, Topology **24** (1985), no. 3, 307–332.

[Por98] Joan Porti, *Regenerating hyperbolic and spherical cone structures from euclidean ones*, Topology **37** (1998), no. 2, 365–392.

[Por02] ———, *Regenerating hyperbolic cone structures from nil*, Geometry and Topology **6** (2002), 815–852.

[Por10] ———, *Regenerating hyperbolic cone 3-manifolds from dimension 2*, preprint (2010).

[PP00] Carlo Petronio and Joan Porti, *Negatively oriented ideal triangulations and a proof of Thurston's hyperbolic Dehn filling theorem*, Expositiones Mathematicae **18** (2000), no. 1, 1–35.

[Rat94] John G. Ratcliffe, *Foundations of hyperbolic manifolds*, Springer-Verlag, 1994.

[Riv94] Igor Rivin, *Euclidean structures on simplicial surfaces and hyperbolic volume*, Annals of Math **139** (1994), no. 2, 553–580.

[Sco83] Peter Scott, *The geometries of* 3*-manifolds*, Bulletin of the London Mathematical Society **15** (1983), 401–487.

[Seg11] Henry Segerman, *Detection of incompressible surfaces in hyperbolic punctured torus bundles*, Geometriae Dedicata **150** (2011), no. 1, 181–232.

[Thu80] William P. Thurston, *The geometry and topology of three manifolds*, `www.msri.org/publications/books.gt3m`, 1980.

[Thu97] ———, *Three-dimensional geometry and topology*, Princeton University Press, 1997.

[Wit88] Edward Witten, *(2+1)-dimensional gravity as an exactly soluble system*, Nuclear Physics B **311** (1988), 46–78.